

Thomas Løften

Catalytic isomerization of light alkanes

Doktoravhandling
for graden doktor ingeniør

Trondheim, desember 2004

Norges teknisk-naturvitenskapelige universitet
Fakultet for naturvitenskap og teknologi
Institutt for kjemisk prosess teknologi

 NTNU

Norwegian University of Science and Technology

Department of Chemical Engineering

Catalytic isomerization of light alkanes

by

Thomas Løften

Doctoral thesis submitted for the degree doktor ingeniør

Trondheim

December 2004

Acknowledgements

First of all I want to thank my supervisor professor Edd A. Blekkan for his guidance and encouragement during these four years.

I am also very grateful to professor Michel Guisnet and Dr. Ngi Suor Gnep for allowing me to stay at their group at the University of Poitiers and for their guidance during my six months there.

Several people have assisted me in the experimental work of this thesis. Kim A. Johnsen, Nguyet-Anh Nguyen, Hilde Moen, Svatopluk Chytil, Roland Bouiti and Philippe Bichon are all thanked for their assistance. Philippe Ayrault is acknowledged for performing the acidity characterization. I will thank Asbjørn Lindvåg in particular for helping me sort out all the problems with the gas chromatographs.

The Norwegian Research Council and NTNU are acknowledged for their financial support of this project. TOTAL E&P Norway are acknowledged for the grant that made my stay in Poitiers possible.

Finally, I would like to thank all my colleagues at NTNU and SINTEF for their support and friendship.

Abstract

In recent years the levels of sulfur and benzene in the gasoline pool have been reduced, and in the future there may also be new regulations on vapor pressure and the level of aromatics and olefins as well. The limitations on vapor pressure and aromatics will lead to reduced use of C₄ and reformate respectively. The branched isomers of C₅ and C₆ alkanes have high octane numbers compared to the straight chain isomers, and are consequently valuable additives to the gasoline pool. To maintain the octane rating, it is predicted that an increased share of isomerate will be added to the gasoline pool.

Today there is a well established isomerization technology with platinum on chlorided alumina as the commercial catalyst for both isomerization of *n*-butane and of the C₅/C₆ fraction. This catalyst is very sensitive to catalyst poisons like water and sulfur, and strict feed pretreatment is required. Zeolites promoted by platinum are alternatives as isomerization catalysts, and has replaced Pt/alumina catalysts to some extent. The Pt/zeolite catalyst is more resistant to water and sulfur compounds in the feed, but it is less active than platinum on chlorided alumina. It does therefore require a higher reaction temperature, which is unfortunate since the formation of the branched isomers of the alkanes is thermodynamically favored by a low temperature.

Because of the limitations of the two types of isomerization catalysts, there is a search for a new catalyst that is resistant to sulfur and water in the feed and is highly active so it can be operated at low temperature. A new type of catalyst that seems to be promising in that respect is sulfated zirconia.

The first part of this study focuses on a series of iron and manganese promoted SZ catalysts. The catalysts were characterized by various techniques such as XRD, TGA, N₂ adsorption and IR spectroscopy of adsorbed pyridine. The catalytic activity in *n*-butane isomerization at 250°C and atmospheric pressure was compared to the physical and chemical properties of the samples. No promoting effect of iron and manganese was found when *n*-butane was diluted in nitrogen. When nitrogen was replaced by hydrogen as the diluting gas the activity of the unpromoted SZ sample was dramatically lowered, while the activity of the promoted catalyst was not significantly changed.

If we only consider the promoted samples, the catalytic activity increases with increasing iron/manganese ratio. We also observe that the activity of the samples is clearly correlated with the number of strong Brønsted acid sites. The total number of strong acid sites (i.e. the sum of Brønsted and Lewis sites) does not change significantly when the promoter content is changing, hence no correlation between catalytic activity and the total number of acid sites is found. This underlines the importance of discrimination between Lewis and Brønsted acidity when characterizing the acidity of the samples.

The second part of this study is focused on a series of noble metal promoted sulfated zirconia. Their catalytic activity in *n*-hexane isomerization at high pressures was compared to a commercial Pt/zeolite catalyst. Among the noble metal promoted samples the catalyst promoted with platinum was the most active. The samples promoted with rhodium, ruthenium and iridium showed equal activity.

Common for all the noble metal promoted catalysts is the large increase in activity when catalysts are reduced with hydrogen compared to when they are pretreated in helium. The increase in activity is most likely connected to the reduction of the metal oxides of the promoters to ensure that the promoters are in the metallic state. Reduction at too high temperatures does however give lower activity. This is probably due to the reduction of surface sulfate groups leading to a loss in acid sites.

The commercial sample was considerably less active than the sample of platinum promoted sulfated zirconia. The commercial catalyst was however more stable than the PtSZ catalyst. All the sulfated zirconia catalysts deactivated, but the initial activity could be regenerated by reoxidation at 450°C followed by reduction at 300°C. The promotion with noble metals appears to inhibit coke formation on the catalyst. But, the main cause of deactivation of the platinum promoted sample is most likely the reduction of sulfate species leading to a loss of acid sites.

The kinetic study of the catalysts indicates that the *n*-hexane isomerization proceeds via a classical bifunctional mechanism where the role of the promoting metal is to produce alkenes, which are subsequently protonated on the acid sites. The reaction orders of hydrogen, *n*-hexane and total pressure are all in accordance with this mechanism. The activation energies of the catalysts are within the typical range of bifunctional catalysts.

All catalysts, except the unpromoted SZ sample, showed close to 100% selectivity to branched hexane isomers and a similar distribution of these isomers. The isomer distribution being the same for both the noble metal promoted catalyst and the Pt/zeolite is another indication that the isomerization proceeds via the bifunctional mechanism over the promoted samples. The different selectivity of the unpromoted SZ catalyst indicates that the isomerization proceeds via a different pathway over this catalyst; this is probably a pure acidic mechanism

The acidity characterization can not explain the differences in isomerization activity. It is however likely that the activity of the promoting metals in the dehydrogenation of alkanes is important since the classical bifunctional mechanism is prevailing.

Table of contents

ACKNOWLEDGEMENTS	III
ABSTRACT.....	IV
TABLE OF CONTENTS	VI
LIST OF PUBLICATIONS AND PRESENTATIONS.....	X
LIST OF SYMBOLS AND ABBREVIATIONS.....	XI
1 INTRODUCTION	1
1.1 Isomerization of Light Alkanes	1
1.2 Sulfated Zirconia	2
1.3 Scope of the Work	4
2 LITERATURE	5
2.1 Thermodynamics.....	5
2.2 Acid Catalysis	6
2.3 Mechanisms	9
2.3.1 Acid catalysis.....	9
2.3.2 The bifunctional mechanism.....	12
2.4 Preparation of sulfated zirconia.....	14
2.5 The active site.....	16
2.6 Promoters.....	18
2.6.1 Iron and manganese and similar transition metals.....	18
2.6.2 Platinum and other noble metals.....	20
2.7 Cracking	22
2.8 Deactivation	23

3	EXPERIMENTAL METHODS	25
3.1	Catalyst Preparation	25
3.1.1	Preparation of iron and manganese promoted sulfated zirconia	25
3.1.2	Noble metal promoted sulfated zirconia.....	26
3.1.3	Preparation of tungsten oxide modified zirconia	28
3.2	Catalyst Characterization	28
3.2.1	Acidity	28
3.2.2	X-ray diffraction	29
3.2.3	Surface area and pore size distribution.....	29
3.2.4	Thermogravimetric analysis.....	29
3.2.5	Temperature programmed reduction.....	29
3.2.6	Sulfur content	29
3.3	Catalytic Tests	29
3.3.1	<i>n</i> -Butane isomerization.....	30
3.3.2	<i>n</i> -Hexane isomerization.....	31
3.4	Calculation of Activity and Selectivities	35
4	RESULTS	36
4.1	Isomerization of n-butane at atmospheric pressure	36
4.1.1	Characterization of the iron and manganese promoted samples	36
4.1.2	Catalytic testing	39
4.1.3	Acidity and catalytic activity of tungsten oxide modified zirconia	45
4.2	Isomerization of n-hexane at elevated pressure	47
4.2.1	Characterization of noble metal promoted catalysts	47
4.2.2	Preliminary catalytic tests at high pressures	51
4.2.3	Comparison of catalytic activity and kinetic study	55
4.2.3.1	<i>PtSZ</i>	55
4.2.3.2	<i>IrSZ</i>	62
4.2.3.3	<i>RhSZ</i>	66
4.2.3.4	<i>RuSZ</i>	69
4.2.3.5	<i>SZ</i>	70
4.2.3.6	<i>Commercial catalyst</i>	72
4.2.3.7	<i>Summary of the kinetic study</i>	75

5	DISCUSSION	77
5.1	Isomerization of n-butane at atmospheric pressure.....	77
5.2	Isomerization of n-hexane at elevated pressure	81
5.2.1	Preliminary catalytic tests	81
5.2.2	The noble metal promoted catalysts	81
5.3	Suggestions for further work	93
6	CONCLUSIONS	94
7	REFERENCES	96
	LIST OF APPENDICES.....	101

List of Publications and Presentations

There is one publication of the results from this study:

T. Løften, N.S. Gnep, M. Guisnet and E.A. Blekkan, "Iron and manganese promoted sulfated zirconia: Acidic Properties and *n*-butane isomerization activity", Accepted for publication in *Catalysis Today*.

Presentations:

- i) Thomas Løften, Kim André Johnsen and Edd A. Blekkan: "Preparation and characterization of sulfated zirconia" Poster at the 10th Nordic Symposium on Catalysis in Helsingør, Denmark, June 2002.
- ii) Thomas Løften: "Isomerization of light alkanes over acid catalysts". Oral presentation at the Vista seminar at Statoil Research Centre, Trondheim, June 2003.
- iii) Thomas Løften: "Isomerization of *n*-butane over iron and manganese promoted sulfated zirconia". Oral presentation at the Norwegian Symposium on Catalysis in Bergen, Norway, November 2003.
- iv) T. Løften, N.S. Gnep, M. Guisnet and E.A. Blekkan: "Iron and manganese promoted sulfated zirconia: Acidic Properties and *n*-butane isomerization activity". Poster at the 11th Nordic Symposium on Catalysis in Oulu, Finland, May 2004.
- v) Edd A. Blekkan, Kim A. Johnsen and Thomas Løften: "Isomerization of light alkanes: Preparation and characterization of platinum promoted sulfated zirconia catalysts". Poster at the 7th Natural Gas Conversion Symposium, Dalian, China, June 2004.
- vi) T. Løften, N.S. Gnep, M. Guisnet and E.A. Blekkan: "Iron and manganese promoted sulfated zirconia: Acidic Properties and *n*-butane isomerization activity". Poster at the 3rd International Taylor Conference, Belfast, UK, 2004.

List of Symbols and Abbreviations

2,2DMB		2,2-dimethylbutane
2,3DMB		2,3-dimethylbutane
2MP		2-methylpentane
3MP		3-methylpentane
a_i		Number of carbon atoms in component i
B		Brønsted acid site
E_A	kJ/mol	Apparent activation energy
F_i	mol/minute	Molar flow of component i
FMSZ (α)F(β)MSZ		Iron and manganese promoted sulfated zirconia α and β is denoting the nominal promoter content in wt%
I/C		isomer/cracking ratio
IrSZ		Iridium promoted sulfated zirconia
L		Lewis acid site
P_{H_2}	bar	Partial pressure of hydrogen
P_{nC_6}	bar	Partial pressure of n -hexane
P_{TOT}	bara	Total pressure
PtSZ		Platinum promoted sulfated zirconia
PtWZ		Platinum promoted tungsten oxide modified zirconia
R^+		Alkyl group

List of Symbols and Abbreviations

RH		Alkane
RhSZ		Rhodium promoted sulfated zirconia
RON		Research octane number
RuSZ		Ruthenium promoted sulfated zirconia
S_i		Selectivity of component i
SZ		Sulfated zirconia
T	°C or K	Temperature
T_d	°C	Temperature of decomposition during TGA
T_D	°C	Temperature of desorption during thermodesorption of pyridine
TGA		Thermogravimetric analysis
TOS	minutes or hours	Time on stream
TPR		Temperature programmed reduction
W	g	Catalyst weight
WHSV	h^{-1}	Weight hourly space velocity
WZ		Tungsten oxide modified zirconia
X	%	Conversion
X_0	%	Initial conversion
XRD		X-ray diffraction

1 Introduction

1.1 Isomerization of Light Alkanes

In recent years the level of sulfur and benzene in the gasoline pool has been reduced, and in the future there may be regulations on vapor pressure and the level of aromatics and olefins as well [1]. This will lead to a change in the gasoline blending stocks. The desulfurization of FCC gasoline could result in a loss in octane number. Furthermore, the limitations on vapor pressure and aromatics will lead to reduced use of C4 and reformate respectively. To maintain the octane rating, it is predicted that an increased share of isomerate will be added to the gasoline pool.

Light hydrocarbons are already important chemicals for the refinery industry and chemical industry in general. Alkylation of isobutane with C3 and C4 alkenes is an important reaction in the production of alkylates used as additives in gasoline. Isobutane can also be dehydrogenated to isobutene for use in the MTBE synthesis. The branched isomers of C5 and C6 have high octane numbers compared to the straight chain isomers, and are consequently valuable additives to the gasoline pool. As an example the difference in octane numbers for *n*-hexane and the branched isomers is shown in Figure 1.1.

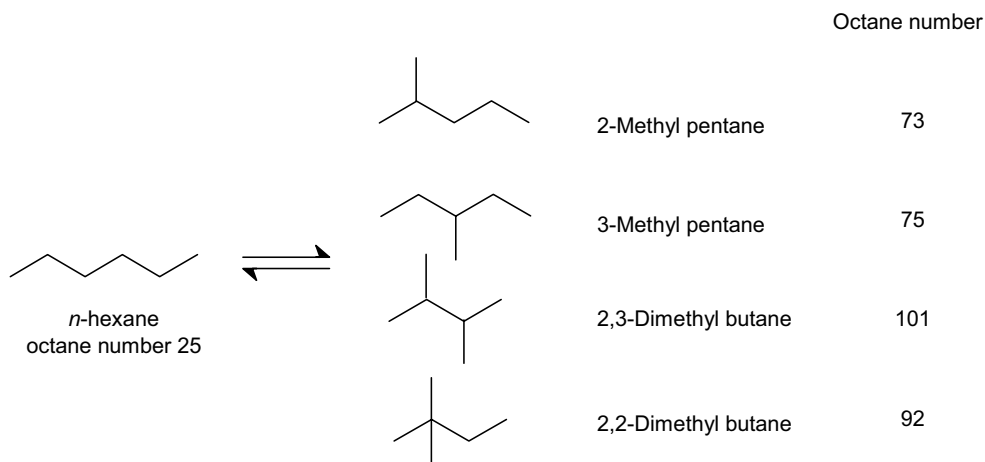


Figure 1.1 Octane numbers (RON) of the hexane isomers [2].

There is a well established isomerization technology available, with an installed capacity today at about 1,500 thousand bspd, and it is growing steadily. The paraffin isomerization technology is dominated by UOP with Penex™ (C5/C6) and Butamer™ (C4) units. Nowadays, the majority of the isomerization units are based on amorphous catalysts (platinum on chlorided alumina), which typically yield 4 points higher RON than the less active zeolite based catalysts [3].

The main objection against the Pt/Al_2O_3 catalyst is that it needs continuous addition of chloride to maintain the activity. The utilization of chlorides is associated with corrosion problems and the handling of the chlorides involves some environmental hazards. In addition to that, the Pt/Al_2O_3 catalyst is extremely sensitive to contaminants in the feed. Water and ammonia in the feed act as permanent poisons to the active sites. Sulfur on the other hand poisons the metallic sites, but this deactivation is reversible. Strict feed pretreatment and drying procedures are therefore needed.

Zeolites promoted by platinum, e.g. HYSOPAR® from Süd-Chemie and HS-10™ from UOP, are alternatives to the metal halide catalysts that are used in the Penex™ process and similar technologies. The zeolites are less acidic than the chlorided alumina, hence they must be operated at a higher temperature, typically at 220-300°C, which is thermodynamically less favorable. On the other hand the zeolite based isomerization catalysts are much more stable and resistant to impurities in the feed like sulfur and water. Typical operating conditions for the conventional isomerization catalysts are given in Table 1.1.

Table 1.1 Operating conditions and feed limitations for the current conventional isomerization catalysts [1, 4]

	<i>Pt/Al₂O₃</i>	<i>Pt/zeolite</i>
Temperature	120-160°C	220-300°C
Pressure	30 bar	30 bar
Feed limitations	Sensitive to water Low sulfur resistance Require continuous addition of chloride	Resistant to water and sulfur in feed
RON yield	83	77

1.2 Sulfated Zirconia

In the last decades there has been a search for a catalyst that can meet the new requirements from both the legislation and the market. One class of catalysts that has received a lot of attention is anion modified metal oxides, which show good acid properties. The focus has been on sulfated zirconia in particular, which was first prepared and used as a hydrocarbon isomerization catalyst in 1962 in Holm and Baileys patent for Phillips Petroleum [5].

Sulfated zirconia (SZ) received renewed interest in the late seventies when Hino and Arata [6] reported that butane could be transformed to isobutane over SZ even at room temperature. They

ascribed the high activity of the catalyst to its superacidic properties, i.e. SZ is claimed to be a stronger acid than concentrated sulfuric acid.

The problem was however that sulfated zirconia deactivated rapidly. To try to overcome this, various transition metals were added as promoters. Among these metals, platinum, iron and manganese gave better activity [7]. Addition of platinum to SZ was found to increase the stability of the catalyst towards deactivation during the isomerization of alkanes [7-9]. The detailed role of platinum is not clear. Hydrogen may dissociate on platinum and either spillover to the SZ surface to produce a protonic site, or it proceeds to hydrogenate the carbonaceous residue and its precursors [10]. It is possible however that the platinum promoted SZ acts as a traditional bifunctional catalyst since it contains both acid and metallic sites [11]. According to the traditional bifunctional mechanism the alkane is dehydrogenated to an olefin over the metallic site before protonation of the olefinic intermediate to a carbenium ion. This carbenium ion is then isomerized to a branched tertiary carbenium ion, which decomposes into a proton and branched olefin. The final step is the hydrogenation of the olefin over a metallic site and a branched alkane is obtained [12].

Hsu and co-workers [13, 14] found that by promoting sulfated zirconia with iron and manganese (FMSZ) the activity for *n*-butane isomerization at room temperature was increased by about three orders of magnitude, and they ascribed the increased activity to an increase in the acid strength of the catalysts [15]. Later this was contradicted by Adeeva *et al.* [16], who reported that there was no difference in the acid strength of neither the Lewis or the Brønsted sites of FMSZ and SZ.

Since the discovery of iron and manganese as promoters for SZ, a wide range of other metals have been studied as promoters, i.e. nickel, antimony, scandium, cobalt, zinc, chromium, vanadium, copper, cadmium, titanium, aluminum, tin, molybdenum, tungsten [17], iridium, platinum, rhodium, ruthenium, osmium and palladium [9].

After nearly thirty years with intensive research there has been published numerous papers on sulfated zirconia [7, 18], very often in connection with isomerization of alkanes. And during these years a new commercial C5/C6 isomerization catalyst based on platinum promoted sulfated zirconia has been introduced to the market [1]. Despite this, the origin of the activity, i.e. the nature of the catalytically active sites, has not been unequivocally identified. Equally unknown is the detailed mechanism of the promoters [19].

1.3 Scope of the Work

The goal of this project is to provide new insight into the behavior of novel highly acidic isomerization catalysts for nC4-nC6 hydrocarbons. The catalyst of main interest in this project is sulfated zirconia, but comparison is made to other catalysts and a commercial isomerization catalyst. The work is especially focused on the effect of promoters such as noble metals like platinum and other transition metals. Traditional activity and selectivity measurements have been used in order to investigate the kinetic parameters of the catalysts, such as reaction order and activation energy. The catalysts have been characterized by various techniques to correlate the physical and chemical properties of the catalyst materials to the catalytic activity and the kinetic parameters.

The work has mainly been performed at the Department of Chemical Engineering at the Norwegian University of Science and Technology (NTNU), and has been supported financially by the Norwegian Research Council. A part of the work was performed at the University of Poitiers, France (Laboratoire de Catalyse en Chimie Organique). This part of the work has been made possible by financial support from TOTAL E&P Norway.

Several people have been involved in the experimental work of this project. Kim Andre Johnsen and Nguyet-Anh Nguyen took part in the preliminary catalyst synthesis and characterization. Hilde Moen contributed in the process of making the set up for *n*-hexane isomerization work properly. Svatopluk Chytil did the preparation and catalytic testing of some mixed metal oxide catalysts. During the stay in Poitiers I received invaluable help and advice from Roland Bouiti and Philippe Bichon. Dr. Philippe Ayrault did all the acidity characterization by FT-IR of adsorbed pyridine. Thermodynamic calculations in Hysys were done by professor emeritus Odd Arne Rokstad.

2 Literature

2.1 Thermodynamics

Isomerization of straight chained alkanes to their branched isomers is a slightly exothermic reaction. Thus the yield of branched alkanes is thermodynamically favored by a low reaction temperature [20].

Thermodynamic calculations done using the software package Hysys (from Hyprotech) applying the thermodynamic model Peng Robinson gave the equilibrium composition of butane and hexane isomers as shown in Figure 2.1 and Figure 2.2 respectively.

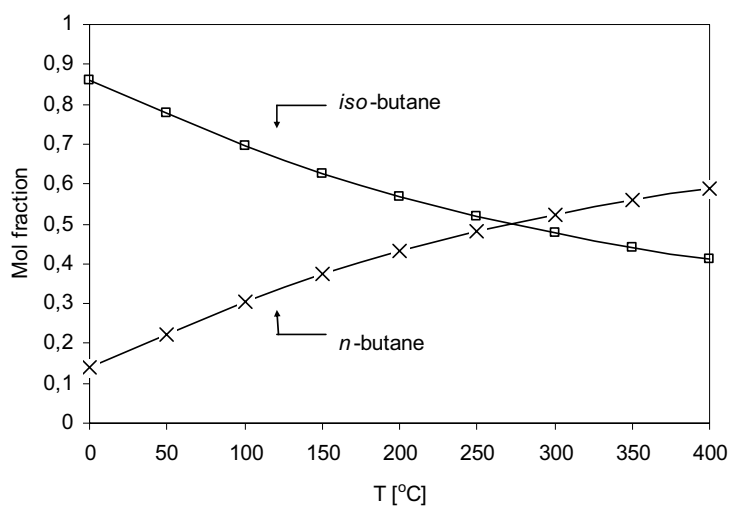


Figure 2.1 Thermodynamic equilibrium for isomers of butane as calculated using the Peng Robinson model. The calculations were performed by associate professor Odd Arne Rokstad [21].

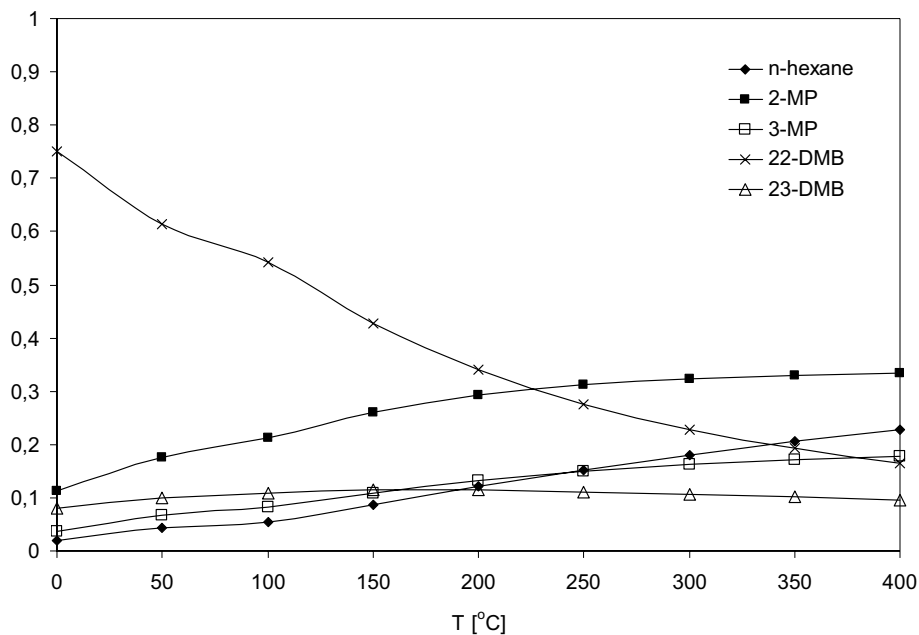


Figure 2.2 Thermodynamic equilibrium for isomers of hexane as calculated using the Peng Robinson model [21].

Among the isomers of hexane, 2,2-dimethylbutane is thermodynamically favored by low temperatures and 2,3-dimethylbutane is relatively unchanged for the whole temperature range. *n*-hexane and the methyl pentanes are on the other hand favored at higher temperatures. Knowing that the dibranched isomers have higher octane numbers, a low reaction temperature is desired and thus a highly active catalyst is needed.

The results from these thermodynamic calculations are in accordance with the calculations published by Ridgway and Shoen [22].

2.2 Acid Catalysis

The mechanism for alkane isomerization has been studied for years, but many of the details are however still disputed. The main questions to be solved in this respect are the way of formation of carbenium ions, the role of different promoters and the role of hydrogen.

The alkane isomerization catalysts of importance can be divided in five groups, which will be described in the following section. The emphasis will be on sulfated zirconia which is the catalyst of main interest in this project.

1. Friedel-Crafts catalysts

The carbenium mechanism for isomerization was developed for the original isomerization catalysts which were of the Friedel-Crafts type (AlCl_3 with additives such as SbCl_3 and HCl). These catalysts are abandoned now because of the problems of corrosion and the disposal of used catalysts [23].

2. Bifunctional catalysts

The Friedel-Crafts type of catalyst was replaced by solid acid catalysts, first by chlorinated alumina and later also by zeolites. The catalyst stability and selectivity are greatly improved by loading a transition metal and operating at a high hydrogen pressure [23]. Solid acids are less active than the homogenous Friedel-Crafts catalyst [23], thus a higher temperature is required to have an acceptable activity. Chlorinated alumina is operated at 120-160°C and zeolite catalysts are operated at 220-300°C [1].

The solid acid participates in the steps involving carbenium ions, while the metallic component offers the metallic hydrogenation-dehydrogenation activity. Therefore, this type of catalysts is referred to as bifunctional catalysts, and the so called bifunctional mechanism is described in more detail in chapter 2.3.

This type of catalyst is utilized today in industrial processes under high hydrogen pressure, as already mentioned. The processes are therefore often called hydroisomerization processes.

3. Sulfated zirconia

Zirconia (zirconium oxide) when modified with anions such as sulfate gives a catalyst with very high acid strength. This catalyst is active for a number of chemical reactions, including hydrocarbon isomerization, methanol to olefins, alkylation, acylation, esterification, condensation and cyclization [7].

Sulfated zirconia was first described as an isomerization catalyst by Holm and Bailey in their patent from 1962 assigned to Phillips Petroleum [5]. The interest in this catalyst reappeared in 1979 when Hino and Arata [6] reported that sulfated zirconia was active for *n*-butane isomerization at 100°C. They ascribed the high activity to the superacidic properties of catalyst, which they measured with the help of Hammett indicators [24]. The method of Hammett indicators have been questioned by Corma [25]. He claims that the Hammett acidity function (H_0) has no physical meaning for solid acids and that the application of Hammett indicators to characterize solid acids can be misleading. Kustov *et al.* [26] investigated SZ by diffuse reflectance IR spectroscopy and found that the acidity of was no more than that of sulfuric acid or H zeolites. This was confirmed by a spectroscopic study with FTIR and ^1H NMR

that showed that SZ and FMSZ have the same acid strength as HY zeolites and are weaker acids than H-ZSM-5 [16].

In 1992 Hsu and coworkers [13, 14] found that *n*-butane could be isomerized at as low temperatures as 35°C over SZ promoted by iron and manganese (FMSZ). The promoters increased the isomerization activity by almost three orders of magnitude, this was ascribed to an increase in the acid strength of the catalysts [15]. In the same way as Hino and Arata [6, 24] did in their seminal work, the high activity of the FMSZ catalyst was ascribed to its superacidic properties. The assignment of superacidity has now been abandoned by most groups. Since the discovery of iron and manganese, the promoting effect of a wide range of other metals has been studied [9, 17], and the role of some of these promoters is described in chapter 2.6.

Not only the strength of the acid matters for enhanced activity and selectivity, but also the type of acidity, i.e. Brønsted or Lewis, is important [7]. There are different opinions on whether it is Lewis or Brønsted acidity that gives sulfated zirconia its catalytic activity, or if it is a combination of the two types. Morterra and coworkers [27] found that Lewis acidity is essential for the isomerization activity, but activity from Brønsted sites are not excluded. This is supported by Yamaguchi *et al.* [28] and Lei *et al.* [29] who found that only Lewis acid sites are present on the catalyst surface. There is however an agreement in most reports that Brønsted sites are present on the SZ surface, but in coexistence with Lewis acid sites [30-33]. Several authors have reported that there is a certain ratio between Lewis and Brønsted acids that gives the optimum catalytic activity in *n*-butane isomerization [34-36], but there is no agreement on what this ratio is.

4. Tungsten oxide supported on zirconia

Another modification of zirconia that has obtained a great interest as an alkane isomerization catalyst is tungsten oxide supported on zirconia, often abbreviated to $\text{WO}_x\text{-ZrO}_2$ or WZ. Hino and Arata found it to be active for *n*-butane isomerization at 50°C [37]. It has been found that the selectivity to branched isomers and stability, but not the activity, of PtWZ is better than for PtSZ [38, 39]. The use of tungsten oxide modified sulfated zirconia is also advantageous compared to SZ because the catalyst contains no sulfate ions which can poison the metal sites [23].

The presence of Pt in WO_x promoted zirconium hydroxide is necessary to obtain a good activity and stability during *n*-hexane isomerization [40]. This indicates that the isomerization proceeds via a kind of bifunctional mechanism as described in chapter 2.3.2. This is supported by Kuba and coworkers [39] who also found that by promoting the WZ catalyst by noble metals such as platinum the activity and selectivity for *n*-pentane isomerization are dramatically improved. The improvement is only marginal in the absence of H_2 but is significant when H_2 is co-fed with the reactant.

5. Heteropoly acids

Another class of highly acidic materials is the heteropoly acids. One of the most interesting compounds for acidic reactions is $\text{H}_3\text{PW}_{12}\text{O}_{40}$ and its cesium salts [41]. These materials are able to catalyze the isomerization of alkanes at moderate temperatures [42, 43]. Na *et al.* [43] found that the stationary activity and selectivity of $\text{Cs}_{2.5}\text{H}_{0.5}\text{PW}_{12}\text{O}_{40}$ were much higher than those of SZ at 573 K, and they concluded that the high catalytic performance of this catalyst was due to its low deactivation and its strong acidity.

Ono and coworkers [23] reported that $\text{H}_3\text{PW}_{12}\text{O}_{40}$ supported on Pd/carbon gave 96% selectivity to hexane isomers at 78% conversion and reaction temperature 150°C. They proposed that the role of palladium was to dissociate H_2 and form hydrogen atoms, which will react with the heteropoly anion and form protons, as shown in equations (2.1) and (2.2). This is suggested to be the same spill-over effect as reported for the PtSZ system [44].



2.3 Mechanisms

The reaction pathway for alkane isomerization can be described by two main mechanisms, the pure acid catalysis and the bifunctional mechanism. This classification corresponds to the two main types of catalysts which were described above, the acid and the bifunctional catalysts.

2.3.1 Acid catalysis

The isomerization of alkanes can be viewed as a chain reaction, which consists of initiation, propagation and termination steps.

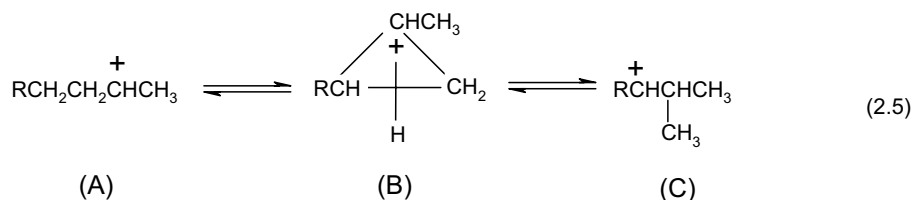
In the acidic mechanism the initiation step over a Brønsted acid site is the formation of carbenium ion. A carbonium ion is formed when the alkane is protonated by a Brønsted acid site, the pentacoordinated carbonium ion splits of dihydrogen and forms the carbenium ion [45]:



The propagation reactions are the skeletal rearrangement of the carbenium ion and the chain transfer reaction.



The skeletal rearrangement involves an intermediate species, the protonated cyclopropane ring (species B in equation (2.5)). This is a delocalized electron deficient structure with much lower energy than the primary carbenium ion [46]. This pathway is called the monomolecular mechanism.



When R is a hydrogen atom (equation (2.5)) this pathway is difficult since it involves the formation of a primary carbenium ion (species C) [47], which is energetically unfavorable [46]. The observed isomerization rate of butane in liquid acids is therefore many orders of magnitude smaller than the isomerization rates of pentane and higher alkanes [48].

In the case of solid acids, however, the rates of butane and pentane isomerization have been reported to be in the same order of magnitude [47]. This indicates that the isomerization of butane in this case proceeds via a different path than in the monomolecular mechanism shown in Equation (2.5). Guisnet *et al.* [49, 50] proved that *n*-butane can be isomerized over H-mordenite via a pathway that does not involve formation of a primary carbenium ion. They showed by isotopic labeling experiments and the presence of C3 and C5 alkanes in the product stream that the mechanism involves a bimolecular alkylation step, followed by isomerization and disproportionation of the dimeric species [50, 51]. This bimolecular mechanism is shown by Adeeva *et al.* [52] to be valid also for sulfated zirconia.

It has also been suggested that this mechanism proceeds over a Lewis acid site. The carbenium ion is formed by hydride abstraction over a Lewis acid site, represented by a coordinatively unsaturated Zr^{4+} center [53]. This is followed by dimerization with butene and fragmentation of the C8 intermediate to yield isobutane or C3 and C5 cracking products as shown in Figure 2.3.

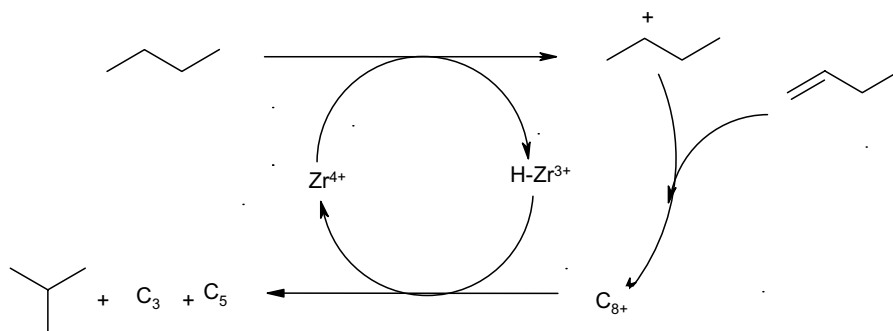


Figure 2.3 *n*-butane isomerization via the bimolecular mechanism catalyzed by a Lewis acid site.

The isomerization of alkanes with more than five carbon atoms will follow the monomolecular scheme as shown in equation (2.5) since the species C then is secondary carbenium ion [20, 47]. A more detailed scheme for the acid catalyzed isomerization of *n*-hexane is shown in Figure 2.4.

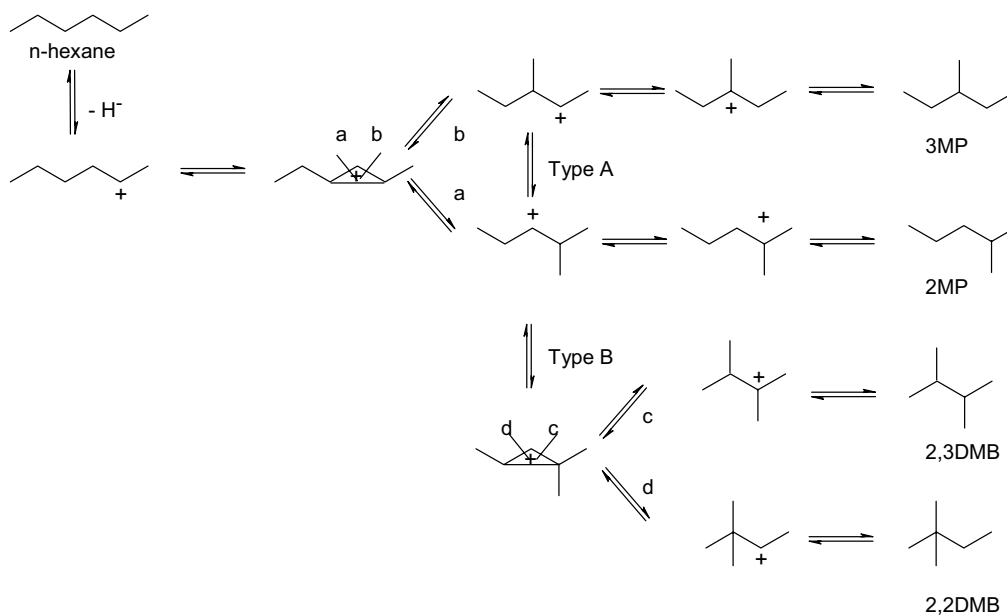


Figure 2.4 The mechanism for *n*-hexane isomerization over pure acid catalyst [54].

2.3.2 The bifunctional mechanism

The classical bifunctional mechanism

The idea of *the bifunctional catalysis*, sometimes referred to as dual function catalysis [12], originates from the use of alumina loaded with transition metals in the reforming processes [23]. The bifunctional catalysts possess what is regarded as two different types of catalytic properties, namely an acidic function which effects the isomerization. And a metallic function, which gives the ability to hydrogenate and dehydrogenate hydrocarbons [12].

For the isomerization of alkanes it is supposed that the alkane is dehydrogenated to an alkene on the metal site. The alkene is then protonated on the acid site to a carbenium ion, which subsequently is isomerized to a branched carbenium ion. The branched carbenium ion gives the proton back to the acid site, the resulting branched alkene is hydrogenated on the metallic site. The branched alkane is formed, and can desorb from the catalyst surface. The reaction scheme is shown in Figure 2.5.

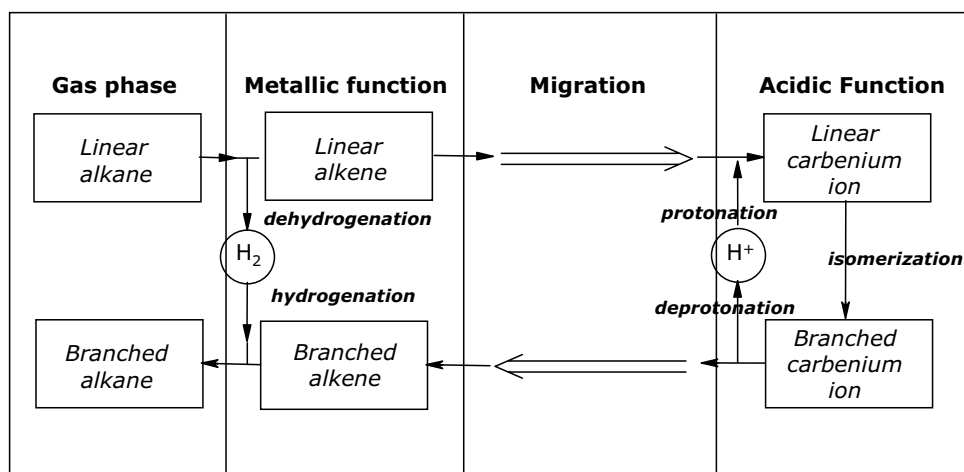


Figure 2.5 The classical bifunctional mechanism as proposed by Mills *et al.* [12] (Drawing after Demirci and Garin [11])

The isomerization step proceeds via a protonated cyclopropane ring as described for the acidic mechanism (equation (2.5)). The difference between the classical bifunctional mechanism and acidic mechanism is in the way the carbenium is formed. In the acidic mechanism it is the alkane that gets protonated and then splits off dihydrogen to give the carbenium ion. For the bifunctional mechanism the order is opposite; the alkane is dehydrogenated and forms an alkene, which then is protonated to give the carbenium ion.

There are two main factors that provide positive evidence for the bifunctional mechanism. Firstly, a high catalytic activity is obtained only when both a metallic component and hydrogen are present. The other evidence is that the reaction order with respect to hydrogen is negative [23].

Alternative bifunctional mechanisms

In recent years it has been reported that hydrogen has a positive reaction order for hydrogen during *n*-hexane isomerization over platinum promoted sulfated zirconia [31, 55, 56], or that the effect of hydrogen reaches a maximum [45, 57] which is also observed in case of *n*-butane [8]. This can not be explained by the classical bifunctional mechanism as proposed by Mills *et al.* [12]. The positive effect of hydrogen in the presence of platinum has been explained by different mechanisms.

Ebitani *et al.* [31, 44] found that by heating PtSZ in the presence of hydrogen in the temperature range 423-623 K, protonic sites were formed with a concomitant decrease in the number and strength of Lewis acid sites, demonstrating that protonic sites originate from molecular hydrogen. They suggest that molecular hydrogen dissociates on the platinum to hydrogen atoms which undergo spillover to the SZ surface and is converted to a proton and a hydride ion (or two protons and two e^-). The enhancement in alkane isomerization activity when hydrogen is present is thus explained by an increase in acidity of the catalyst. A model for the hydrogen spillover is shown in Figure 2.6. The idea that the simultaneous presence of platinum and hydrogen leads to an increase in the acidity of SZ by is supported by Falco *et al.* [58]. Their idea is the same; hydrogen is dissociated on platinum producing protonic sites on the support. They find, however, that the metallic properties and the activity of platinum are decreased by a strong interaction with the support. At the same time this interaction leads to an enhancement of the activity of the acid support.

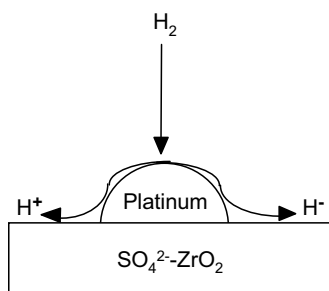


Figure 2.6 Model for the dissociation of H_2 and spillover to the surface of sulfated zirconia.

Iglesia *et al.* [56] also observed an increase in the isomerization rate with increasing hydrogen pressure, in this case for *n*-heptane isomerization. They claim that the desorption step is the rate-limiting step for the isomerization reaction. Dihydrogen can provide hydride ions, but to form these hydrogen ions a dissociation site like platinum is required. Thus, the conversion rate increases since more hydride ions are provided for the rate-limiting desorption step. As a result of the shorter surface residence time, desorption occurs before the undesired C-C scission events and the cracking steps

are inhibited. This is also observed in the case of *n*-hexane isomerization [55]. At low hydrogen partial pressures or in the absence of hydrogen the lifetime of the surface intermediates is longer. Under these conditions oligomerization and cracking will dominate at short residence times and polymerization and coke formation at long residence times.

Manoli *et al.* [57] did observe a maximum in *n*-hexane isomerization activity with increasing hydrogen partial pressure which cannot be explained by the traditional bifunctional mechanism. They proposed that a “compressed bifunctional site” exists on the surface of PtSZ, where concerted metal-acid catalysis prevails. Sachtler *et al.* [59] had already suggested the existence of such ensembles, which they called “collapsed bifunctional sites”. These combined active ensembles are formed when sulfate groups meet platinum sites in their close vicinity [60]. The maximum in catalytic activity as a function of hydrogen pressure is explained as follows [60]: At low hydrogen pressures the supply of hydrogen is scarce. Near the maximum, the lifetime of the surface species is optimal; this is supported by the findings of Sachtler *et al.* [47]. When the hydrogen partial pressure is too high hydrogen will compete with the intermediates on the active sites and the intermediates will desorb too quickly.

Duchet and co-workers [45, 61] explains the influence of hydrogen over platinum promoted sulfated zirconia in another way. At low hydrogen pressures hydrogen increases the concentration of hydride species, this leads to an acceleration of the desorption of the carbenium ions, and hence an increase in the overall rate. The decrease in activity at higher hydrogen pressures is explained by the competition between protons and carbenium ions on the Lewis base site.

2.4 Preparation of sulfated zirconia

There are many parameters that are determining for the activity of sulfated zirconia, i.e. deactivation, acidity, hydration state, sulfur content, activation temperature, crystallinity and promoters [62]. All of these parameters are connected to the preparation of the material, and often these parameters interact. This underlines the importance of choosing the right conditions when synthesizing the catalyst.

The most common route for synthesis of sulfated zirconia is the two-step method which is illustrated schematically in Figure 2.1. The first step is the precipitation of zirconium hydroxide. This is done by adding a base, e.g. ammonium hydroxide, to an aqueous solution of a zirconium salt. The zirconium source can be zirconyl chloride ($ZrOCl_2$), zirconyl nitrate ($ZrO(NO_3)_2$), zirconium chloride ($ZrCl_4$), or zirconium nitrate ($Zr(NO_3)_4$) [18]. The precipitate is washed and dried before impregnation of the sulfate. The sulfating agent can be sulfuric acid or ammonium sulfate. The sulfated zirconium hydroxide is calcined at 600-650°C to give the optimal catalytic activity [63, 64], they find that in this temperature range the tetragonal crystalline phase is formed, which is considered to be the active phase of sulfated zirconia [65]. Pure zirconia is transformed from the tetragonal to the monoclinic phase at a calcination temperature above 600°C. This transformation is prevented when doping

zirconia with SO_4^{2-} [7]. When calcining at higher temperatures sulfur is lost and the surface area decreases [30].

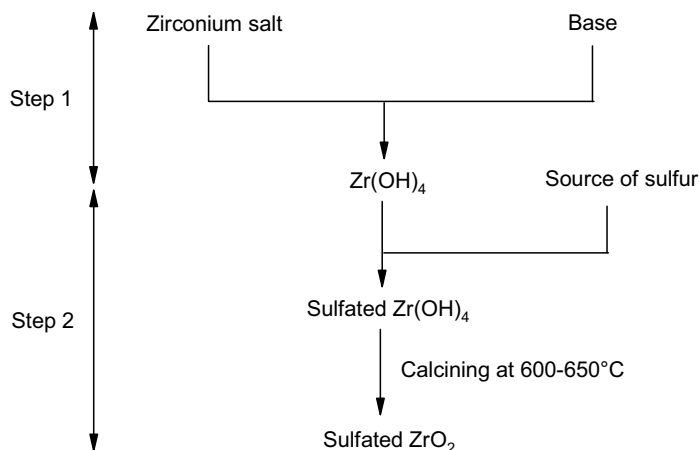


Figure 2.7 The two step synthesis route for preparation of sulfated zirconia [18].

The other synthesis route to sulfated zirconia is the one-step sol gel method. This method was first described by Ward and Ko [66]. In this procedure a zirconium sulfate alcogel is produced by addition of diluted sulfuric acid to zirconium *n*-propoxide. If the alcogel is dried at supercritical conditions a zirconium-sulfate aerogel with high specific surface area is obtained [67]. It was found that the sulfate ions were initially trapped in the bulk of the aerogel, but upon calcination and crystallization of zirconia the sulfate is expelled onto the surface [18, 66].

The calcination temperature determines important catalyst properties such as sulfur content, surface area, phase composition and activity [30, 63, 64]. It has also been found that the catalyst properties depend on the batch size during calcination [68]. During the calcination an exothermic reaction occurs which can lead to overheating. The heat transfer and hence the temperature overshoot is influenced by the batch size; this affects the physical and catalytic properties of the produced sulfated zirconia.

Another preparation parameter that can influence the properties of sulfated zirconia is the mechanical stress the material is exposed to during milling or grinding. Klose *et al.* [19] found that both the crystallinity and catalytic activity was changed after milling and grinding, and they find an operator influence during the grinding likely. The influence of the batch size and a common laboratory practice such as grinding underlines the difficulty of investigating sulfated zirconia. It may also explain why a fundamental understanding of this system has not been reached despite 25 years of intensive research [19].

2.5 The active site

The nature of the active site, whether it is of the Brønsted or the Lewis type, as well as the exact structure of the site has been disputed since the discovery of sulfated zirconia [7]. Several attempts have been made to disclose the true nature of the active site and in the following section some of the suggested models are presented.

Kumbhar *et al.* [69] suggested the following model for the formation of the acid site after impregnation with sulfuric acid and calcination.

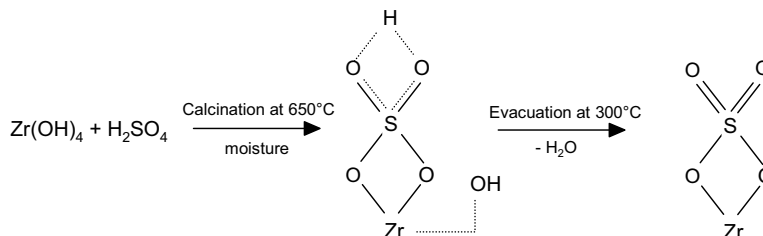


Figure 2.8 Structure of sulfated zirconia proposed by Kumbhar *et al.* [69]

Hino and Arata [33] found that the surface structure was sulfate (SO_4) combined with Zr elements in the bridging bidentate state. The Lewis acid site of Zr^{4+} becomes remarkably stronger by the inductive effect of $\text{S}=\text{O}$ in the complex (illustrated by the arrows in Figure 2.9). It appears that many of the structures used to explain the catalysis of sulfated zirconia are represented by the model of the active site shown in Figure 2.9.

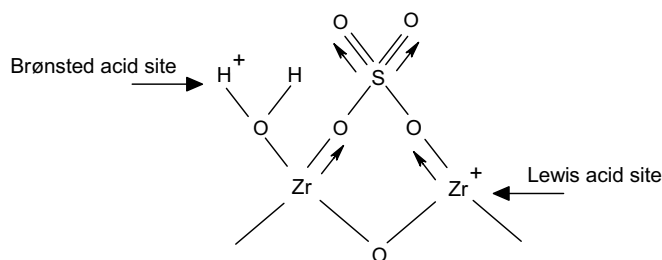


Figure 2.9 Hino and Arata's model for the active site of sulfated zirconia containing both Lewis and Brønsted acid sites [33].

It has been shown that if water molecules are present, the Lewis acid sites are converted to Brønsted acid sites [33]. And the other way; Brønsted sites are converted to Lewis sites if water molecules are removed as represented by Figure 2.10.

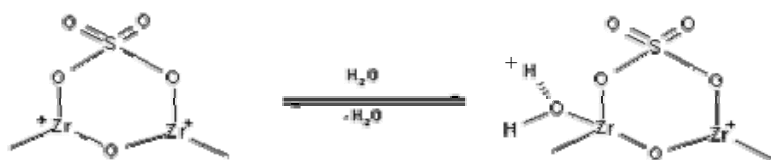


Figure 2.10 The model for the interconversion of Lewis acid sites to Brønsted acid sites [33, 70].

Davis and coworkers [32] proposed a model for what happens to the structure of sulfated zirconia upon heating to higher temperatures, which is common when the catalyst is pretreated before the reaction. The data suggested that sulfur was lost as the dried material is heated to higher temperatures [32]. The model of Davis, as shown in Figure 2.11, is based on Hino and Arata's model, but explains how surface sulfate is lost as SO_3 on heating above 923 K.

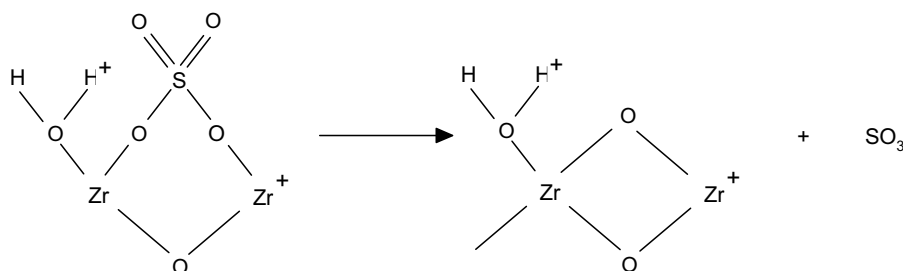


Figure 2.11 Model proposed by Davis *et al.* [32].

Kustov *et al.* [26] discovered that the acidic sites of the catalyst are formed when the terminal ZrOH groups are substituted by HSO_4^- ions. The protons of the Brønsted sites are hydrogen-bonded with neighboring basic oxygen atoms of the sulfate ions or with basic oxygen of the ZrO_2 support as shown in Figure 2.12.

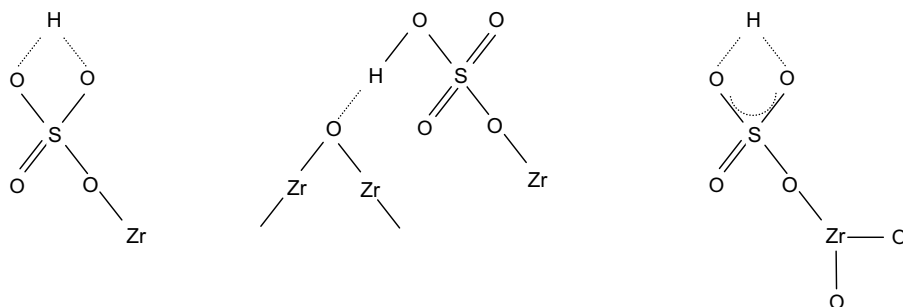


Figure 2.12 The three different models for the active site on sulfated zirconia proposed by Kustov *et al.* [26].

Most of the models that are proposed contain either Lewis or Brønsted sites, or in some cases both types of acid sites are proposed to exist on the catalyst surface, but separately. Adeeva *et al.* [16] suggested a model of a surface complex in which the Lewis and Brønsted acid sites are combined in close proximity. In this model (Figure 2.13) the OH group of the sulfate is hydrogen bonded to a surface oxygen of zirconia, in the same way as suggested in model from Kustov *et al.* [26].

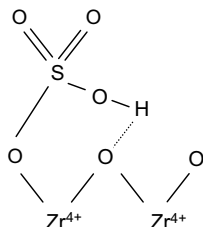


Figure 2.13 Model of the active site which combines Lewis and Brønsted sites in close proximity as suggested by Adeeva *et al.* [16].

2.6 Promoters

The promoters that will be described here are divided into two classes according to how their function is described in the literature. One class is iron and manganese and similar transition metals, these metals are by some authors claimed to increase the acid strength of the catalyst [13, 15]. Others focus on their ability to produce olefinic intermediates [16, 71-73]. Even if the way these promoters work is disputed, it is generally accepted that they increase the activity of sulfated zirconia. The other class of promoters is platinum and other noble metals. The function of these promoters is to inhibit deactivation of the catalyst during alkane isomerization [7]. Platinum is usually connected to its ability to increase the catalyst stability [56], but it is also found that platinum enhances the activity of by increasing the acidity of the catalyst [44].

2.6.1 Iron and manganese and similar transition metals

In their seminal work on this class of catalysts Hsu and co-workers [13, 14] found that by promoting sulfated zirconia with 1.5 wt% iron and 0.5 wt% manganese (FMSZ) the activity for *n*-butane isomerization at room temperature was increased by about three orders of magnitude. The combination of iron and manganese have been studied in great extent [13, 63, 72, 74-89], because of a possible synergetic effect between these two promoters. One such effect may be that manganese stabilizes the dispersion of iron, while iron enhances the catalytic activity of SZ [76].

Other transition metals have been found to promote the isomerization of alkanes. Lange *et al.* [71] found that effectiveness of metal promoters in *n*-butane isomerization at 373 K to be in the order Mn>Fe>Co>Zn, which means that the activity increases when moving to the left in the first row in the periodic table. This is apparently in disagreement with what was found by Vera *et al.* [90]. They found

the order to be $\text{Cr} \approx \text{Fe} < \text{Co} < \text{Ni}$, the activity decreases when moving from left to right in the periodic table. It should be noted that the reaction temperature is higher in the latter case, 473 K. The first row transition metals show qualitatively the same effect, but the mode of operation is however unknown [89].

Hsu and coworkers ascribed the increased activity to an increase in the acid strength of the catalysts [15]. Later other theories for the role of iron and manganese as promoters have been proposed. Adeeva *et al.* [16] reported that there was no difference in the acid strength of neither the Lewis nor Brønsted sites of FMSZ and SZ. They point out two other possibilities for the increased isomerization activity of FMSZ catalyst compared to their unpromoted counterparts. Greater stabilization of the highest transition state on FMSZ compared to on SZ is one of them. The second possibility is that the formation of olefinic intermediates is facilitated on FMSZ.

Yori and Parera [73] claim that the formation of alkenes is the rate determining step in the mechanism for *n*-butane isomerization. The transition metals or their oxides provide the dehydrogenating capacity that can produce C4 alkenes, and when the pool of alkenes is increased it will lead to an increase in the isomerization rate [73]. Tabora and Davis [72] and Lange *et al.* [71] supported that iron and manganese contribute in the formation of olefinic species on catalyst surface. They suggested however that alkenes are formed in a non-catalytic redox reaction rather than in a catalytic cycle, thus iron and manganese act as initiators. The long term activity is likely to be due to other sites in the surface [80].

Wan *et al.* [80] also claim that the role of iron and manganese is in the formation of alkenes, but that it happens in a catalytic cycle rather than single turnover reaction. They propose that the acid and metal sites exist in close proximity, and that the combination of those sites contributes to a bifunctional mechanism.

In addition to the role of iron and manganese in the formation of hydrogen deficient intermediates, it has been emphasized that the metal promoters also enhance the stability of these intermediates [81, 91].

Most studies on FMSZ catalysts are performed at low temperatures, from 35 to 100°C. In this temperature range iron and manganese promoted SZ are shown to have a remarkably high activity for isomerization of alkanes compared to unpromoted SZ [13, 71, 81]. At higher temperatures the situation is different. Gao and coworkers [92] reported that the initial activity of FMSZ was 67% of the activity of the unpromoted SZ at 250°C. They reported that the activity of a FMSZ catalyst (1.5 wt% Fe, 0.5 wt% Mn) was 2-3 times higher than the activity of unpromoted and aluminum promoted SZ at 35°C. At 250°C, however, they find that the FMSZ catalyst is less active than unpromoted SZ and exhibits a much poorer stability than both aluminum promoted and unpromoted SZ. The promotion effect of iron and manganese is according to Morterra *et al.* [86] due to a redox process that triggers

the acid catalyzed reaction at much lower temperatures than on unpromoted SZ. It is likely that the iron and manganese additives still play a catalytic role at higher temperatures (150°C), but that they under these conditions acts against the isomerization mechanism. This might be the accumulation of olefinic intermediates that eventually leads to the formation of oligomers capable of poisoning the active sites.

2.6.2 Platinum and other noble metals

Platinum is the metal that is most widely studied as a promoter for sulfated zirconia. Although it has been done extensive research on the PtSZ system there is no consensus on neither the role of platinum nor the state of platinum on the catalyst surface.

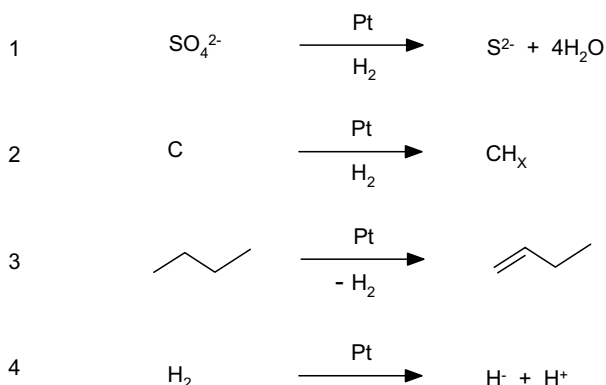
The role of platinum

According to the classical bifunctional mechanism the role of platinum is to produce olefins which in the case of *n*-butane isomerization react with a carbenium ion to form the C8 intermediate. In the case of isomerization of C5+ alkanes the olefin is protonated, and the formed carbenium ion is then isomerized via the monomolecular mechanism to give the branched isomer.

Addition of platinum has been reported to increase the stability of SZ catalysts [8]. Laizet *et al.* [4] explained the stabilizing effect of platinum by its ability to limit coke formation. Hydrogen can dissociate on platinum sites and spill over to the SZ surface to hydrogenolyze carbonaceous residue and its precursors [53, 55]. In that way the effect of hydrogen is related to the clean-up of the catalyst surface, and one can expect a positive order of hydrogen. Manoli *et al.* [60] claims on the other hand that the hydrogenolyzing activity of platinum is too low to be important in removing coke from the catalyst surface.

Ebitani and coworkers [44] found that platinum besides enhancing the stability of the catalyst also increases its activity. They suggested that hydrogen dissociates on platinum sites and spill over to the SZ surface to generate acid sites, this was supported by the findings of Falco *et al.* [93] in the case of platinum promoted WO_x/ZrO_2 . It has been found that platinum was not only important in the generation of acid sites, but also provides hydride ions that eliminates ionic intermediates from the surface before β -scission occurs, thus cracking and polymerization reactions are avoided and the isomerization selectivity is increased [10, 56, 93].

The role of platinum on SZ can be summarized by the following four reactions:



Reaction 1 is the reduction of sulfate groups which can lead to masking of the sulfate groups and must be avoided [53]. Reaction 2 is the hydrogenation of coke precursors and this reaction will benefit from an increase in the hydrogen pressure. Reaction 3 is the dehydrogenation of alkanes important in the formation of hydrogen deficient intermediates. This reaction implies a negative kinetic order of hydrogen. Reaction 4 is the hydrogen spillover reaction forming protons which can increase the acidity of the sample or hydrides that eliminates ionic intermediates from the catalyst surface, this implies a positive order of hydrogen.

The state of platinum

Another matter of controversy is the state of platinum. There are three main possibilities on the surface of sulfated zirconia; it can exist as metallic platinum (Pt^0), in the sulfided state or in the oxidized state.

Ebitani *et al.* found that platinum on SZ can dissociate H_2 but can scarcely chemisorb hydrogen [94]. They propose on the basis of XPS data that the unique properties of PtSZ catalysts originate from the fact that a large fraction of the platinum remains in the state of the cation in form of PtO_x and PtS , and the metallic fraction is low [94, 95]. These findings are supported by Comelli and coworkers [96], who found that the *n*-hexane isomerization activity does not depend on if PtSZ is reduced or not. They also observed that hydrogen did not chemisorb on neither the reduced sample nor the unreduced sample, in addition they did not observe the characteristic peak of platinum reduction. These results can be explained by that platinum is covered by sulfur, which is suggested by XPS analysis.

Paál *et al.* on the other hand found no signs of PtS particles on the SZ surface [60, 97]. Their results correspond to that platinum is in the metallic state surrounded by an adsorbed overlayer and that the platinum particles exhibited rather Pt-O than Pt-S interactions [60]. This is quite similar to the XANES/EXAFS data from Shishido *et al.* [98] which suggest that platinum exists as oxidized platinum particles with a metallic core.

Sayari and Dicko found by XPS, XRD and TPR that platinum on PtSZ upon calcination at high temperatures (600°C) was reduced to its metallic state. They proposed that SO₂ produced by decomposition of sulfate ions reduces Pt.

Other noble metals

Other noble metals than platinum have not been widely studied as promoters for SZ catalysts. Hino and Arata [9] tested the *n*-butane isomerization activity of SZ with Ir, Pt, Rh, Ru, Os, and Pd as promoters. Their activities, in decreasing order, were found to be Ir, Pt > Rh > Ru > Os > Pd > unpromoted. The product selectivities were quite similar to those when the isomerization reaction is catalyzed by superacids.

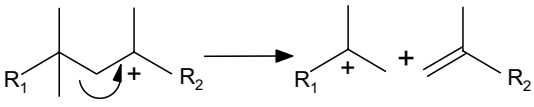
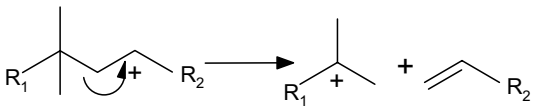
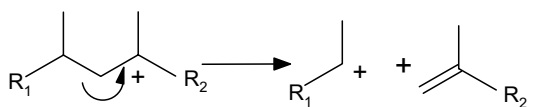
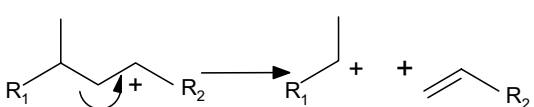
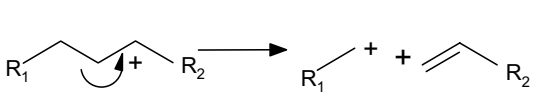
Palladium was tested as a promoter by Larsen *et al.* [99]. PdSZ had a lower *n*-butane isomerization activity than unpromoted SZ, and the Pd function cannot stabilize the reaction at low H₂/*n*C₄ ratios.

Isomerization reactions of *n*-heptane, *n*-octane and *n*-nonane were studied over PtSZ, PdSZ and IrSZ catalysts [11]. The isomer selectivity decreases in the order Pt > Pd > Ir. This effect is explained by their difference in electron withdrawing efficiency.

2.7 Cracking

Isomerization of *n*-alkanes over acid and bifunctional catalysts is often followed by cracking. The breaking of C-C bonds in carbenium ions will happen to the bond in β-position to the positively charged carbon atom, this mechanism is known as β-scission. Weitkamp and coworkers [100] classified the principal modes of β-scission. The classification is based on the type of carbenium ion which is cracked and the type of carbenium ion formed, e.g. type D is the transformation from a secondary to a primary carbenium ion. The rate constants decrease from type A to type D β-scission.

Table 2.1 The modes of β -scission of alkylcarbenium ions [100].

Type of cracking	Minimum number of C atoms	Example
A	8	tert. \rightarrow tert. 
B1	7	sec. \rightarrow tert. 
B2	7	tert. \rightarrow sec. 
C	6	sec. \rightarrow sec. 
D	4	sec. \rightarrow prim. 

It should be noted that cracking of type D is impossible since it involves the formation of a thermodynamically unstable primary carbenium ion. The direct cracking of *n*-hexane will therefore not occur, but hexane will crack consecutively to the isomerization in a type C β -scission reaction.

The results of Comelli *et al.* [55] suggest that the cracking products are formed through polymeric intermediates. Comelli *et al.* observe that isomerization of *n*-hexane over PtSZ is always accompanied by hydrocracking, hydrogenolysis products on the other hand are not observed.

2.8 Deactivation

Sulfated zirconia is a very active catalyst for the isomerization of alkanes, unfortunately the catalyst deactivates rapidly. There are several possible mechanisms for deactivation of SZ catalysts. One of the most commonly suggested causes is the formation of coke or oligomers at the active sites [8, 64, 101-104]. The rate of deactivation has been found to be related to the concentration of alkenes, which are known to be coke precursors, in the feed [62]. The activity of SZ, and FMSZ catalysts in particular,

is reported to be connected to their ability to produce hydrogen deficient intermediates, thus the catalytic activity of the catalyst is coupled to the rate of deactivation [17]. Föttinger [102] and Gonzalez [104] found that the activity could be completely restored by burning of the coke at 450-500°C. Since the activity can be restored, Gonzalez and Li [104] ruled out sulfur loss as a cause for deactivation, though sulfur reduction cannot be excluded. Buchholz *et al.* [101] on the other hand found that sulfated zirconia could only be partly regenerated in air. They ascribed the reversible part of the deactivation to carbon formation and the irreversible deactivation to loss of sulfur from the surface.

On the basis of XPS spectra of the catalyst before and after deactivation Resofszki *et al.* [105] rule out carbon deposition as the reason for deactivation, instead they point out the reduction of S^{6+} to S^{4+} as reason to deactivation, this was previously suggested by Ng and Horvát and Yori *et al.* [106, 107]. Yori *et al.* [107] found that when the sulfur was reoxidized, producing again the sulfate ion, it led to recovery of the catalytic activity. Ng and Horvát [106] claimed that sulfur loss in the form of H_2S was a mechanism of deactivation in addition to reduction of the surface sulfate. Sulfur can also be lost by migration from the surface to the bulk of the zirconia [18].

Li and Stair [108] observed by UV Raman spectroscopy that the surface phase of sulfated zirconia changed during the deactivation process, from the tetragonal phase of the fresh catalyst to the monoclinic phase of the deactivated sample. The bulk phase maintains the tetragonal phase before and after the reaction test. After oxidizing the sample at 500°C for 2 hours the Raman spectra showed that the tetragonal surface phase was recovered.

Another possible mechanism for deactivation of promoted catalysts is the loss of the promoters. Paál and coworkers [109] claimed deactivation can be due to the combination of the recrystallization of the zirconia phase, the loss of surface OH and disappearance of platinum when it is partially 'buried' under zirconia layers. This will lead to the disruption of the most active metal-acid ensembles, i.e. the proposed "compressed bifunctional site" [60]. By blocking the rapid hydrogen transfer from Pt and sulfate sites, another non-acidic reaction initiation route is opened, involving oxidation of the reactant and reduction of S^{6+} entities to S^{4+} .

3 Experimental methods

3.1 Catalyst Preparation

3.1.1 Preparation of iron and manganese promoted sulfated zirconia

These materials were prepared according to the two-step precipitation method as described in chapter 2.4. The level of the preparation parameters, such as pH, molarity of sulfuric acid and drying temperature were mainly chosen according to Comelli *et al.* [96], though some of the parameters were adapted to the procedure given by Arata [110].

40 g of zirconyl (IV) chloride octahydrate ($ZrOCl_2 \cdot 8H_2O$, 98+%, Acros) was dissolved in 500 ml distilled water.

Ammonium hydroxide ($NH_3(aq)$ 25%, Merck) was added dropwise into the aqueous solution with stirring until the solution reached a pH value of 10. Precipitation of zirconium hydroxide is observed immediately after addition of ammonium hydroxide.

The precipitated hydroxide was aged at room temperature for 20 hours and then filtrated and washed with distilled water (4.5 liters) until no chloride ions could be detected in the wash water. (Test: Addition of $AgNO_3$ to a sample of wash water. Precipitation of a white solid ($AgCl$) indicates presence of chloride ions → further washing is needed.)

The filtrate was dried at 100°C for 24 hours, then crushed and sieved to a fraction smaller than 125 μm .

Addition of metal promoters and sulfur

The total content of metal promoter was always kept at 2 wt%. Nitrates of manganese ($Mn(NO_3)_2 \cdot 4H_2O$, 98%, Fluka AG) and iron ($Fe(NO_3)_3 \cdot 9H_2O$, 99%, Fluka AG) was used as agents for the promoters.

The desired amount of the metal nitrate was dissolved in distilled water (2.1 ml distilled water/ gram hydroxide).

The solution of metal nitrates was added to the zirconium hydroxide, then stirred for 10 minutes and the liquid was finally evaporated at 100°C for 18 hours.

The next step was addition of sulfuric acid. Sulfuric acid was added do the dried sample of promoted zirconium hydroxide (0.5M H_2SO_4 ; 2.1 ml per gram of hydroxide). The solution was stirred for five

minutes and then aged for one hour. The liquid was decanted and the solid was dried at 100°C for 24 hours. The dried solid was crushed and sieved to a fraction smaller than 125 µm.

Finally the dried zirconium hydroxide was calcined at 600°C for 3 hours in flowing air (600 Nml/minute). The heating rate was set to 6°C/minute.

3.1.2 Noble metal promoted sulfated zirconia

A series of noble metal promoted sulfated zirconia samples were prepared by the two-step precipitation method as described in chapter 2.4. The platinum content was chosen to be 0.75 wt%, as this was shown to be sufficient to prevent catalyst deactivation under hydroisomerization [9], and a further increase in platinum content does not give an increase in the catalytic activity [20, 111]. The molar concentrations of the other promoters were chosen to be equivalent to that of platinum.

100 g of $ZrOCl_2 \cdot 8H_2O$ (98+ %, Acros) was dissolved in 1000 ml of distilled water. Then 17.5 ml of ammonium hydroxide (NH_3 (aq), 25%, Merck) was added to the solution rapidly. Zirconium hydroxide precipitated immediately. The pH of the solution was measured to be 10 after precipitation.

The precipitate and solution were stirred for 2 hours. The precipitate was filtrated and then washed with 9 liters of distilled water (Chloride ions were not detected in the filtrate after washing with 8 liters). The solid particles were dried at 100°C overnight.

384 ml 0.3N H_2SO_4 was added to the dried hydroxide (76.55 dried hydroxide, 5 ml acid/g of solid), and stirred for 1 hour. The solution was filtrated, and the sulfated solids were dried at 100°C overnight.

The dried sulfated hydroxide was calcined with flowing air (300 Nml /min) at 600°C for 3 hours (Figure 3.1).

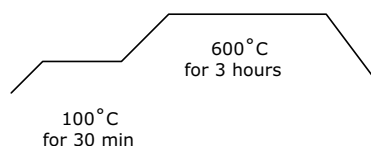


Figure 3.1 Temperature program during the calcination of the sulfated hydroxide

37 grams of sulfated zirconia were obtained, and divided into seven equally sized parts (5.3 g). Five of these were impregnated with various noble metals, one was not promoted and one part was kept uncalcined for reference.

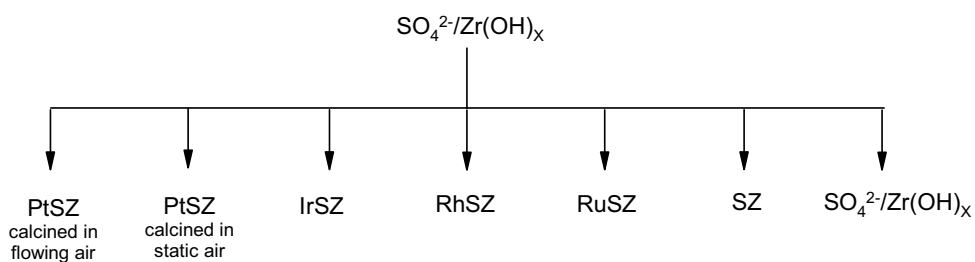


Figure 3.2 The noble metal promoted sulfated zirconia samples.

PtSZ calcined in static air and the $\text{SO}_4^{2-}/\text{Zr}(\text{OH})_x$ are not discussed further in this work.

Addition of promoter

The noble metal salt was dissolved in distilled water. The solution was added to 5.30 g of the sulfated zirconia by the incipient wetness technique. The amounts used of the various metal salts are shown in Table 3.1. The solid was dried overnight at 100°C.

Table 3.1 Metal content in the noble metal promoted sulfated zirconia samples

Promoter	Pt	Ir	Rh	Ru
Source	$\text{H}_2\text{PtCl}_6 \cdot 6\text{H}_2\text{O}$	$\text{H}_2\text{IrCl}_6 \cdot 6\text{H}_2\text{O}$	$\text{Rh}(\text{NO}_3)_3 \cdot 2\text{H}_2\text{O}$	RuCl_3
Supplier	Johnson Matthey	Johnson Matthey	Johnson Matthey	Johnson Matthey
Weight per gram SZ [mg]	21.5	20.6	8.4	8.3
Metal content [wt%]	0.75	0.75	0.41	0.40
Metal content [$\mu\text{mol/g}$ SZ]	40	40	40	40

The dried solid is calcined with flowing air (300 Nml /min) at 450°C for 3 hours (Figure 3.3). The unpromoted sample was 'impregnated' with distilled water and calcined the same way as the promoted samples to get the history of the samples as identical as possible.

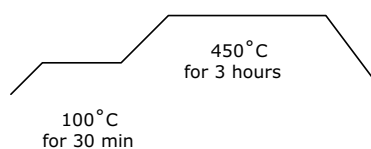


Figure 3.3 Temperature program during the calcination of the promoted sulfated zirconia

3.1.3 Preparation of tungsten oxide modified zirconia

The platinum promoted tungsten oxide modified zirconia catalyst was prepared according to synthesis routes described by De Rossi and co-workers [112], though there are some modifications to the procedure [113, 114].

20 g of $\text{ZrO}(\text{NO}_3)_2 \cdot x\text{H}_2\text{O}$ (Fluka) was dissolved in 200 ml of distilled water. Then 14 ml of ammonium hydroxide (NH_3 (aq), 20%, Prolabo) was added to the solution rapidly. Zirconium hydroxide precipitated immediately. The pH of the solution was in the range 9-10 after precipitation.

The mixture of precipitate and liquid solution was stirred for 1 hour. The precipitate was filtrated and then washed with 800 ml of distilled water. The solid particles were dried at 100°C overnight.

The dried hydroxide was crushed with a mortar and pestle and then calcined at 300°C for 3 hours (Air, 166 Nml/min) according to the procedure given by Arata and Hino [113]. The calcined material was then impregnated with ammonium metatungstate (AMT, $(\text{NH}_4)_{10}\text{W}_{12}\text{O}_{41} \cdot 5\text{H}_2\text{O}$). To 4 grams of ZrO_2 it was added 0.91g AMT dissolved in 2.6 ml of distilled water. The impregnated zirconium hydroxide was dried at 100°C over night. The material is finally calcined at 800°C for 3 hours (air, 166 Nml/min).

Impregnation of platinum

To obtain a material containing 1 wt% platinum 0.041 g $\text{H}_2\text{PtCl}_6 \cdot 6\text{H}_2\text{O}$ (Interchim) dissolved in 1.2 ml distilled water was added to 2.3 gram of the final $\text{WO}_x\text{-ZrO}_2$ by the incipient wetness technique.

The impregnated material was dried overnight at 100°C before calcination at 500°C for 3 hours (Air 77 Nml/min).

3.2 Catalyst Characterization

3.2.1 Acidity

FT-IR measurements were carried out with a Nicolet Magna IR 550 (resolution 2 cm^{-1}) in the transmission mode on thin wafers ($12\text{-}16\text{ mg/cm}^3$) prepared under 4 MPa pressure and activated in situ in the IR cell. The activation conditions were as following: in flowing dry air (60 ml min^{-1}) at 450°C for 3 h and then in vacuum (10^{-3} Pa) at 300°C for 1 h. Pyridine was introduced at 1 to 2 torr pressure at 150°C for 15 minutes, then outgassed at the same temperature for 1 h. The IR spectra were carried out at room temperature after (i) the activation period and (ii) pyridine thermodesorption in vacuum ($10^{-1}\text{ Pa} - 1\text{ h}$) at increasing temperatures: 150, 250, 350 and 450°C . The area of the bands corresponding to the Brønsted- and the Lewis-acid sites were measured by integration. The procedure is adapted from Tran *et al.* [30].

3.2.2 X-ray diffraction

The crystallinity of the samples was characterized by powder X-ray diffraction (XRD). The XRD spectra were obtained by a Siemens D5005 X-ray diffractometer with Cu K α radiation, scanned at a rate of 2° min⁻¹.

3.2.3 Surface area and pore size distribution

Nitrogen adsorption-desorption isotherms were measured using a Micromeritics TriStar 3000 instrument, and the data were collected at the nitrogen liquid temperature, 77 K. All samples were outgassed at 473 K overnight prior to measurement. The surface area was calculated from the Brunauer-Emmett-Teller (BET) equation while the total pore volume and the pore size distribution were calculated from the nitrogen desorption branch applying the Barrett-Joyner-Halenda (BJH) method.

3.2.4 Thermogravimetric analysis

Thermogravimetric Analysis (TGA) of the catalyst samples was performed with a Perkin Elmer TGA7 Thermogravimetric analyzer. The experiments were performed at a heating rate of 20°C/min from 50°C to 900°C in a nitrogen stream (80 Nml/min).

3.2.5 Temperature programmed reduction

Temperature Programmed Reduction (TPR) is an experimentally simple technique that indicates the reducibility of a material. The TPR apparatus is described in detail elsewhere [115].

The experiments were performed at a heating rate of 10°C/min from 25°C to 900°C with 7 % hydrogen in argon. The hydrogen consumption was measured by a Shimadzu GC-8A gas chromatograph equipped with thermal conductivity detector (TCD).

3.2.6 Sulfur content

The total sulfur content of some of the samples was analyzed by the LECO combustion method by NGU (The Geological Survey of Norway). The sample is inserted in an oven in oxygen atmosphere at 1375°C. Sulfur is oxidized to SO₂ which is detected with IR cells.

3.3 Catalytic Tests

The catalytic testing of the samples is divided in two parts. Isomerization of *n*-butane under atmospheric pressure was used mainly as test reaction for screening of isomerization catalyst, and to compare the catalytic activity with the acidity of the samples. The other part is the investigation of various kinetic parameters and comparison of the catalytic activity of the series of SZ samples for *n*-hexane isomerization at elevated pressures.

3.3.1 *n*-Butane isomerization

The catalytic isomerization of *n*-butane was performed in a fixed bed quartz reactor operated at a low conversion. Prior to the reaction the catalyst was pretreated in situ with flowing air at 450°C for 3 hours before cooling down to reaction temperature. The product was analyzed on line by a Varian 3400 GC equipped with a Valco multiposition valve (10 positions) and a flame ionization detector. The experimental set-up is shown in Figure 3.4.

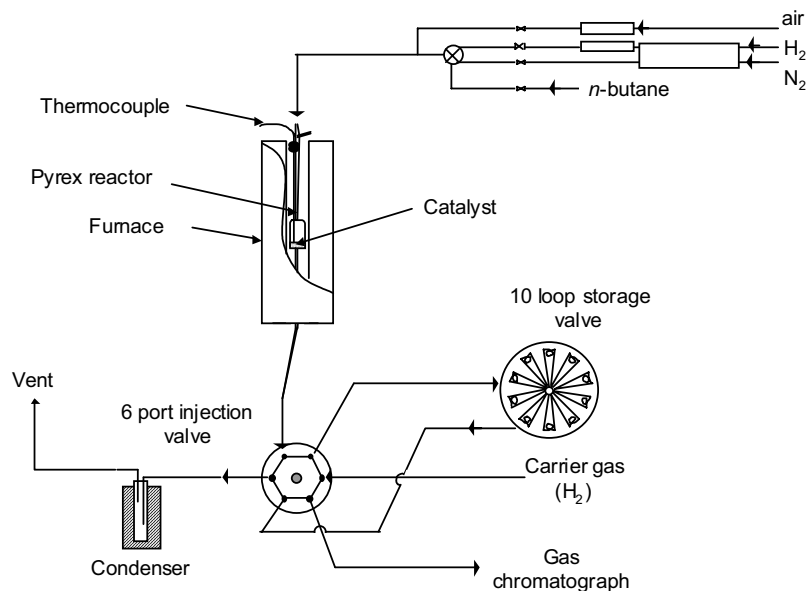


Figure 3.4 Experimental set-up for isomerization of *n*-butane under atmospheric pressure

The catalyst particles ($160 < d < 400 \mu\text{m}$) was placed in a pyrex reactor (Height 4 cm, diameter 1.5 cm). The thermocouple was placed in the middle of the catalyst bed

Standard procedure for *n*-butane isomerization tests:

Catalyst weight: 300 mg

Pretreatment: Air (60mL/min) at 450°C for 3 hours

diluent/*n*-butane ratio = 9

Diluent was either hydrogen or nitrogen

Reaction temperature: 250°C

Atmospheric pressure

Samples taken at 1 min, 1 min 15 seconds, 1 min 30 seconds, 2 min, 5 min, 10 min, 25 min, 40 min, 60 min

3.3.2 *n*-Hexane isomerization

Preliminary experiments

Some preliminary experiments for *n*-hexane isomerization were performed at the University of Poitiers, France. The experimental set-up is described in detail by Bichon [116].

The reactor is a tube of stainless steel with the following characteristics:

- length: 40 cm
- outer diameter: 1.7 cm
- inner diameter: 1.3 cm

Standard conditions during a catalytic test:

- Pretreatment: N₂ or H₂ (60 mL/min) at 450°C for 2 hours
- Total pressure: 30 bar
- H₂/*n*-hexane ratio = 9
- Reaction temperature: 250°C
- Catalyst weight: 0.500 g
- WHSV: 2.25 – 13 h⁻¹
- Catalyst particles: 160<d<400 μm
- Between catalytic tests (overnight) the catalyst was kept in the reactor under hydrogen flow (60 mL/min) at 30 bar.

The liquid (*n*-hexane) was fed by a HPLC pump (Gilson Model 307) and the hydrogen was metered using a mass flow controller (BROOKS 5850TR).

The composition of product stream was analyzed on line with a gas chromatograph (Varian 3400) equipped with a flame ionization detector and a DB-1 column (J&W Scientific L=60m, diameter=0,25 μm, film thickness: 1μm)

n-Hexane isomerization –Catalytic test and kinetic study

The isomerization of *n*-hexane at elevated pressures over noble metal promoted catalysts was performed at NTNU in Trondheim. The experimental set-up is shown in Figure 3.7.

The reaction was performed in steel tube reactor with an inner diameter of 9.4 mm. The reactor was placed in an electric furnace, and controlled using an internal thermocouple (K-type). There was one bypass line in parallel with the reactor.

n-Hexane was fed from cylinders (shown in Figure 3.5) pressurized with nitrogen. The flow of *n*-hexane was controlled by a liquid flow controller (Bronkhorst Model L1C2-FAC-22-P). The *n*-hexane

was fed into the hydrogen stream and evaporated in the preheater which had a temperature around 220°C before the reactor inlet.

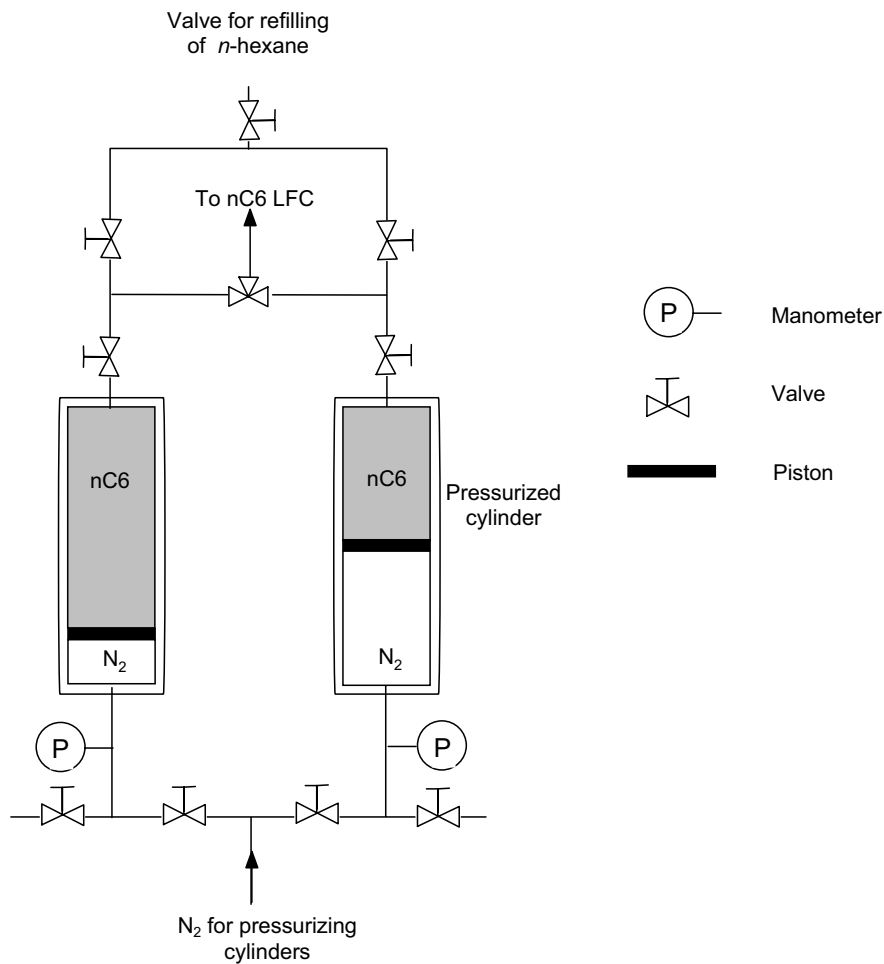


Figure 3.5 *n*-hexane feed system. The cylinders are pressurized by N₂.

The gases (helium, hydrogen and air) were fed using electronic mass flow controllers (Bronkhorst EI-Flow).

The pressure in the reactor is controlled by a back-pressure regulator (Tescom Model 26-1766-24).

The catalyst bed was placed in the middle of the steel tube as shown in Figure 3.6.

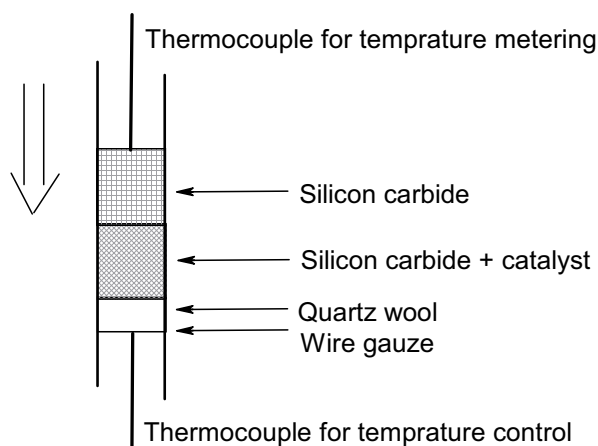


Figure 3.6 Cross-section of the catalyst bed for *n*-hexane isomerization

The catalysts were pretreated in either a hydrogen or helium flow at atmospheric pressure. The samples of SZ were heated at rate of 3°C/min up to 300°C and kept at this temperature for 3 hours, before cooling down to reaction temperature.

Typical reaction conditions during the catalytic test were:

- Pretreatment: He or H₂ (440 Nml/g.cat) at 300°C for 3 hours
- Total pressure: 5-30 bar
- Diluting gas: Hydrogen
- Standard H₂/*n*-hexane ratio = 9
- Reaction temperature: 180 - 250°C
- Catalyst weight: 0.100 - 0.500 g
- Catalyst particle size: 90<d<180 μm
- SiC/catalyst = 3 (mass ratio)
- WHSV: 12 – 90 h⁻¹

- between catalytic tests (overnight) the catalyst was kept in the reactor under hydrogen flow (66 Nml/min) at 30 bar.

The composition of product stream was analyzed on line with a gas chromatograph (HP 5890 series II) equipped with a flame ionization detector and HP Pona column (L=50m, diameter=0,20 mm, film thickness: 0.5 μm). The column was kept at isothermal conditions, 35°C.

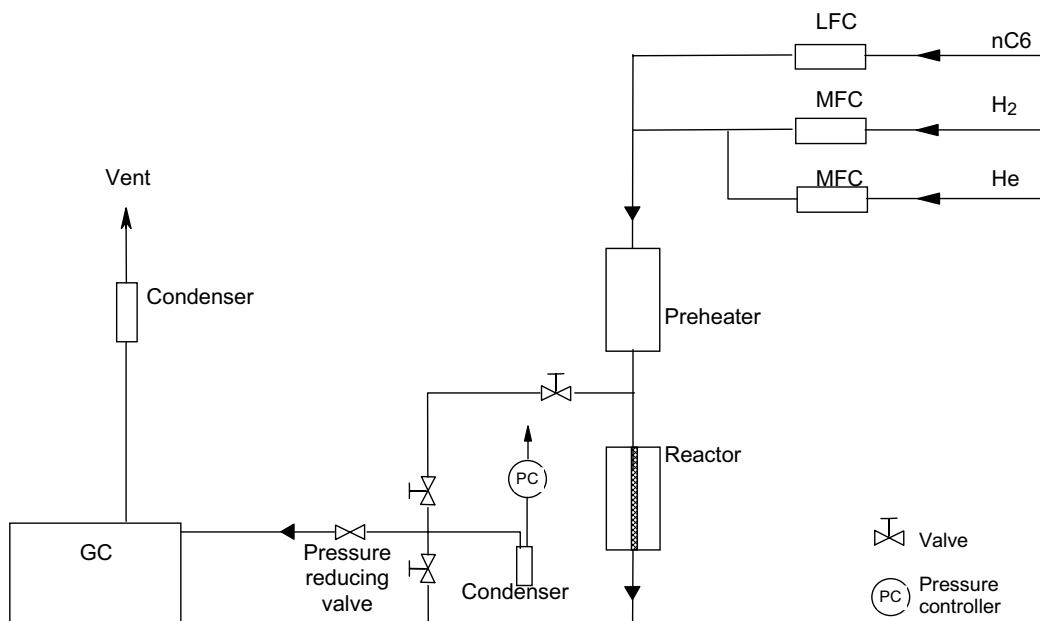


Figure 3.7 Experimental set-up used for *n*-hexane isomerization at NTNU

Procedure

The catalyst was mixed with silicon carbide particles with the same size as the catalyst ($90 < d < 180 \mu\text{m}$) and put on top of a quartz wool plug. Another layer of coarser silicon carbide particles were put on top of the catalyst layer.

The next step was to leak test the reactor system by pressurizing the system with the pre-treatment gas, i.e. hydrogen or helium.

The catalyst was heated in the flow of the pretreating gas ($440 \text{ Nm}^3/\text{g cat}$) at rate of $3^\circ\text{C}/\text{minute}$ up to 300°C . The temperature was held at 300°C for 3 hours before cooling down to standard reaction temperature, 200°C .

The activation energy was determined by changing the reaction temperature while keeping the other parameters at the standard conditions. The WHSV was however adjusted to give comparable conversion at the different temperatures, and to make sure that the conversion was within the limits of differential conditions.

When examining the effect of the total pressure on the catalytic activity, all parameters were set to the standard conditions, and only the total pressure is varied.

During the examinations of the effect of the hydrogen partial pressure the WHSV and the partial pressure of *n*-hexane were kept constant, while the hydrogen/*n*-hexane ratio and total pressure were changed. When examining the effect of the *n*-hexane partial pressure the hydrogen partial pressure was kept constant, while the hydrogen/*n*-hexane ratio and total pressure were varied. In the latter case the WHSV was adjusted to give almost equal conversion for all P_{nC6} .

3.4 Calculation of Activity and Selectivities

The conversion of *n*-hexane (in %) is calculated by equation (3.1):

$$X = 100 \frac{(F_{nC6, in} - F_{nC6, out})}{F_{nC6, in}} = 100 \left(1 - \frac{F_{nC6, out}}{F_{nC6, in}} \right) \quad (3.1)$$

In equation (3.1) F_{nC6} is corresponding to the molar flow of *n*-hexane.

When calculating the activity (i.e. the reaction rate, $-r_{nC6}$) of the catalyst it is assumed that the reaction is operated at differential conditions. Thus the reactor approximates an ideal CSTR, and equation (3.2) give the reaction rate [117]:

$$-r_{nC6} = \frac{F_{nC6} X}{W} = \text{WHSV} \cdot X \quad (3.2)$$

In equation (3.2) W is corresponding to catalyst weight.

The selectivities (S) of the component i were calculated using equation (3.3):

$$S_i = \frac{a_i / 6 (F_{i, out} - F_{i, in})}{F_{nC6, in} \cdot X} \quad (3.3)$$

a_i corresponds to number of carbon atoms in component i and F_i corresponds to the molar flow of component i .

4 Results

This chapter is divided in two main parts. The first part treats the experimental data regarding the isomerization of *n*-butane at atmospheric pressure, and includes the data from the catalyst characterization as well as the catalytic testing. The second part deals with the kinetic investigation of *n*-hexane isomerization over various acid catalysts at elevated pressure and the physical and chemical characterization of these catalysts.

4.1 Isomerization of *n*-butane at atmospheric pressure

The isomerization of *n*-butane was carried out at atmospheric pressure in a fixed bed quartz reactor. A series of five iron and manganese promoted samples, referred to as FMSZ, were the catalyst of main interest for these experiments. The total content of promoters is always 2 wt%, e.g. a sample which contains 0.5 wt% manganese contains 1.5 wt% of iron. The catalyst are termed according to their composition where (1.5)F(0.5)MSZ describes the catalyst with 1.5 wt% iron and 0.5 wt% manganese, and SZ is the unpromoted sample. Some samples of tungsten oxide modified zirconia were tested as well to give an indication of their activity for alkane isomerization, and the results for these catalysts are shown at the end of this chapter.

4.1.1 Characterization of the iron and manganese promoted samples

The catalyst samples have been characterized by various techniques as described in chapter 3. The results from the physical and chemical characterization of the iron and manganese promoted SZ samples are given in Table 4.1, while the results from the acidity characterization are given separately in Table 4.2

Table 4.1 Physical and chemical properties of the iron and manganese promoted SZ samples.

Sample	BET surface area [m ² /g]	Sulfur content [wt%]	Crystalline phase	T _d [°C]*
(1.0)F(1.0)MSZ	101	2.62	Tetragonal	820
(1.5)F(0.5)MSZ	127	2.55	Tetragonal	666 and 813
(2.0)FSZ	90	2.05	Tetragonal	684 and 831
(2.0)MSZ	106	1.91	Tetragonal	813
SZ	93	2.01	Tetragonal	673 and 820

* T_d corresponds to the decomposition temperature for sulfate in the thermogravimetric analysis.

From X-ray diffraction it was found that the samples were exclusively in the tetragonal phase, the details for the X-ray diffractograms are shown in Appendix 1. The derivative of the weight loss as a

function of temperature is shown in Figure 4.1. The TGA data show at which temperatures the sulfate groups are decomposed. All the samples lose sulfate in the range 813-831°C, while only (1.5)F(0.5)MSZ, (2.0)FSZ and unpromoted SZ also lose sulfur in the low temperature range 666-684°C.

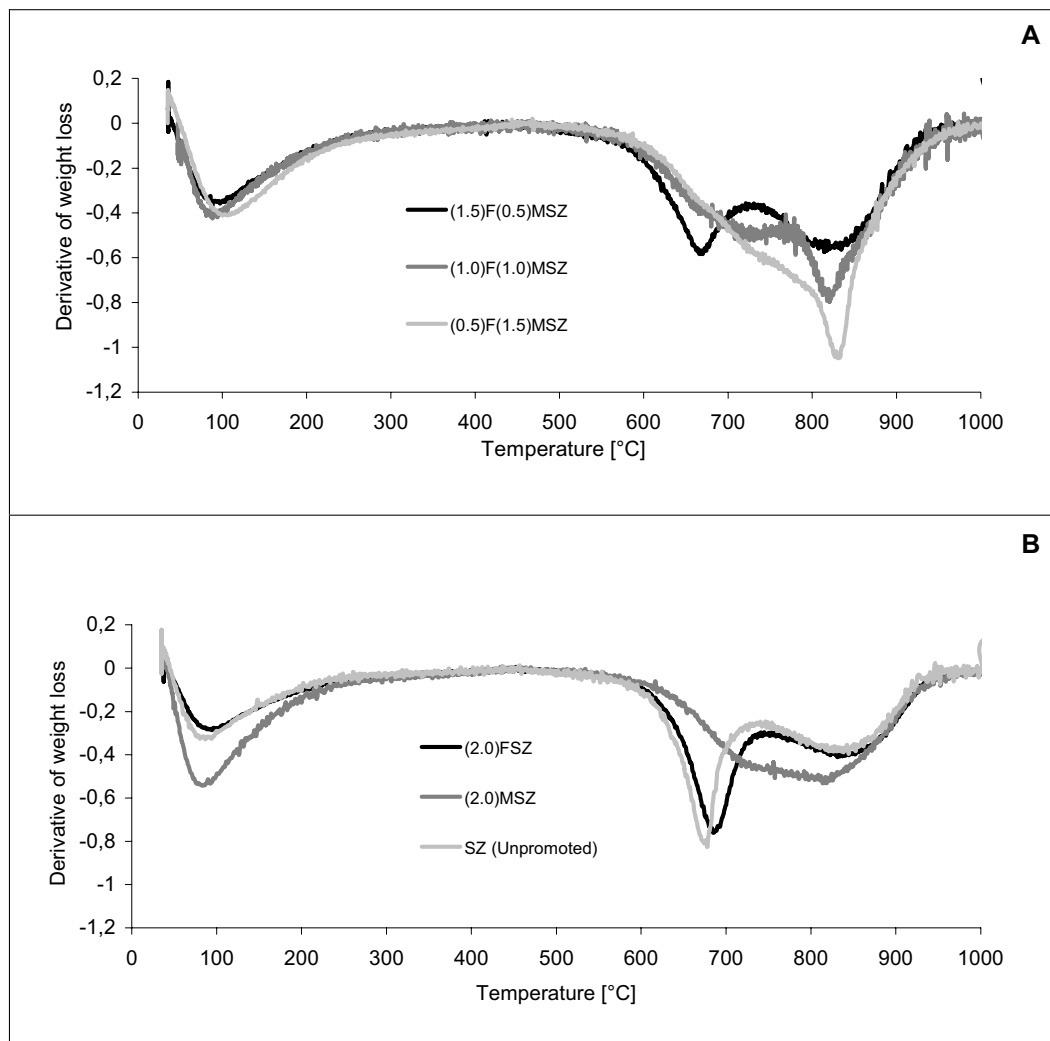


Figure 4.1 The derivative of the weight loss during thermogravimetric analysis.

The type and the strength of the acid sites were determined by FTIR spectroscopy of adsorbed pyridine, and the results are given in Table 4.2. In this work we have found it appropriate to differentiate between strong and weak sites in the following way; the sites that are able to retain pyridine after evacuation at 350°C or higher temperatures are referred to as *strong sites*. The acid sites that retain pyridine at 150°C are the sum of both weak and strong acid sites, and are thus referred to as either *All Brønsted acid sites* or *All Lewis acid sites*. The sum of the Brønsted and Lewis acid sites are called *Total acid sites*.

The concentration of Brønsted and Lewis acid sites were estimated from the intensities of the pyridinium band at 1544 cm^{-1} and of the band corresponding to coordinated pyridine at 1447 cm^{-1} , respectively, using the extinction coefficients $1.13\text{ cm}^2/\mu\text{mol}$ for Brønsted band and $1.28\text{ cm}^2/\text{mol}$ for the Lewis band [30]. In Figure 4.2 the IR spectrum for (1.5)F(0.5)MSZ is given, the intensities of the Brønsted and Lewis bands are decreasing with increasing desorption temperature, and they disappear completely at 450°C . The number of acid sites at each desorption temperature are summarized in Table 4.2

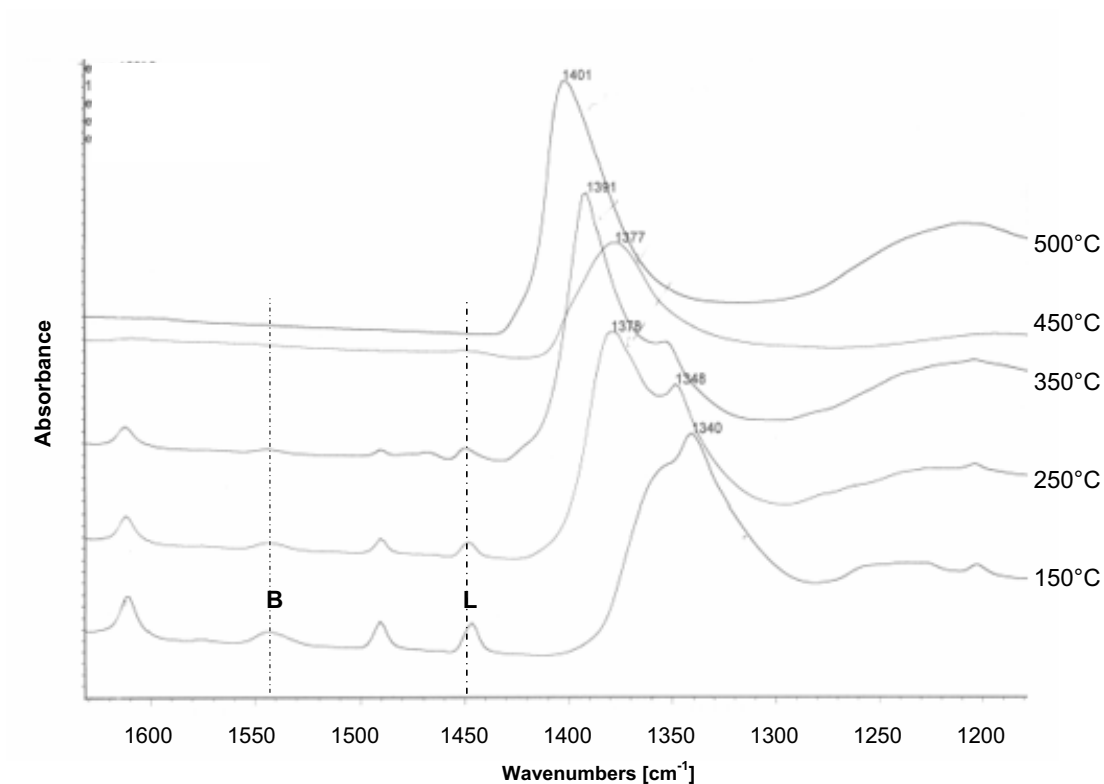


Figure 4.2 Example of IR spectra. Catalyst: (1.5)F(0.5)MSZ. Brønsted sites (B) at 1544 cm^{-1} and Lewis sites (L) at 1447 cm^{-1} . Each curve corresponds to the sample after desorption at a temperature, which is indicated on the right side of the figure. The large band in the region $1425\text{--}1325\text{ cm}^{-1}$ corresponds to S=O.

Table 4.2 Acidity of the iron and manganese promoted SZ samples. The number of Lewis (L) and Brønsted (B) acid sites is determined by FTIR spectroscopy of adsorbed pyridine. The IR spectra were carried out at increasing temperatures: 150, 250, 350, 450 and 500°C.

Desorption Temperature	150°C		250°C		350°C		450°C		500°C	
	L	B	L	B	L	B	L	B	L	B
(1.0)F(1.0)MSZ	105	76	48	34	38	11	0	0	-	-
(1.5)F(0.5)MSZ	130	135	70	65	30	25	0	0	-	-
(2.0)FSZ	72	138	39	79	22	39	0	0	-	-
(2.0)MSZ	138	122	74	49	45	6	0	0	-	-
SZ	82	128	48	75	17	33	7	19	5	5

The unpromoted sample has strong acid sites that retains pyridine even at 500°C, while the promoted samples does not retain pyridine above 350°C.

4.1.2 Catalytic testing

The catalysts were tested for *n*-butane isomerization in a fixed bed reactor at 250°C and atmospheric pressure. *n*-Butane was diluted in nitrogen (diluent/*n*-butane ratio = 9). A detailed description of the set-up and the reaction conditions are given in chapter 3.3. The catalysts deactivated rapidly under these conditions as shown for (1.5)F(0.5)MSZ in Figure 4.3. Typical selectivity to isobutane was 90-100%, other reaction products were propane and pentanes. Similar profiles and selectivities were obtained for the other catalyst as well (Appendix 4). The experiments showed good reproducibility (Appendix 3).

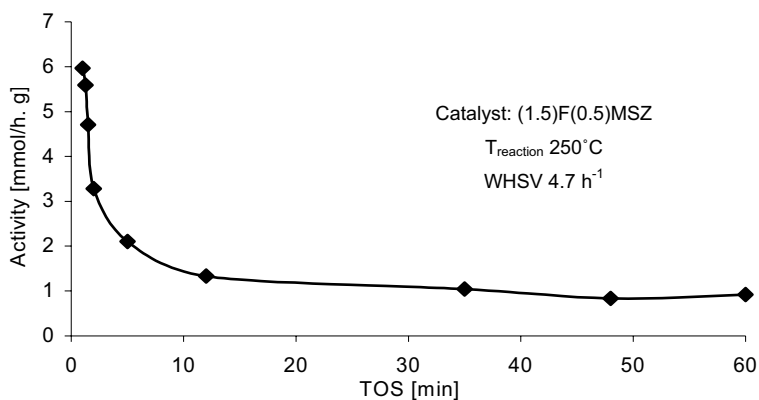


Figure 4.3 Typical activity profile during the isomerization of *n*-butane over a FMSZ catalyst.

The initial (1 min TOS) and long term (60 min TOS) conversion for all the iron and manganese promoted catalysts are summarized in Table 4.3. Two experiments where nitrogen was replaced by hydrogen as the diluting gas are also included in the table.

Table 4.3 Activity for *n*-butane isomerization of FMSZ samples. Reaction conditions: T = 250°C, P = 1 atmosphere, diluent/*n*-butane = 9, WHSV = 4.7 h⁻¹. The catalysts were pretreated in air at 450°C for 3 hours.

<i>Sample</i>	<i>Conversion [%] at 1 min TOS</i>	<i>Conversion [%] at 60 min TOS</i>	<i>Diluent</i>
(1.0)F(1.0)MSZ	3.5	0.4	N ₂
(1.5)F(0.5)MSZ	4.7	0.8	N ₂
(2.0)FSZ	6.2	0.7	N ₂
(2.0)MSZ	1.0	0.3	N ₂
SZ	10.7	1.1	N ₂
(1.5)F(0.5)MSZ	6.8	0.6	H ₂
SZ	1.4	1.2	H ₂

Correlation between promoter content and n-butane isomerization activity

The activities of the FMSZ catalysts after 1 minute and 60 minutes time on stream as function of their nominal promoter content are shown in Figure 4.4. (The activity is expressed as level of the conversion, all experiments were carried out at the same space velocity, WHSV = 4.7 h⁻¹). Only the nominal metal content is given, since the real metal content of the samples has not been determined. Notice that the unpromoted sample exhibit higher activity than all of the promoted samples both initially and after deactivation.

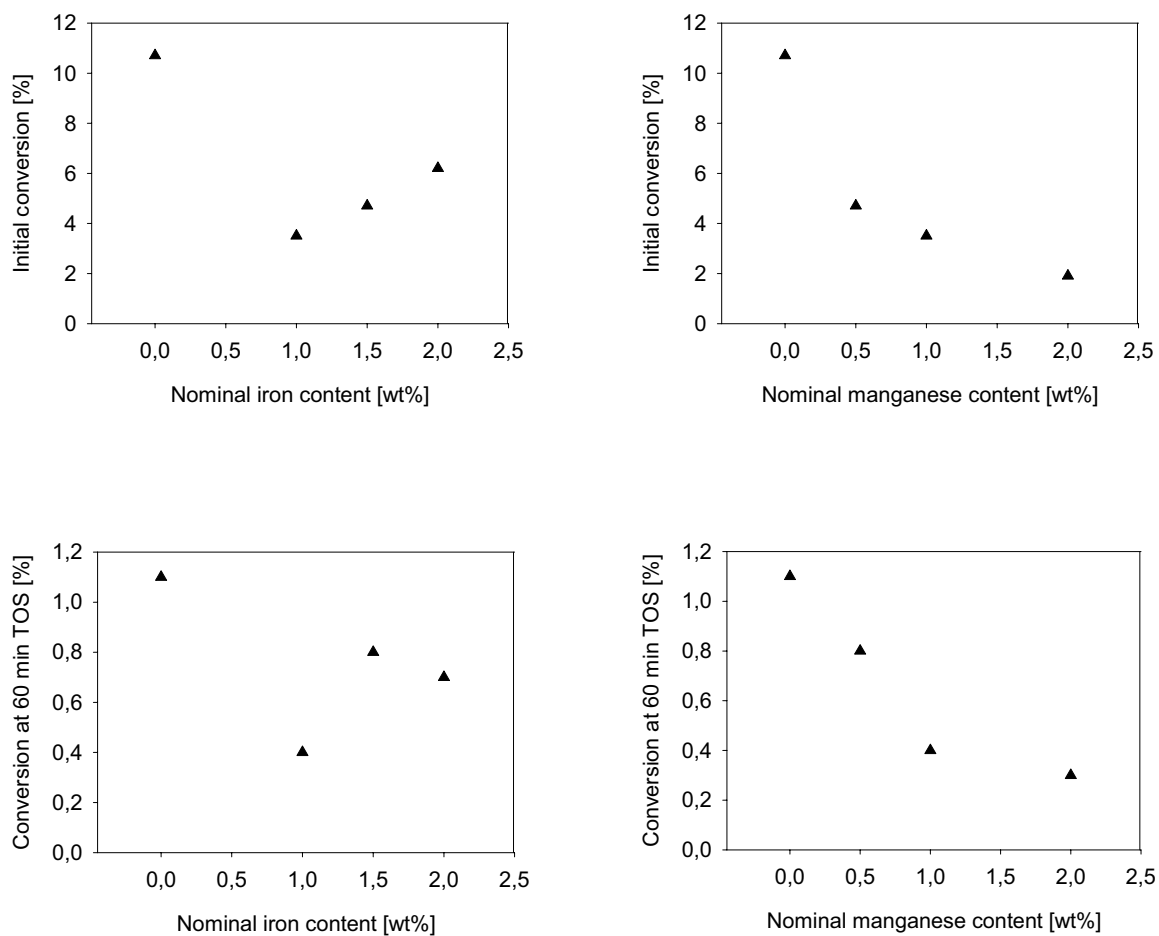


Figure 4.4 *n*-Butane conversion as a function of the promoter content of the catalysts. Initial conversion is the conversion after 1 minute time on stream. $T=250^{\circ}\text{C}$, $P=1$ atmosphere, $\text{WHSV}=4.7\text{ h}^{-1}$ $\text{N}_2/n\text{-butane} = 9$.

Correlation between acidity and n-butane isomerization activity

The acidity of the catalysts was determined by FTIR spectroscopy of adsorbed pyridine. As described above we differentiate between the strength of the acid sites by thermodesorption of pyridine at stepwise increasing temperatures. The sites that can retain pyridine after evacuation at 350°C and higher temperatures are referred to as strong acid sites, while the sites retained at 150°C are called *all Brønsted acid sites* or *all Lewis acid sites*.

Figure 4.5 a and c show that there is no good correlation between *all acid sites* and the initial conversion, but for the strong sites (Figure 4.5 b and d) the trends are clearer. The initial conversion is increasing with the number of strong Brønsted acid sites. The unpromoted sample is an exception, but it should be noticed that this sample contains some acid sites that are stronger than what is the case for the promoted samples (Table 4.2). The situation is the contrary for the strong Lewis acid sites where conversion decreases with the number of strong acid sites.

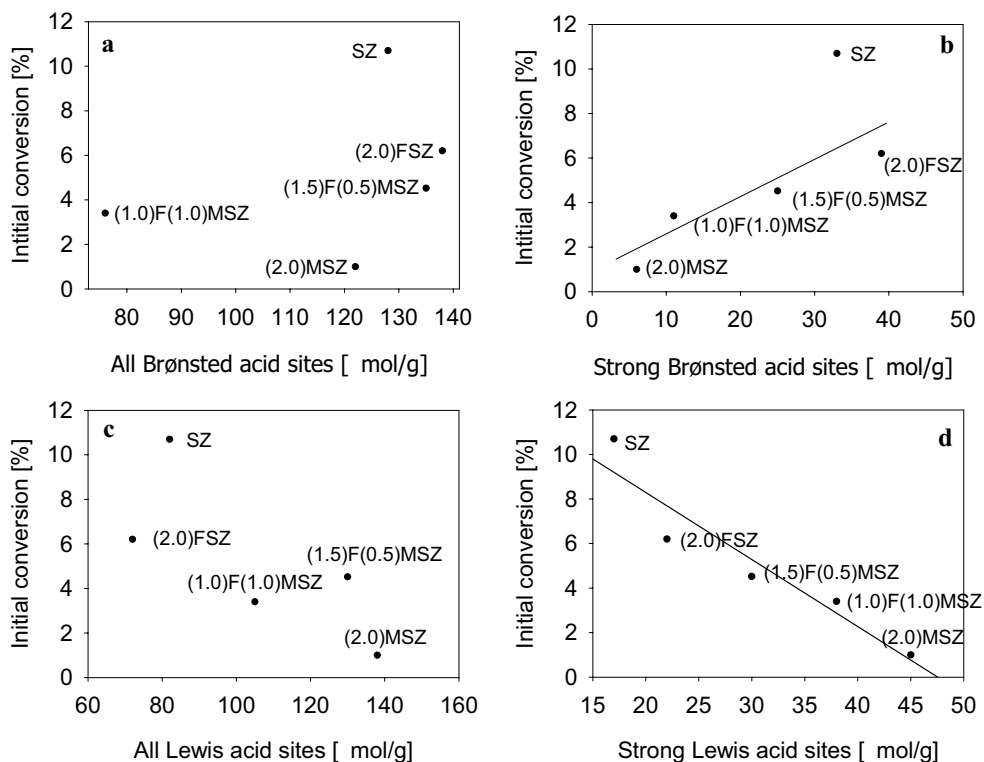


Figure 4.5 Initial conversion as a function of acid sites. *All sites* corresponds to the sites left after thermodesorption at 150°C, and *Strong sites* to sites measured after thermodesorption at 350°C. Reaction conditions: 250°C, 1 atm, N_2/n -butane = 9, WHSV = 4.7h⁻¹

The trends for the deactivated catalysts are the same as for the initial conversion as shown in Figure 4.6, though the trends are not as clear as in shown Figure 4.5 b and d.

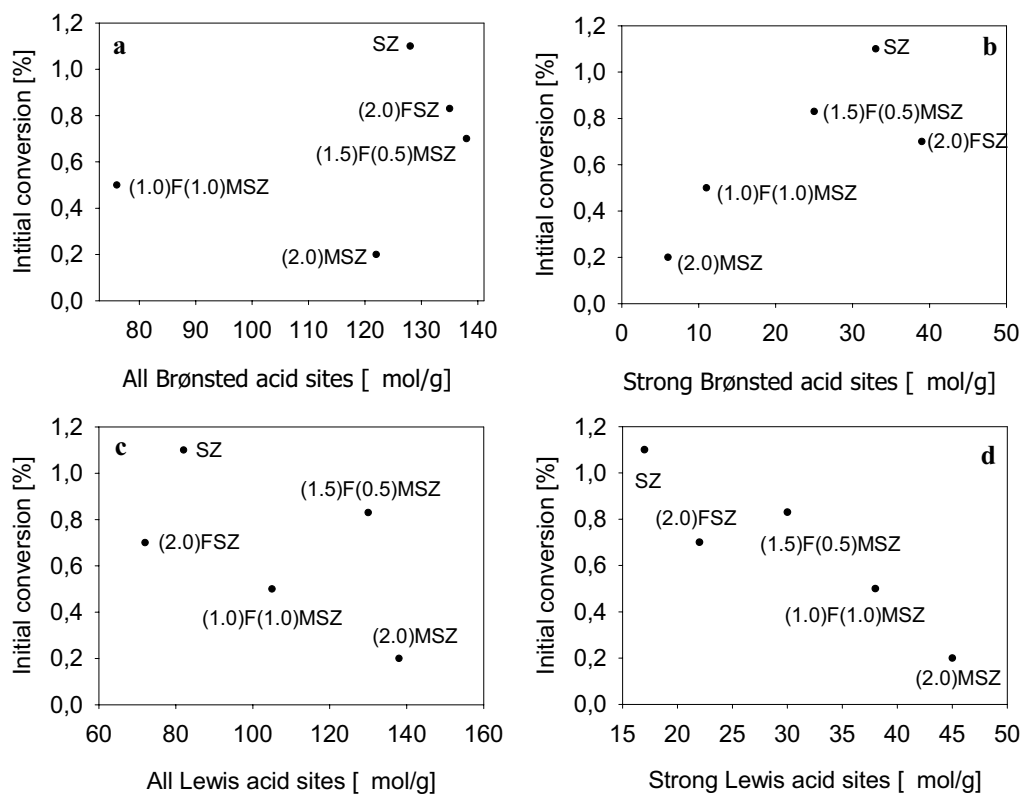


Figure 4.6 Conversion after deactivation (60 minutes TOS) as a function of catalyst acidity. *All sites* corresponds to the sites left after thermodesorption at 150°C, and *Strong sites* to sites measured after thermodesorption at 350°C. Reaction conditions: 250°C, 1 atm, N_2/n -butane = 9, WHSV = $4.7h^{-1}$

In two experiments nitrogen was replaced by hydrogen as the diluting gas. This resulted in different activity profiles than what was observed in the case of nitrogen. The *n*-butane conversion over unpromoted SZ is strongly inhibited in the presence of hydrogen (Figure 4.7), while in the case of (1.5)F(0.5)MSZ the activity profile is basically the same in hydrogen and nitrogen. The initial conversion is in fact higher in the case where hydrogen is the diluent.

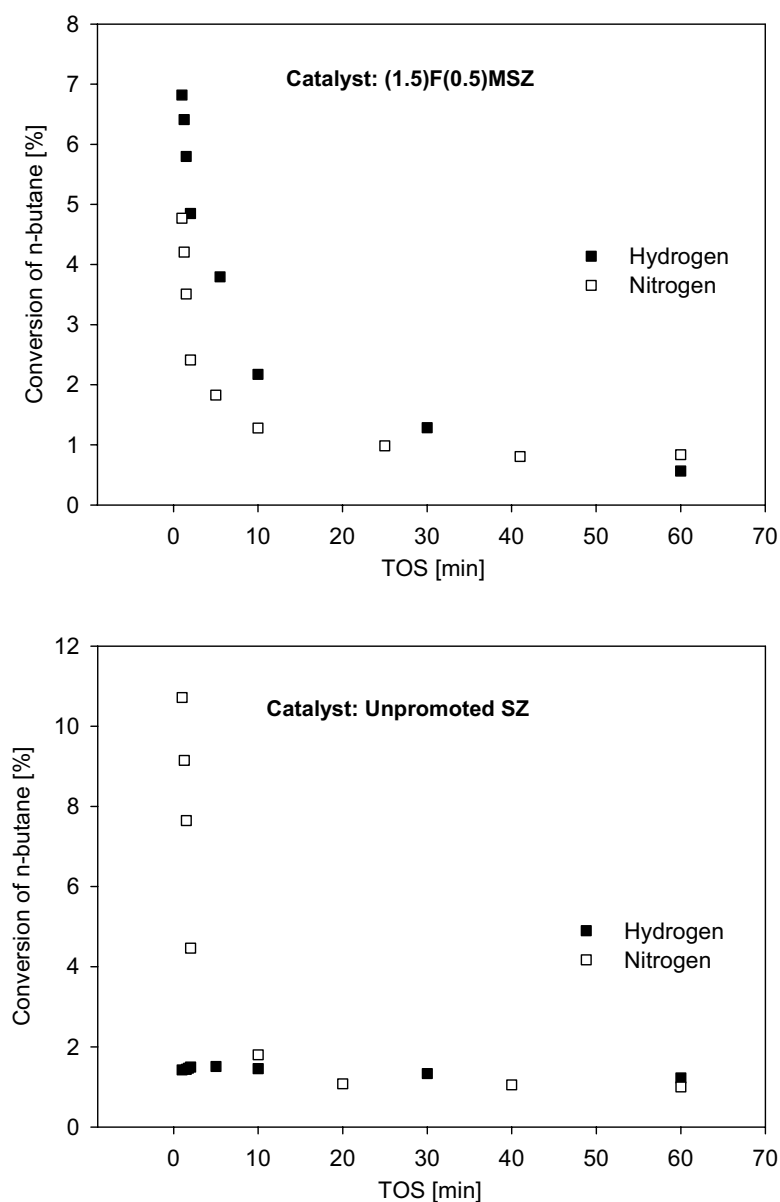


Figure 4.7 Effect of diluting gas on *n*-butane conversion. Iron and manganese promoted SZ in the upper pane and unpromoted SZ in the lower. Reaction conditions: 250°C, 1 atm, diluent/*n*-butane = 9, WHSV = 4.7h⁻¹

4.1.3 Acidity and catalytic activity of tungsten oxide modified zirconia

The acidity of two samples of tungsten oxide modified zirconia (WZ) was characterized in the same way as the iron and manganese promoted SZ samples. The concentration and strength of the acid sites are much lower than in the case the FMSZ catalyst. No further characterization was done, except catalytic testing. The WZ sample fits well into the correlation plot for *strong acid sites* and initial activity shown in Figure 4.8.

Table 4.4 Acidity of the WZ and PtWZ samples.

Desorption temperature	150°C		250°C		350°C		450°C		500°C	
Acid sites [$\mu\text{mol/g}$]	L	B	L	B	L	B	L	B	L	B
WZ	32	34	14	16	2	2	0	0	-	-
PtWZ	47	17	16	3	3	0	0	-	-	-

The catalysts were tested for *n*-butane isomerization activity at standard conditions as described in chapter 3.3. The catalyst showed remarkably much lower activity (Table 4.5) than the iron and manganese promoted SZ catalysts, but the deactivation was also less pronounced for the WZ catalysts.

Table 4.5 Activity for *n*-butane isomerization of WZ and PtWZ. Reaction conditions: T=250°C, P=1 atmosphere, diluent/*n*-butane= 9, WHSV=4.7 h⁻¹. The samples were pretreated in air at 450°C.

Sample	Conversion [%] at 1 min TOS	Conversion [%] at 60 min TOS	Diluent
WZ	0.05	0.04	N ₂
PtWZ	0.18	0.10	N ₂

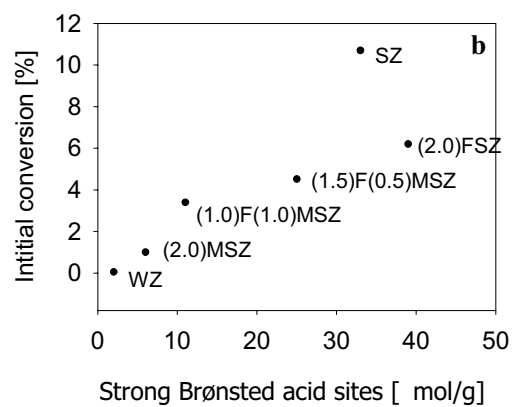


Figure 4.8 Initial conversion as a function of catalyst acidity. The WZ sample fits into the series of FMSZ catalysts. *Strong Brønsted acid sites* correspond to sites measured after thermodesorption at 350°C. Reaction conditions: 250°C, 1 atm, N₂/n-butane= 9, WHSV = 4.7h⁻¹

4.2 Isomerization of *n*-hexane at elevated pressure

This part of the study is divided in three parts. The first part treats the characterization of the physical and chemical properties of the catalyst samples. In the second part the results of the preliminary catalytic tests at high pressure are presented. These experiments were performed at the University of Poitiers with the set-up described by Bichon [116]. Finally, the third part, the kinetic study of *n*-hexane isomerization over various noble promoted sulfated zirconia samples and a commercial isomerization catalyst. These catalytic tests were performed at NTNU.

4.2.1 Characterization of noble metal promoted catalysts

Various techniques have been employed to characterize the samples of noble metal promoted sulfated zirconia. The structural properties and the total sulfur content of the samples are summarized in Table 4.1. All the samples have almost identical surface area, pore width and pore volume. From X-ray diffraction it was found that the only crystalline phase is the tetragonal zirconia phase. The sulfur content of the samples differs some, but it is almost within the limits of the uncertainty of the analysis method (+/- 10 % relative error; given by the analyst). The X-ray diffractograms and the N₂ adsorption-desorption curve are shown in Appendix 2 and 5.

Table 4.6 Physical and chemical properties of the noble metal promoted SZ samples

Sample	BET surface area [m ² /g]	Average pore width [nm]	Pore volume [cm ³ /g]	Crystalline phase	Sulfur content [wt%]
PtSZ	134	46	0.20	Tetragonal	1.78
IrSZ	133	47	0.20	Tetragonal	2.16
RuSZ	132	46	0.19	Tetragonal	1.63
RhSZ	134	47	0.20	Tetragonal	2.02
SZ	133	47	0.19	Tetragonal	2.23

Figure 4.9 shows the TPR profiles of the catalysts. One major reduction peak which corresponds to the reduction of sulfate groups is observed for all samples. For the unpromoted sample the maximum of the peak is observed at 616°C, when a noble metal is added to the samples the maximum of the sulfate peak is shifted towards lower temperatures. The maximum is observed at 515-517°C when iridium, ruthenium and platinum are added to SZ and at 532°C when rhodium is added. For RhSZ, IrSZ and RuSZ a low temperature reduction peak for the metal oxide is observed with maxima at 160, 170 and 195°C, respectively. For the platinum promoted sample no peaks were observed in the low temperature area where one can expect to find the PtO_x reduction peak [118]. The distinct smell of H₂S could be recognized when the reactor was opened after the analysis for all samples.

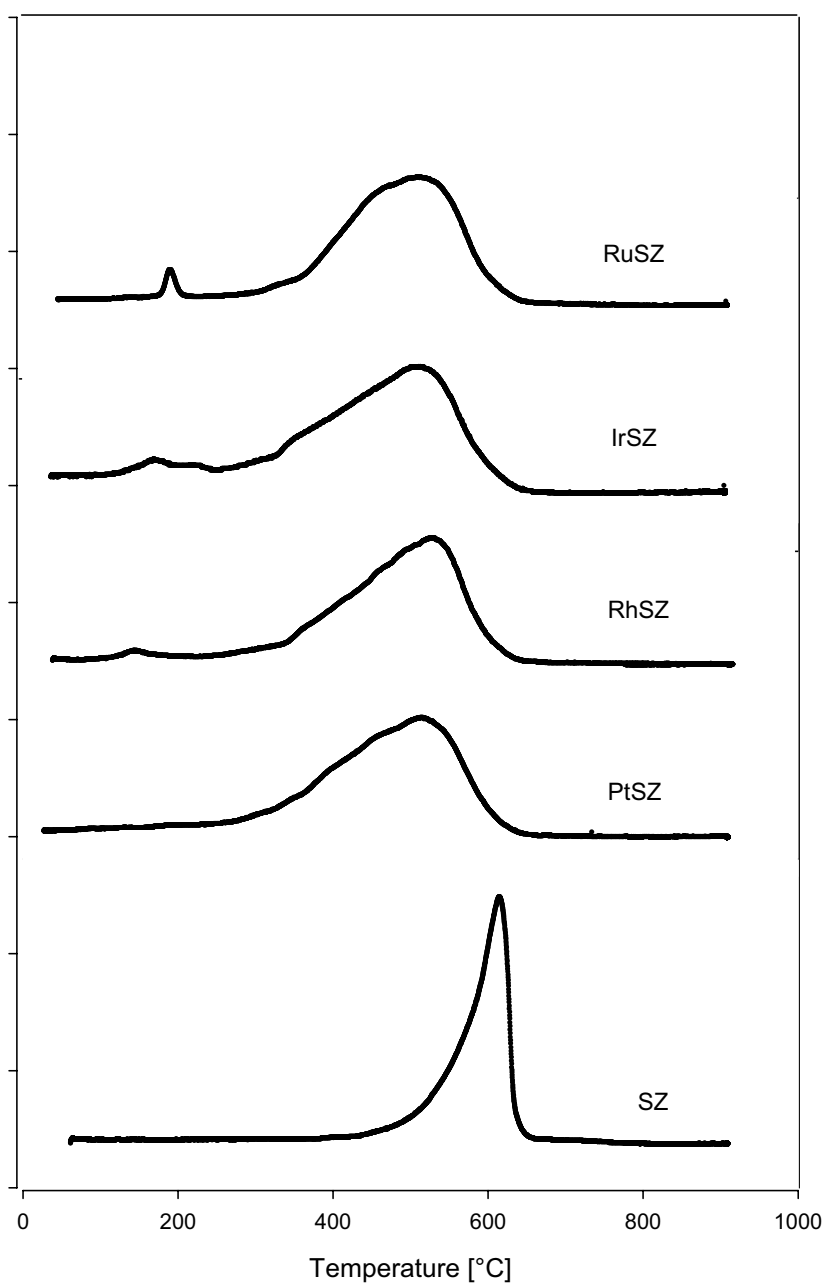


Figure 4.9 TPR profiles of the noble metal promoted samples.

The type and strength of the acid sites were determined by IR spectroscopy as described in chapter 4.1.1. The platinum promoted sample was analyzed after two different pretreatments, one was

pretreated in helium, and the other was reduced at 450°C, like the rest of the promoted samples. The unpromoted sample is treated with air at 450°C, thus the pretreatment before characterization is different from pretreatment before the catalytic test. The samples were pretreated this way because after pretreatment at 300°C the spectra are not well defined.

The IR region of the Brønsted and Lewis bands (1430-1670 cm^{-1}) after adsorption of pyridine and evacuation at 150°C is shown in Figure 4.10. Note that there are two Lewis bands for the PtSZ samples (1446 and 1457 cm^{-1}). The strength and concentration of the acid sites measured for by thermodesorption all the samples are summarized in Table 4.7.

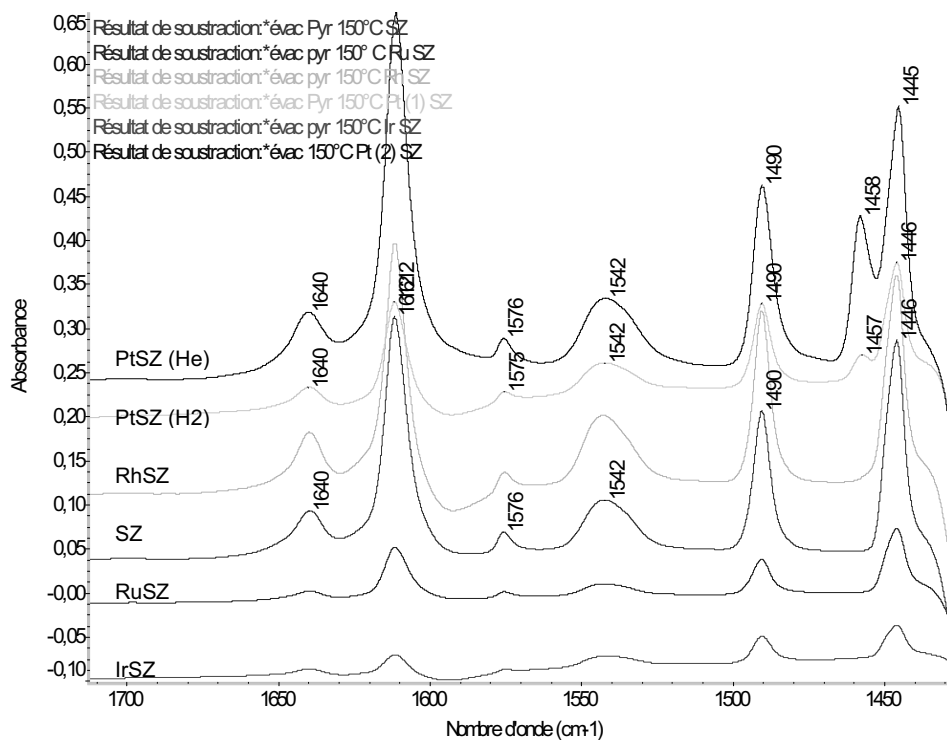


Figure 4.10 The Brønsted and Lewis band after adsorption of pyridine and evacuation at 150°C. (Nombre d'onde = Wave number)

The OH bands in the region 3400-3800 cm^{-1} are reported in Figure 4.11. The wave numbers for the OH bands are similar, but it is difficult to obtain information on acid strength from the OH region for these samples.

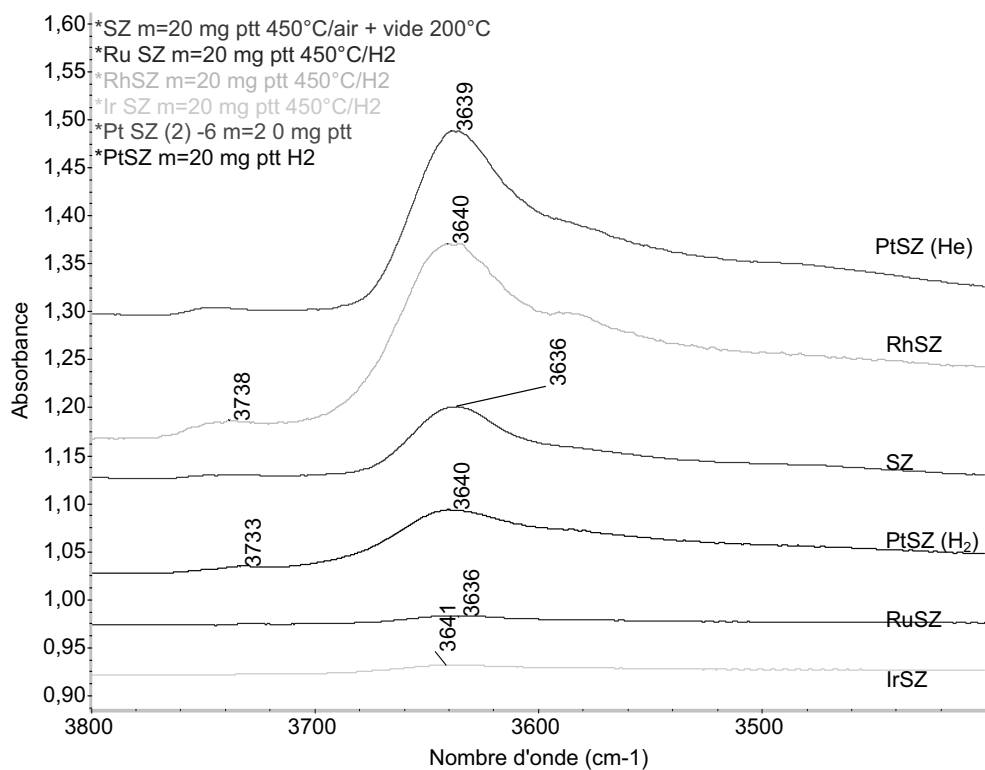


Figure 4.11 IR spectra in the OH region for the noble metal promoted samples after pretreatment (Nombre d'onde = Wave number)

Table 4.7 Acidity of the noble metal promoted SZ samples. The number of Lewis (L) and Brønsted (B) acid sites is determined by FTIR spectroscopy of adsorbed pyridine. The IR spectra were carried out at increasing temperatures: 150, 250, 350 and 450 °C

Desorption Temperature	150°C		250°C		350°C		450°C	
	L	B	L	B	L	B	L	B
PtSZ (H ₂)	103	61	70	22	28	7	14	0
PtSZ (He)	264	137	230	89	136	59	0	0
IrSZ	26	23	16	12	3	6	0	0
RuSZ	47	22	27	14	12	5	0	0
RhSZ	131	130	64	69	18	0	0	0
SZ	140	93	83	75	39	39	10	5

Pretreatment in hydrogen reduces the number of acid sites, thus the sample pretreated in helium, PtSZ(He), appears as the most acidic of the samples. IrSZ and RuSZ have less acid sites than the two other promoted samples reduced in hydrogen.

4.2.2 Preliminary catalytic tests at high pressures

The preliminary catalytic test were performed in fixed bed steel tube reactor at 250°C and pressure in the range 10-30 bar with hydrogen as the diluent, as described in chapter 3.3.2. Two different catalysts were tested, the first was a sample of iron and manganese promoted sulfated zirconia, (1.5)F(0.5)MSZ, which was also tested for *n*-butane isomerization activity (Chapter 4.1). The second catalytic test was performed over platinum promoted sulfated zirconia. This sample was prepared according to the procedure in chapter 3.1.3, and its nominal platinum content was 0.75 wt%, but it was not tested or characterized by any technique except the catalytic test.

Iron and manganese promoted sulfated zirconia

The effects of the reaction temperature, total pressure and partial pressure of hydrogen and *n*-hexane partial pressure on the *n*-hexane isomerization activity were examined. A typical run is presented in Figure 4.12. As it is shown in the figure, the catalyst deactivates and reaches a plateau where the conversion is stable before the new conditions are set. At the end of the test the catalyst is tested at the standard conditions again to see if there has been any further deactivation during the run. Between the tests, over night, the catalyst was kept under flowing hydrogen. This treatment led to an increase in the initial activity the following day, but after the initial deactivation the activity of the catalyst was back to same level as, or lower than, the previous day.

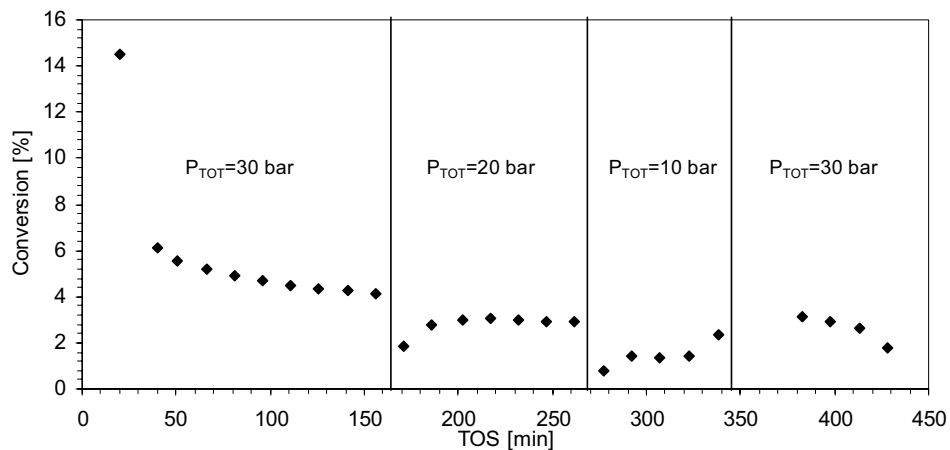


Figure 4.12 Effect of the total pressure. Reaction conditions: Catalyst: (1.5)F(0.5)MSZ, $T=250^{\circ}\text{C}$, $\text{WHSV}=2.3\text{ h}^{-1}$, $\text{H}_2/\text{nC}_6=9$).

In these experiments ratio between isomerization and cracking products (I/C) were in the range 5-10. This corresponds to approximately 80-90% selectivity to branched nC6 isomers. The catalyst was continuously deactivated. In Figure 4.13 the deactivation from day to day during the experiment with the iron and manganese promoted sample is shown. The conversion at standard conditions at the end of each day was taken as measure for the deactivation. Only the three first days are shown, after the third day the conversion did not stabilize. After three days of catalytic testing at different conditions the residual conversion was 33% of the initial conversion.

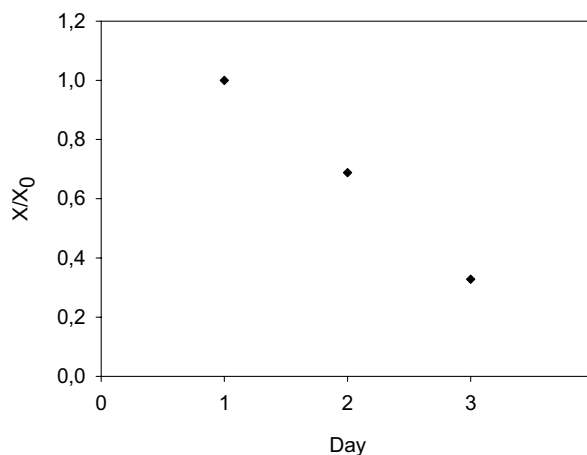


Figure 4.13 Deactivation during the experiment for iron and manganese promoted sulfated zirconia. X_0 is the conversion at the end of day 1.

Since the catalyst deactivated continuously it was not possible to estimate the effects of reaction temperature, total pressure and partial pressure of hydrogen and *n*-hexane partial pressure. The results of these tests are shown in Appendix 6.

Platinum promoted sulfated zirconia

The platinum promoted catalyst was more stable than the FMSZ sample. Although it deactivated slightly each day (Figure 4.14) it was stable enough to determine the activation energy and the reaction orders with respect to hydrogen, *n*-hexane and total pressure. The catalytic tests were performed in the same way as for the iron and manganese promoted sample. An example of a run is shown in Figure 4.14 where the effect of the *n*-hexane pressure on the conversion was examined. The rest of the runs for this catalyst are shown in Appendix 6. The conversion seems to be relatively stable, at the end of the run the starting conditions are checked and a slight deactivation is observed. After six days of catalytic testing the conversion had decreased to 40% of the initial conversion (Figure 4.17).

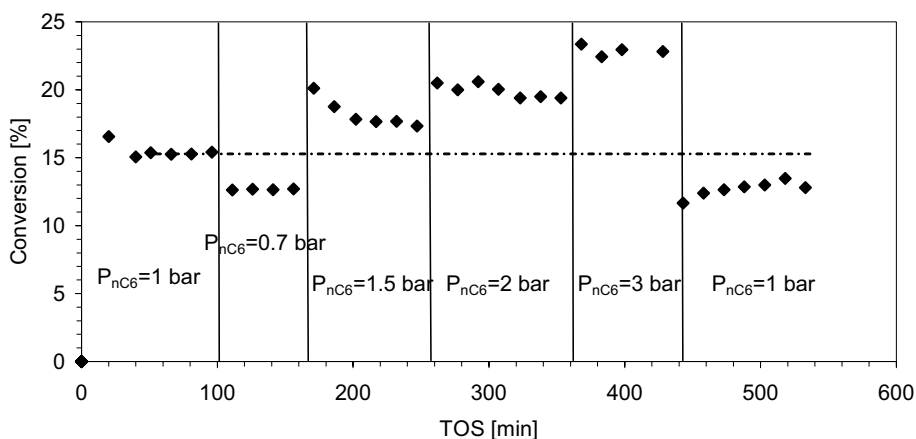


Figure 4.14 Example of how a catalytic test was performed. Reaction conditions: $T=250^{\circ}\text{C}$, $\text{WHSV}=7.9\text{ h}^{-1}$, $P_{\text{H}_2}=9\text{ bar}$. Catalyst: 0.75 wt% PtSZ.

The activation energy was determined to be 93 kJ/mol. The reaction order with respect to hydrogen is -1.1, while the reaction order for *n*-hexane is 0.4.

Figure 4.15 shows that the selectivity to isomers, presented as the ratio between isomer and cracking product (I/C), decreases as the conversion increases.

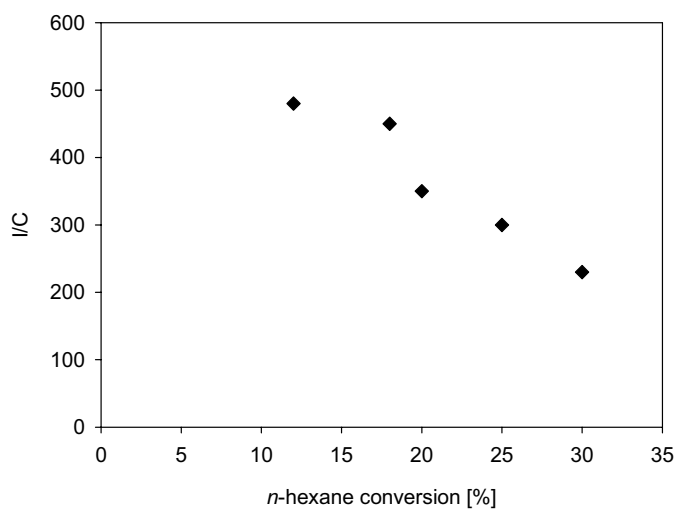


Figure 4.15 Selectivity (I/C) as a function of n-hexane conversion. Reaction conditions: T=250°C, WHSV=7.9 h⁻¹, P_{TOT}=10 bara, H₂/nC6=9. Catalyst: 0.75 wt% PtSZ.

The distribution of the branched C6 isomers as a function of the conversion is shown in Figure 4.16.

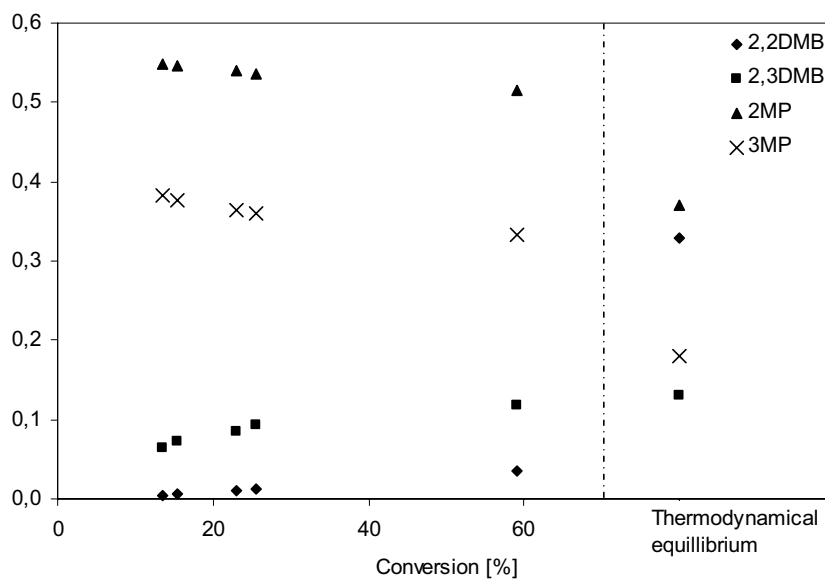


Figure 4.16 Isomer distribution as a function of n-hexane conversion. Reaction conditions: T=250°C, P_{TOT}=10 bara, H₂/nC6=9. Catalyst: 0.75 wt% PtSZ. The isomer distribution at thermodynamical at equilibrium is included in right side of the figure.

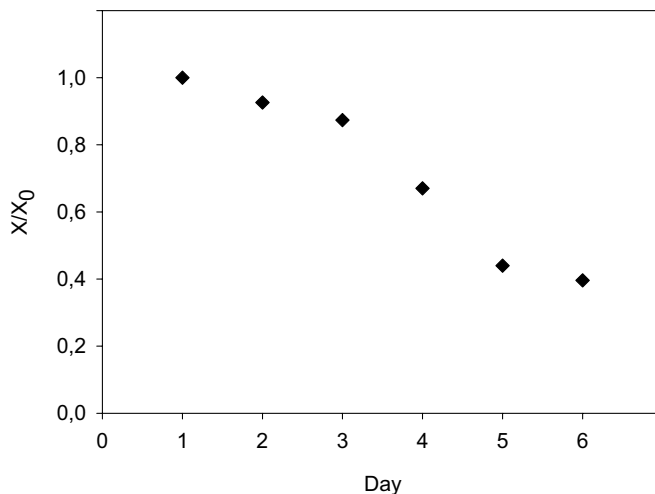


Figure 4.17 Deactivation during the experiment for platinum promoted sulfated zirconia. X_0 is the conversion at the end of day 1. Conversion measured at standard conditions.

4.2.3 Comparison of catalytic activity and kinetic study

Five different samples of sulfated zirconia promoted with different noble metals (i.e. Pt, Ir, Ru and Rh) and one commercial isomerization catalyst were tested in the experimental set up described in chapter 3.3.2. Kinetic parameters of these catalysts for *n*-hexane isomerization are determined. The catalyst have been tested either after reduction in hydrogen or pretreatment in helium.

The parameters of the standard condition were chosen to give a conversion that gave differential conditions for all catalysts. For the commercial catalyst a higher reaction temperature, 235°C, was chosen to give an adequate conversion, otherwise the standard condition was the same. The experiments were performed in the same way as in the preliminary experiments. The catalyst deactivated until a level of stable conversion was reached. After reaching stable conversion, the new conditions are set. At the end of the test the catalyst is again tested at the standard conditions to see if there has been any further deactivation during the run. Between the tests, over night, the catalyst was kept under flowing hydrogen, or helium in the case of helium pretreated samples.

4.2.3.1 PtSZ

PtSZ pretreated in hydrogen

The PtSZ sample was the most active of all samples that were tested. The isomer distribution does not change much with the level of conversion in the range 5-31 %. When the conversion increases there is

slightly more dimethyl butanes formed at the sacrifice of 3-methyl pentane. The kinetic study is summarized in Figure 4.18.

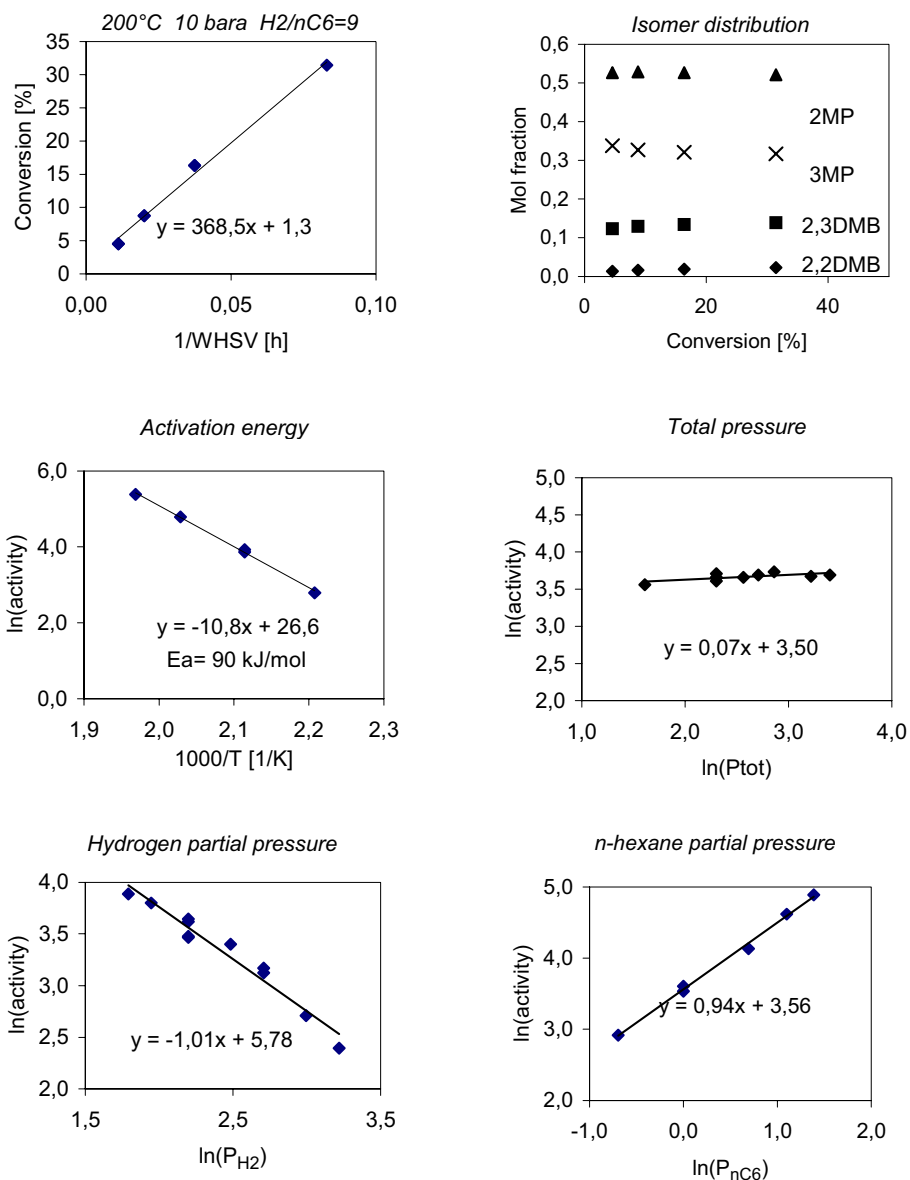


Figure 4.18 Kinetic study of PtSZ reduced in hydrogen 300°C. Standard conditions: 200°C, $P_{TOT}=10$ bara, $H_2/nC_6=9$.

The reaction orders were estimated to 0.07, -1.01 and 0.94 for total pressure, hydrogen partial pressure and *n*-hexane partial pressure respectively, while the activation energy was found to be 90

kJ/mol. The branched isomers of hexane were main products of the reaction, and no cracking products were observed until the conversion exceeded 20%. In the conversion range 20-30% the I/C ratio was in the range 400-500, which corresponds to around 99.8% selectivity to isomers.

Figure 4.20 shows that the catalyst seemed to be fairly stable, but it deactivated slightly during each day of experiment. The conversion at standard conditions at the end of the day is taken as an indication of the deactivation, after 6 days of catalytic testing the remaining activity was 64% of the initial activity (Figure 4.19). It should be noticed that the conditions during the catalytic test was varied from day to day.

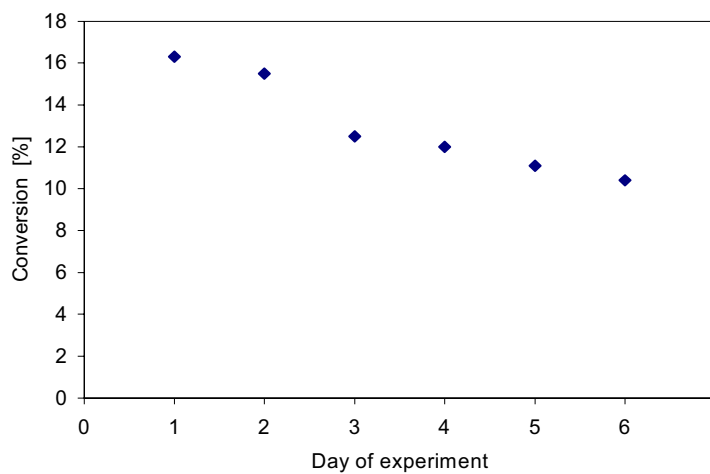


Figure 4.19 Deactivation during catalytic testing of the PtSZ sample. Conversion measured at standard conditions.

Regeneration

The catalyst was regenerated by reoxidation in oxygen (2% oxygen in nitrogen) at 450°C for 5 hours followed by reduction by the standard procedure. The catalyst regained its initial activity as shown in Figure 4.20.

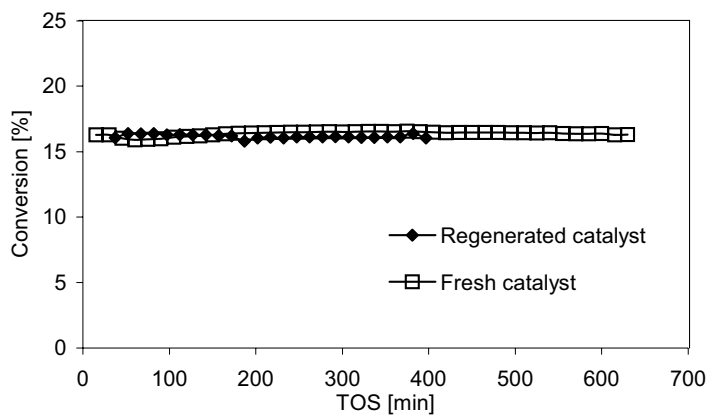


Figure 4.20 PtSZ regains its initial activity after reoxidation at 450°C for 5 hours. Reaction conditions (200°C, 10 bara, $H_2/nC_6=9$, $WHSV=26.7\ h^{-1}$)

PtSZ pretreated in helium

The effect of pretreating PtSZ in helium at 300°C instead of reducing the sample in hydrogen is quite dramatic. In the case of the reduced catalyst there was an insignificant deactivation initially, but in case of the helium pretreated sample there is an increase in the activity of the catalyst. After 400 minutes time on stream the conversion reaches a plateau where it is nearly stable. At this plateau the activity is only 13% of the initial activity of the reduced sample at standard conditions. In spite of that the pretreatment leads to considerable difference in catalytic activity, the activation energy and the reaction orders are almost identical in the two cases. The result from the catalytic tests of the helium pretreated PtSZ are summarized in Figure 4.21 and Figure 4.22.

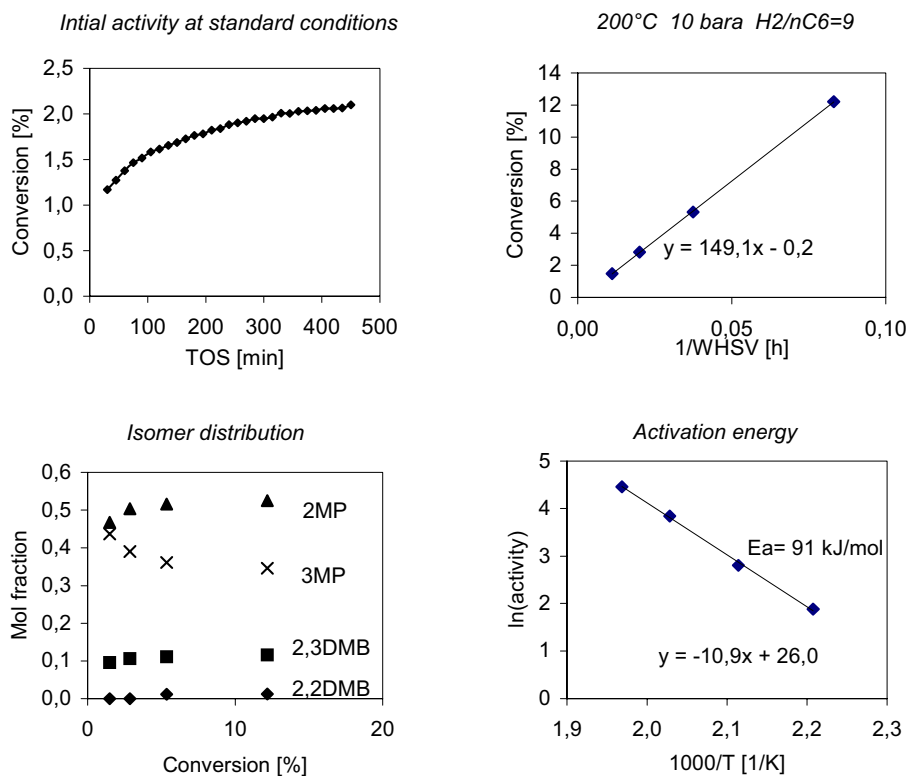


Figure 4.21 Catalytic testing of PtSZ pretreated in helium. Standard conditions: T=200°C, P_{TOT}=10 bara, H₂/nC₆=9.

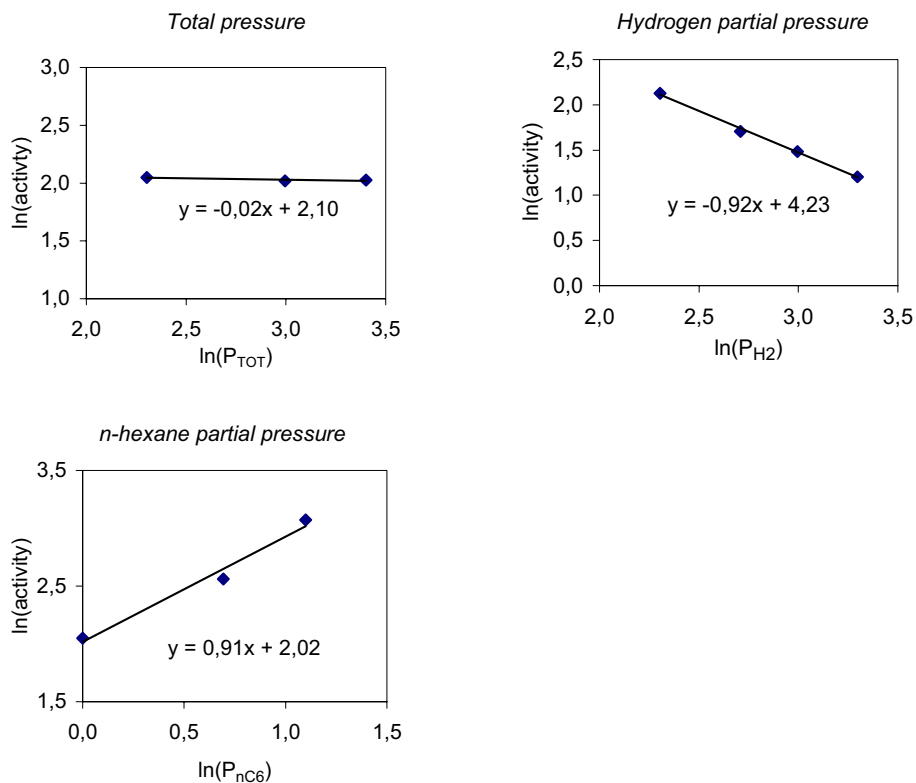


Figure 4.22 Reaction orders of *n*-hexane isomerization over PtSZ pretreated in helium. Standard conditions: $T=200^\circ\text{C}$, $P_{\text{TOT}}=10$ bara, $\text{H}_2/\text{nC}_6=9$.

Pretreatment procedure

The conversion at standard condition is reported for six tests after different pretreatment procedures in Figure 4.23. When considering the reduced samples a maximum in conversion is observed for the catalyst reduced at 250°C . After reduction at 300°C the catalyst shows approximately 50% of the activity of the catalyst reduced at 250°C , but even though the activity is lower after increasing the reduction temperature, the stability is better. When the reduction temperature is increased to 325°C the level of conversion dropped substantially, and a further increase to 337°C gave a catalyst that yielded practically no conversion at standard conditions.

Pretreatment in helium at 300°C gives a considerably less active catalyst than if the catalyst is reduced at the same temperature. When the temperature is further increased to 337°C the activity drops considerably, and the opposite order is observed; the sample pretreated in helium is 3 times more active than the reduce one.

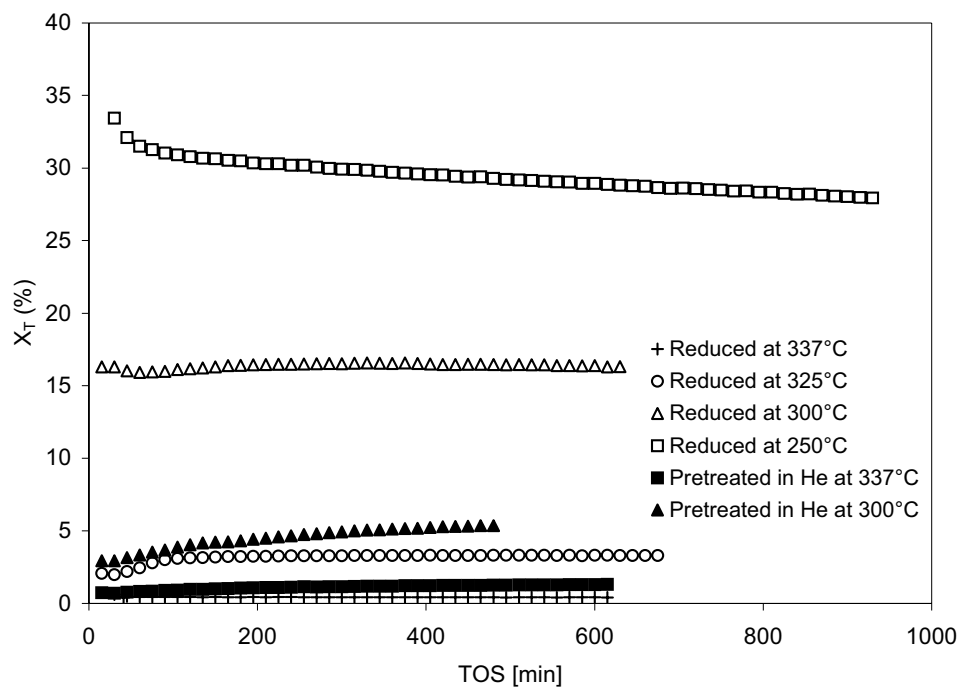


Figure 4.23 The effect of pretreatment on the initial conversion at standard conditions (200°C, 10 bara, $WHSV=26.7h^{-1}$).

4.2.3.2 IrSZ

IrSZ pretreated in hydrogen

The activity of the iridium promoted catalyst is one third of the activity of PtSZ at standard conditions. Even if the IrSZ catalyst is less active, the activation energy, the isomer distribution and the reaction orders with respect to hydrogen and *n*-hexane are quite similar to that of PtSZ. The results are summarized in Figure 4.24 and Figure 4.25.

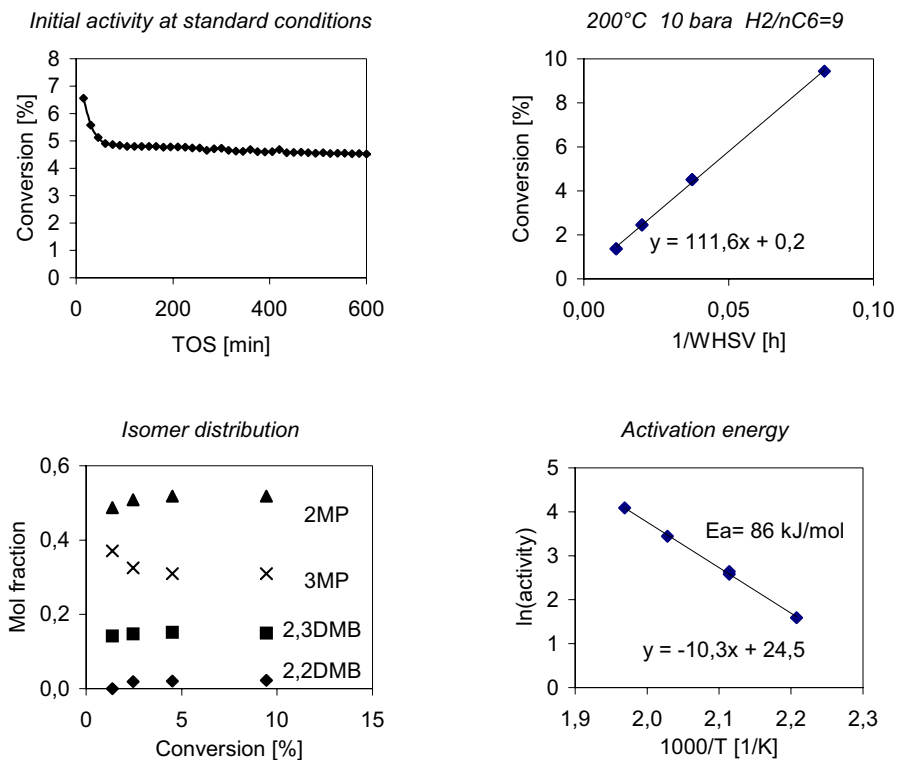


Figure 4.24 Catalytic test of IrSZ pretreated in hydrogen. Standard conditions: T=200°C, P_{TOT}=10 bara, H₂/nC₆=9.

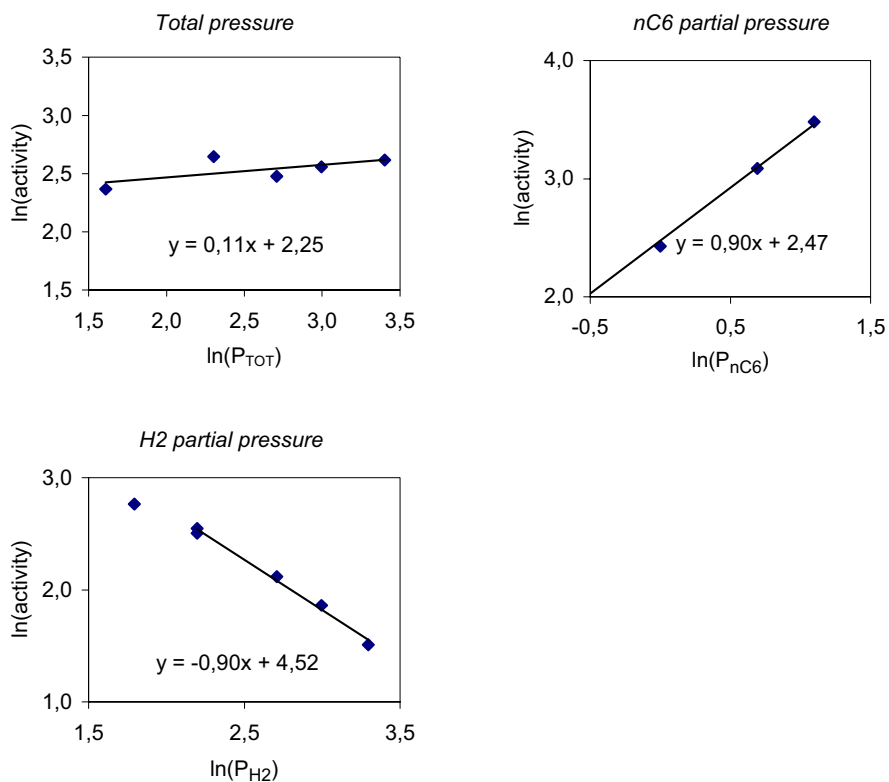


Figure 4.25 Reaction orders over IrSZ pretreated in hydrogen. Standard conditions: $T=200^{\circ}\text{C}$, $P_{\text{TOT}}=10$ bara, $\text{H}_2/n\text{C}_6=9$.

IrSZ pretreated in helium

The effect of pretreating the IrSZ sample in helium instead of hydrogen at 300°C is the same as for the platinum promoted sample; the helium pretreated sample exhibits considerably lower activity and an initial increase in activity with time on stream is observed. The increase in activity continued throughout the experiment, and this makes it difficult to compare the activities at different conditions. However, the activation energy was found to be the same as in the previous cases (86 kJ/mol) and the reaction order with respect to the total pressure was -0.3, which is different from the previous cases. The product distribution is the same as for the reduced IrSZ sample. The activity of this catalyst is low and is steadily increasing as shown in Figure 4.27, this gives a relatively high uncertainty in the determination of kinetic parameters. The experiment was therefore terminated without determining the reaction orders of *n*-hexane and hydrogen. The catalytic test is summarized in Figure 4.26.

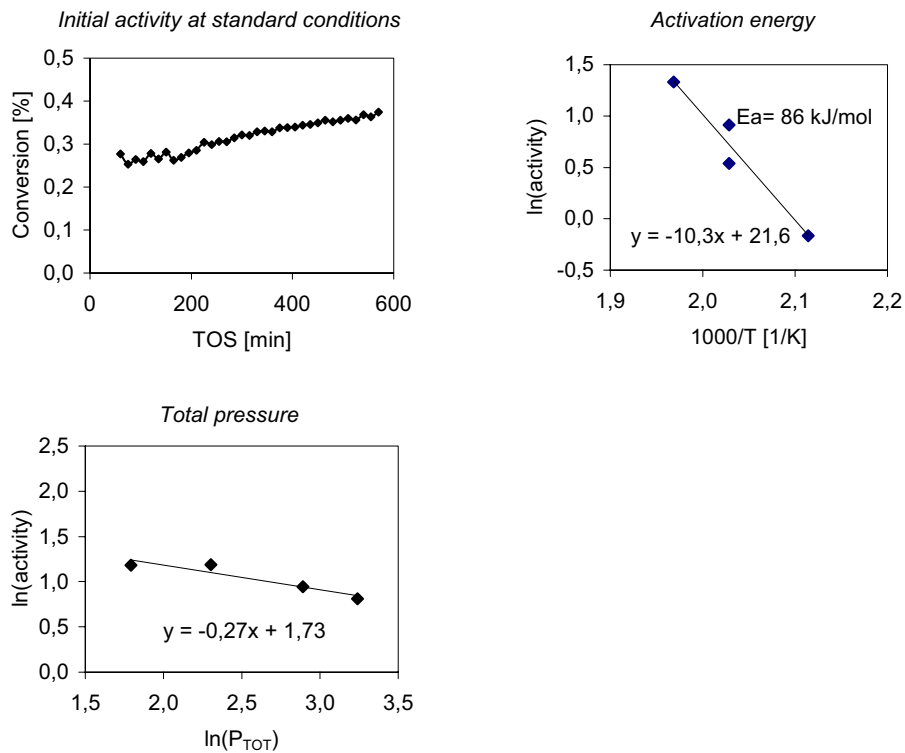


Figure 4.26 Catalytic test of IrSZ pretreated in helium. Standard conditions: $T=200^{\circ}\text{C}$, $P_{\text{TOT}}=10$ bara, $\text{H}_2/\text{nC}_6=9$.

The activity of the IrSZ sample was increasing during the catalytic testing, especially when the reaction temperature was raised during the test. The activity increased by 50% after raising the temperature to 235°C (Figure 4.27). At the end of the experiment the activity is nearly the double of the activity at the beginning of the test.

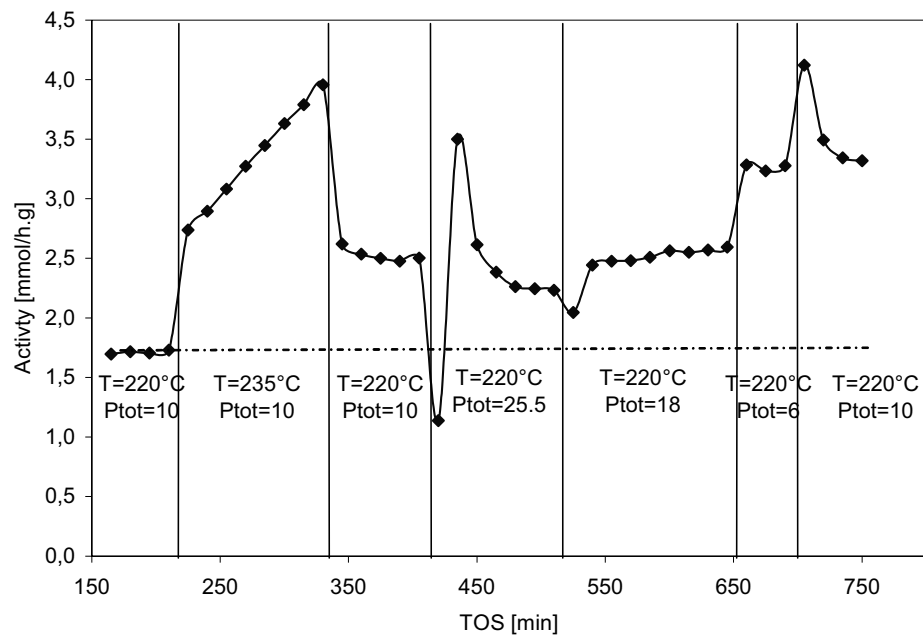


Figure 4.27 Investigation of the effect of reaction temperature and total pressure over IrSZ pretreated in helium. The dashed line indicates the activity at the beginning of the test. Conditions: $WHSV=12h^{-1}$, $H_2/nC6=9$.

4.2.3.3 RhSZ

RhSZ pretreated in hydrogen

The rhodium promoted sample exhibited an initial activity close to that of IrSZ. It showed however a slight increase in activity initially, as opposed to IrSZ which deactivated during the first 50 minutes of reaction. The reaction orders of RhSZ are also different from IrSZ and PtSZ, while the reaction order is -1 with respect to hydrogen for the two last, it is -0.5 for RhSZ. Since the reaction order with respect to *n*-hexane is almost unchanged, +1.0, it means the reaction order to the total pressure is positive, 0.6.

The activation energy of RhSZ is 67 kJ/mol, which is lower than for that of IrSZ and PtSZ. The isomer distribution is the same as for IrSZ.

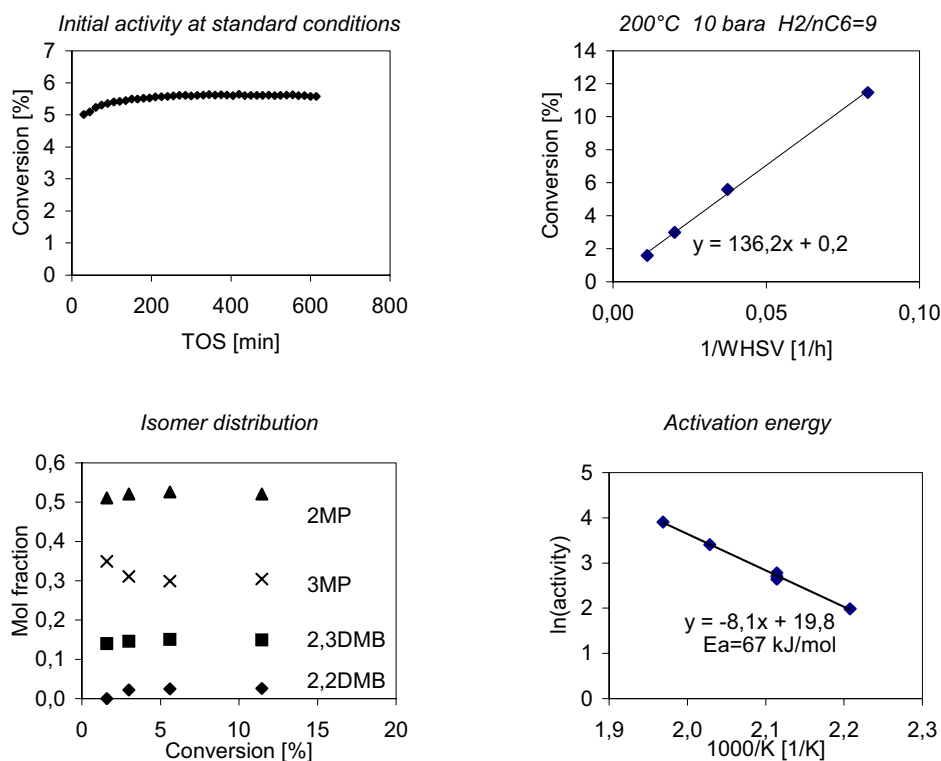


Figure 4.28 Catalytic test of RhSZ pretreated in hydrogen. Standard conditions: $T=200^\circ\text{C}$, $P_{\text{TOT}}=10$ bara, $\text{H}_2/\text{nC}_6=9$.

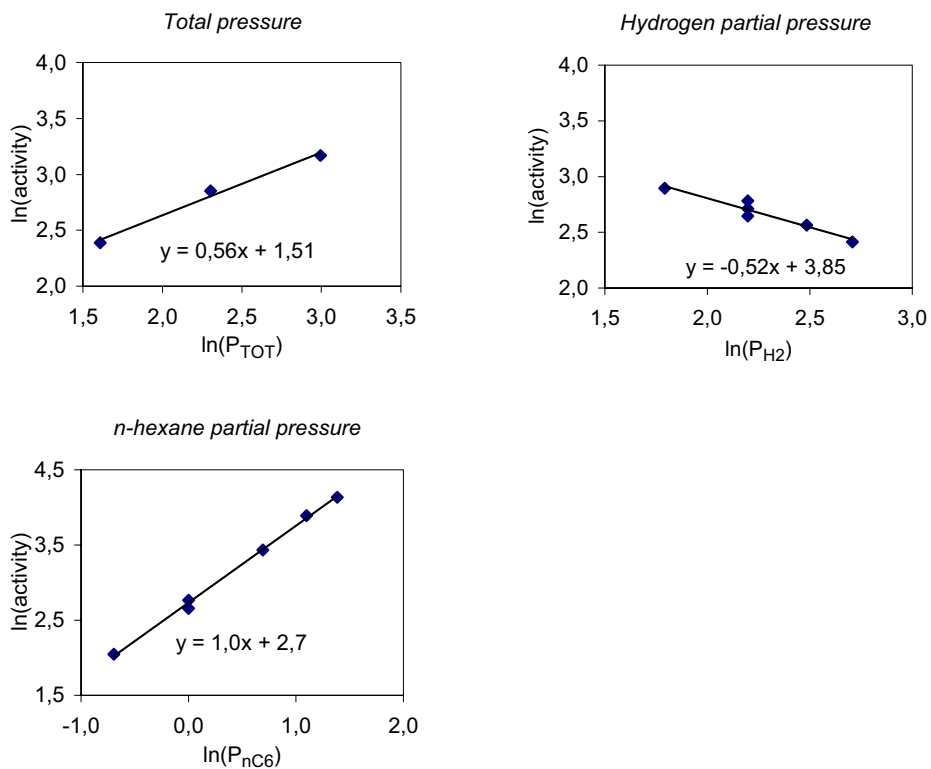


Figure 4.29 Reaction orders over RhSZ pretreated in hydrogen. Standard conditions: $T=200^\circ\text{C}$, $P_{\text{TOT}}=10$ bara, $\text{H}_2/\text{nC}_6=9$.

RhSZ pretreated in helium

When RhSZ is pretreated in helium instead of hydrogen, the same dramatic drop in activity as for PtSZ and IrSZ is observed. The reaction order with respect to *n*-hexane changes to 0.6 while it is almost unchanged for hydrogen (-0.6), and thus the order for the total pressure is close to 0. In case of IrSZ pretreated in helium it was observed a continuous increase in activity during the catalytic test, this was not the case for RhSZ where the activity stayed low and unchanged. The product distribution was the same as for the previous samples.

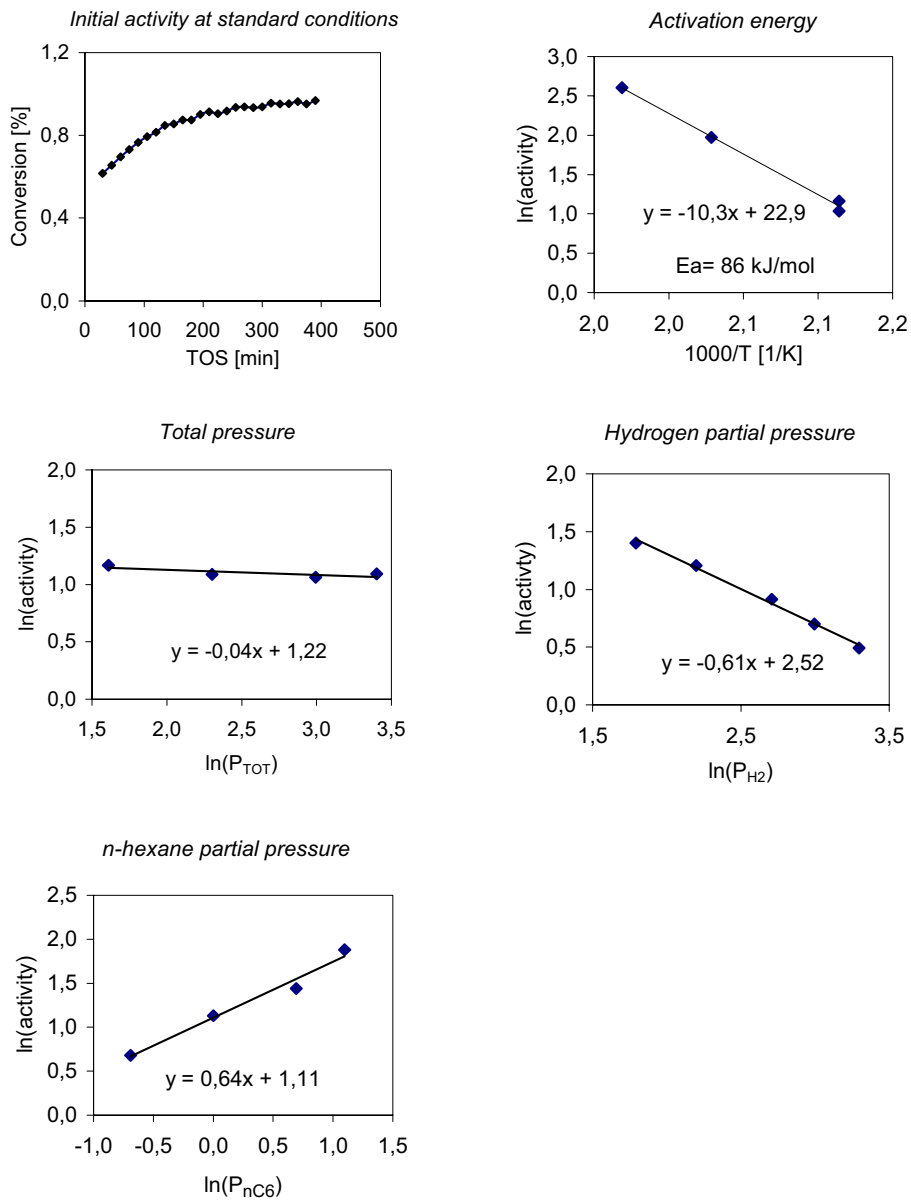


Figure 4.30 Catalytic test of RhSZ pretreated in helium. Standard conditions: T=200°C, P_{TOT}=10 bara, H₂/nC6=9.

4.2.3.4 RuSZ

RuSZ pretreated in hydrogen

The RuSZ sample was tested at temperatures somewhat lower than what is reported for the other samples because of a change in the experimental set-up. The activity of RuSZ was of the same order as IrSZ and RhSZ when they were tested at the same conditions (not reported here). The sample deactivates continuously and especially at temperatures above 200°C, this made the estimation of kinetic parameters difficult, and this is also the reason why this sample was not investigated further.

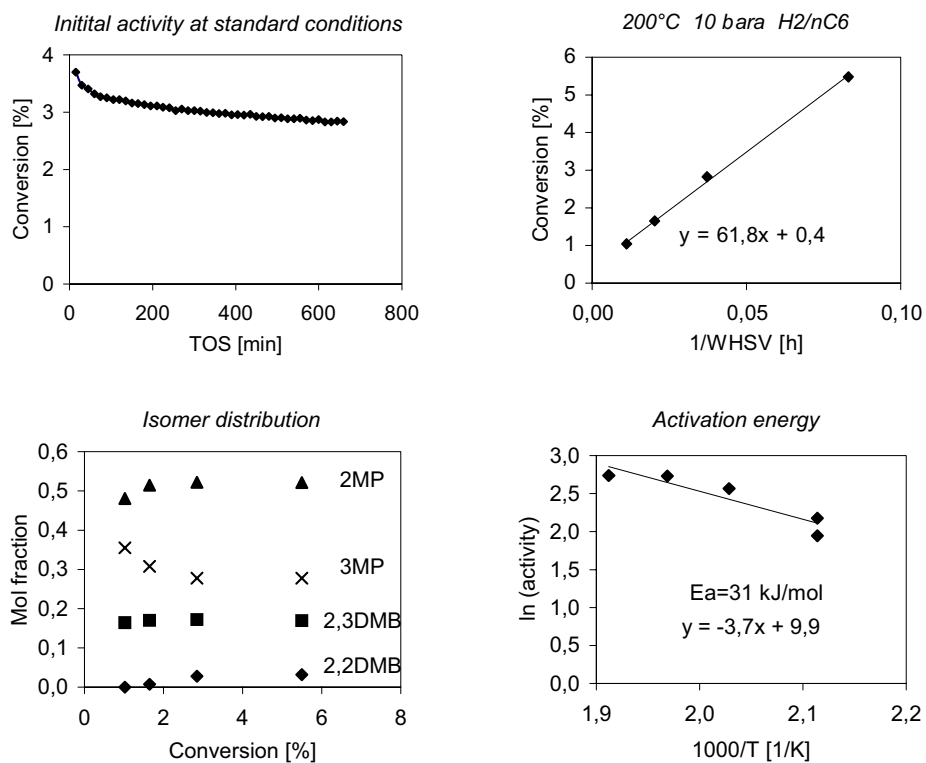


Figure 4.31 Catalytic test of RuSZ pretreated in hydrogen. Standard conditions: T=200°C, P_{TOT}=10 bara, H₂/nC₆=9.

4.2.3.5 SZ

The unpromoted SZ sample exhibited much poorer catalytic activity and stability compared to all of the promoted samples. The continuous deactivation made it impossible to estimate all the kinetic parameters of SZ. The activity as a function of hydrogen partial pressure seems to pass through a maximum, but the activity of the catalyst is very low, and there are just small changes in activity which gives a large uncertainty in the determination of the reaction order.

The selectivity to cracking products is substantially higher than for the promoted catalysts. The I/C ratio was around 30, corresponding to 96-97% selectivity to isomers, at 2.4% conversion. At such low conversion the promoted catalysts gave 100% selectivity to the isomers. However, unpromoted SZ show higher selectivity to dimethylbutanes than the promoted catalysts do (Table 4.9). The ratio between methylpentanes and dimethylbutanes (MP/DMB) is 3 for SZ at 2.4% conversion, while for the promoted catalysts and the commercial catalyst this ratio is around 6 at comparable conversions.

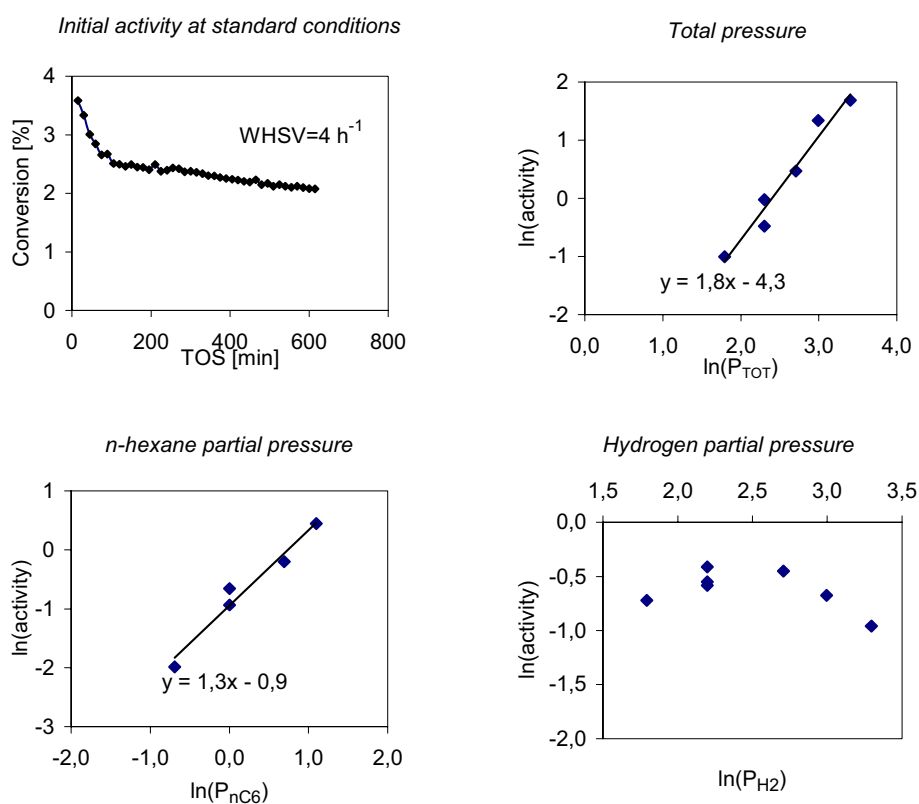


Figure 4.32 Catalytic test of SZ pretreated in hydrogen. Standard conditions: $T=200^\circ\text{C}$, $P_{\text{TOT}}=10$ bara, $\text{H}_2/\text{nC6}=9$.

It was as in the case of PtSZ possible to regenerate the activity of the catalyst after reoxidation at 450°C for 5 hours. The deactivation was even faster for the regenerated catalyst than the fresh sample (Figure 4.33).

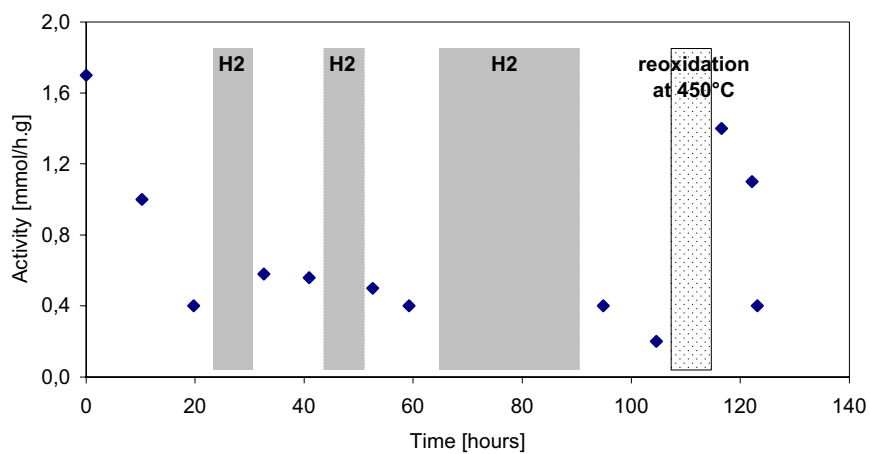


Figure 4.33 Deactivation and regeneration of unpromoted sulfated zirconia. Activity measured at standard conditions: 200°C, 10 bara, H₂/nC₆=9, WHSV=4/h In between the measurements at standard conditions other conditions have been examined.

4.2.3.6 Commercial catalyst

The commercial catalyst was pretreated according to the procedure given by the supplier. The catalytic test was performed at 235°C, a temperature that is not too different from the catalytic tests of the SZ samples, but still gives a conversion that is adequate. Otherwise the standard conditions are the same as for the samples of sulfated zirconia.

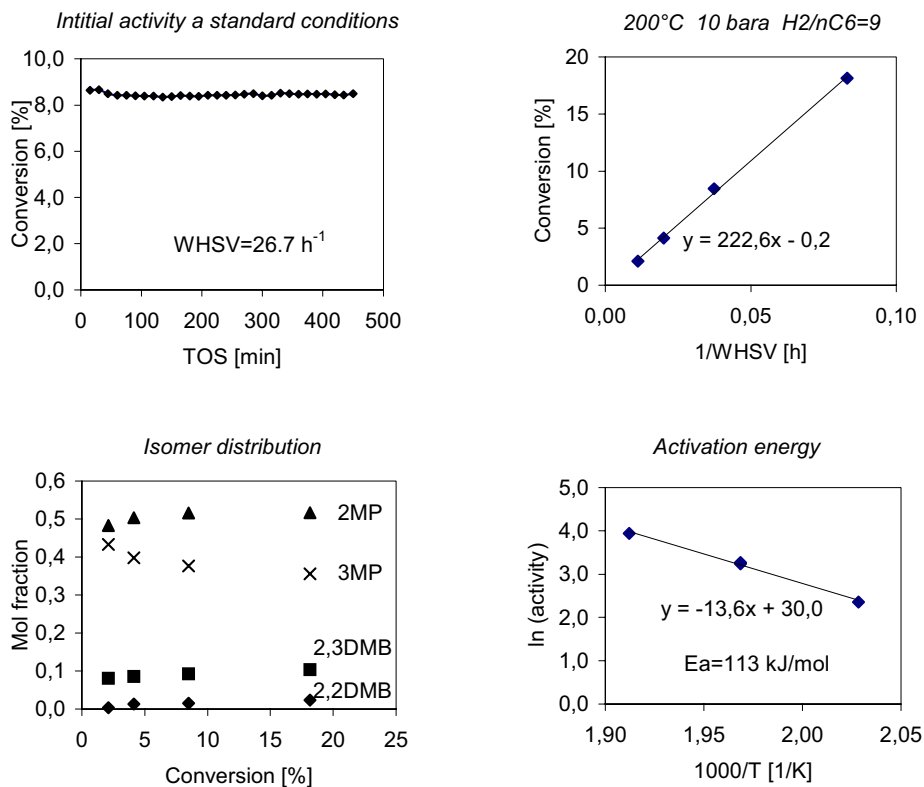


Figure 4.34 Catalytic test of commercial isomerization catalyst. Reaction conditions: 235°C, 10 bara, H₂/nC₆=9, WHSV=26.7/h

The reaction orders for hydrogen, *n*-hexane and total pressure were determined using a different reactor set-up. The thermocouple was placed differently from the new set-up where the other catalysts were tested. The temperature in the catalyst bed was about 210°C when examining these kinetic parameters, thus the activity measured in the old set-up is lower even if it apparently is at same conditions as in the new set-up.

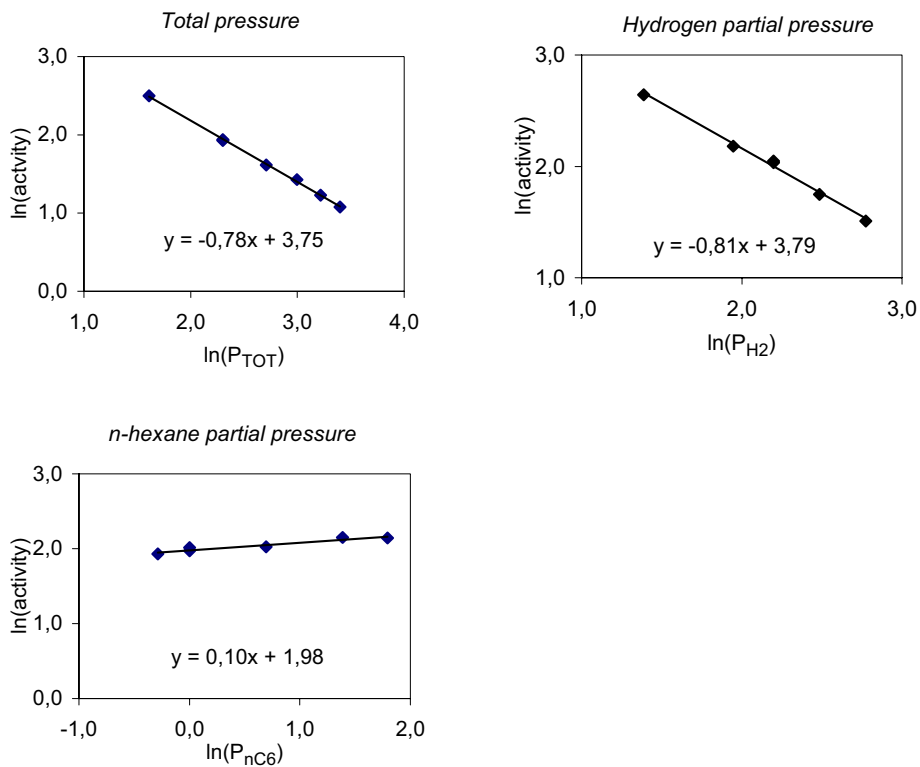


Figure 4.35 Reaction orders for hydrogen, *n*-hexane and total pressure. Standard conditions: $T=235^{\circ}\text{C}$, $P_{\text{TOT}}=10$ bara, $\text{H}_2/\text{nC}_6=9$.

The product distribution of the commercial catalyst is quite similar to the metal promoted SZ catalysts. The MP/DMB ratio was nearly the same for the two catalysts, the selectivity to isomers was slightly higher: 99.6 % selectivity at 43% conversion.

The commercial catalyst did not deactivate under these conditions, on the contrary it was observed a slight increase in the activity during the catalytic testing as shown in Figure 4.36.

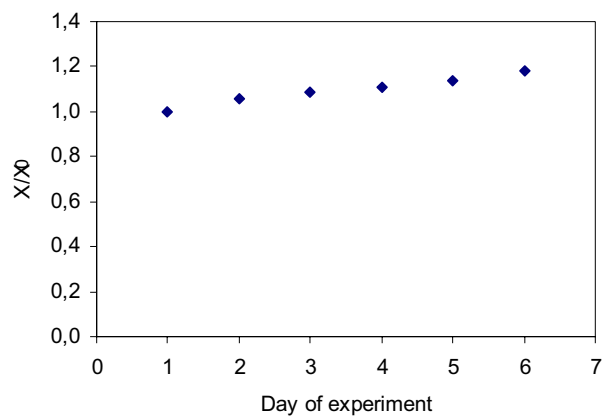


Figure 4.36 Development of the activity of the commercial isomerization catalyst during the catalytic testing. The conversion (X) is measured at standard conditions ($T=235^{\circ}\text{C}$, $P_{\text{TOT}}=10$ bara, $\text{H}_2/\text{nC}_6=9$), X_0 is the initial conversion.

4.2.3.7 Summary of the kinetic study

The comparison of the catalytic activity, the kinetic parameters and the isomer distribution for all the catalysts are summarized in Table 4.8 and Table 4.9. The activity of PtSZ sample at 235°C is included for comparison with the commercial isomerization catalyst.

Table 4.8 Activity and kinetic parameters of the various catalysts for n-hexane isomerization

Sample	Pretreatment	Activity ¹ [mmol/g.h]	E_A [kJ/mol]	Reaction order		
				Total	H ₂	n-hexane
PtSZ	H ₂	51	90	0.07	-1.0	0.9
	He	6.5	91	0.02	-0.9	0.9
IrSZ	H ₂	14	86	0.1	-0.9	0.9
	He	0.37	86	-0.3	n.d	n.d
RhSZ	H ₂	17	67	0.6	-0.5	1.0
	He	3.0	86	0.04	-0.6	0.6
RuSZ	H ₂	8.8 ²	31	n.d	n.d	n.d
SZ	H ₂	0.97	n.d	1.8	n.d	1.3
Commercial catalyst	H ₂	26	113	-0.8	-0.8	0.1
PtSZ at 235°C	H ₂	217	-	-	-	-

¹ Isomerization rate at standard conditions: $P_{TOT}=10$ bara, $T=200^\circ\text{C}$ (235°C for the commercial catalyst), $H_2/nC_6=9$

² Activity measurement performed in old set-up. The actual temperature in the catalyst bed is around 180°C .

Table 4.9 Isomer distribution for the various catalysts. Measurements were taken at standard conditions.

<i>Catalyst</i>	X_T [%]	<i>2MP</i>	<i>3MP</i>	<i>2,3DMB</i>	<i>2,2DMB</i>	<i>2MP/3MP</i>	<i>MP/DMB</i>
PtSZ	4	52	32	14	2.3	1.6	5.2
	13	53	33	13	1.9	1.6	5.6
IrSZ	4	52	32	15	1.9	1.6	4.9
	10	52	31	15	2.2	1.7	4.8
RhSZ	4	53	31	14	2.1	1.7	5.1
	12	52	30	15	2.6	1.7	4.7
RuSZ	4	52	28	17	2.8	1.9	4.0
SZ	2.5	48	28	21	4.0	1.7	3
Commercial catalyst	4	50	40	8.5	1.3	1.3	9.2
	13	52	35	11	2.7	1.5	6.6
Thermodynamical equilibrium		33	15	13	39	2.2	0.93

5 Discussion

In this work the isomerization activity of various acid catalysts has been investigated. And through the kinetic study of these catalysts the mechanism of the isomerization reaction will be elucidated, and the catalytic properties will be related to the chemical and physical properties of the samples.

5.1 Isomerization of *n*-butane at atmospheric pressure

Effect of promoters

The isomerization of *n*-butane has been reported to proceed via a bimolecular mechanism [49, 50] over acid catalysts, e.g. H-mordenite and sulfated zirconia, as described in chapter 2.3. The addition of iron and manganese to sulfated zirconia is claimed to facilitate this reaction pathway by enhancing the production of alkenes, which are important reaction intermediates in this mechanism [71-73].

Figure 4.4 shows that the unpromoted SZ sample is more active, both initially and after deactivation, than all of the FMSZ samples. This means that iron and manganese act as inhibitors rather than promoters under these conditions. The promoting effect of iron and manganese on sulfated zirconia in the isomerization of *n*-butane has been examined by several authors [15, 71-74, 76, 89, 91, 92]. Most studies are performed at low temperature, 35-100°C. In this temperature range iron and manganese are reported to have a promoting effect [15, 71, 72, 76, 89, 91]. Gao and co workers [92] reports that the activity of a FMSZ catalyst (1.5 wt% Fe, 0.5 wt% Mn) is 2-3 times higher than the activity of unpromoted and aluminum promoted SZ at 35°C. But at 250°C they find that the FMSZ catalyst is less active than unpromoted SZ and exhibits a much poorer stability than both aluminum promoted and unpromoted SZ. The initial activity of FMSZ is 67% of the activity of the unpromoted SZ. These results comply with the results of our study where the initial conversion over the (1.5)F(0.5)MSZ is about 45% of the conversion over unpromoted SZ.

It should be stressed that the preparation of promoted and unpromoted catalysts are not exactly identical. The promoted samples are impregnated with promoter (soaked in an aqueous metal nitrate solution) and dried at 100°C for 18 hours before sulfation. The impregnation step was skipped for the unpromoted sample. It is known that sulfated zirconia is very sensitive to the preparation parameters and procedures [19, 62, 68], and one might speculate that this could affect the properties of the final catalyst product, for example the hydration state or the textural properties.

Another possible explanation for the absence of a promoting effect of iron and manganese can be that the FMSZ catalysts are very active at the relatively high reaction temperature 250°C. If the initial activity is high the samples will deactivate so fast that real initial activity is concealed. Morterra *et al.* [86] found it likely that the iron and manganese additives still play a catalytic role at higher temperatures (150°C), but that it under these conditions acts against the isomerization mechanism.

This might be the accumulation of olefinic intermediates that eventually leads to the formation of oligomers capable of poisoning the active sites [86].

When only the promoted samples are considered, conversion decreases with increasing manganese content both at 1 minute and 60 minutes TOS. Initial conversion increases with increasing iron content, but for long-term activity (60 minutes TOS) there is a maximum in the activity with 1.5 wt% iron content and 0.5 wt% manganese. There seem to be a positive effect of iron on the activity which is expected from the reports in literature. Manganese is claimed to increase the dispersion of iron on the catalyst surface [76]. Optimum composition of the FMSZ catalyst was found to be 2wt% iron and 0.65wt% manganese, a further addition of manganese did not improve the catalytic activity [76]. This is in line with the negative effect of manganese we observe.

The unpromoted sample is unquestionably the most active catalyst at standard conditions with nitrogen as the diluent. However, the promoting effect of Fe and Mn seems to be more significant in a hydrogen atmosphere, as discussed under.

Effect of diluent

It is generally agreed that the isomerization of *n*-butane proceeds through a bimolecular pathway [50, 52]. Hydrogen inhibits this pathway since it inhibits the formation of hydrogen deficient species like carbenium ions and butenes which are crucial in this mechanism [76, 119], and it is suggested that in hydrogen atmosphere the isomerization over unpromoted SZ proceeds via the slower monomolecular pathway [119, 120]. It is proposed that the addition of promoters such as iron and manganese diminishes the negative effect of hydrogen over sulfated zirconia by promoting the production and stabilization of these hydrogen deficient intermediates [71-73, 80, 91]. In the experiments when nitrogen is the diluting gas, iron and manganese did not promote the isomerization of butane (Figure 4.4). It is however expected that the promoting effect of iron and manganese appear when nitrogen is replaced by hydrogen.

The isomerization activity of the unpromoted sample is considerably inhibited when *n*-butane is diluted in hydrogen. The high initial activity which is usually observed in a nitrogen atmosphere is not seen. The conversion is low initially and stays at the same level throughout the run as shown in Figure 4.7. The iron and manganese promoted catalyst on the other hand exhibits slightly higher activity in hydrogen than in nitrogen. These results are in accordance with the bimolecular mechanism since only C3 and C5 are observed as byproducts in the reactor effluent (see Appendix 4), and the positive effect of iron and manganese in hydrogen are in agreement with the results of Garcia *et al.* [76] and Song *et al.* [74, 81].

The unpromoted SZ sample has more and stronger Brønsted acid sites than (1.5)F(0.5)MSZ (Table 4.2). This indicates that the promoting effect of iron and manganese in hydrogen atmosphere must be related to some other properties than the acidity. This is probably related to the redox properties of the

oxides of Fe and Mn. Millet and coworkers [75] characterized iron and manganese after catalytic testing (*n*-butane isomerization). Their results suggest that the reducible iron species on FMSZ have been reduced in the catalytic conditions, most probably in the course of the oxidative dehydrogenation of *n*-butane to butene. Tabora and Davis [72] have also suggested that the Fe/Mn system forms butene initially in a single turnover oxidative reaction, this may explain why the FMSZ catalyst deactivates quite rapidly. In fact the deactivation is even faster in hydrogen than in nitrogen, though one would expect the contrary since hydrogen is reported to inhibit coke formation [8, 44].

Correlation between acidity and n-butane isomerization activity

As previously mentioned, most authors have studied *n*-butane conversion over FMSZ catalyst in the low temperature range, 30-100°C. Early reports, like Hsu and coworkers [15], attributed the promoting effect of iron and manganese to superacidic properties. They found by TPD of alkyl and fluorobenzenes that the FMSZ catalyst contained much stronger acid sites than the unpromoted catalyst. Later Davis *et al.* [82] found that for FMSZ and SZ the results from TPD of benzene cannot be correlated with the *n*-butane isomerization activity at 35°C. This is also supported by the findings of Adeeva *et al.* [16] who showed that there is no difference in the acid strength of neither Lewis nor Brønsted sites of FMSZ and SZ. Instead the redox properties of the FMSZ catalysts are usually emphasized to explain the differences in activity [80].

Figure 4.5b shows that there is a good correlation between strong Brønsted acid sites (sites that can retain pyridine after desorption at 350°C) and the initial catalytic activity. If the weaker acid sites are included too, the correlation is not that good (Figures 4.5 a and c). The same trends, although not so clear, are also observed for the deactivated catalyst (Figure 4.6). This indicates that acid sites of a certain strength are needed to catalyze *n*-butane isomerization at the present conditions. The unpromoted sample does not seem to fit into the rest of the catalyst series, but the IR data from thermodesorption of adsorbed pyridine (Table 4.2) show that SZ contains both more and stronger acid sites than all of the promoted samples. This can explain the extraordinary activity of unpromoted SZ compared to the other catalysts.

The WZ and PtWZ samples also fit into this picture, as shown in Figure 4.8. These samples possess few and very weak acid sites compared to that of the FMSZ samples, and they exhibit, as expected, very low *n*-butane isomerization activity.

Since the activity is clearly related to the acidity and the iron content is related to the activity (if only the promoted samples are considered) there has to be a relation between acidity and promoter content as well, as shown in Figure 5.1. The number of strong Brønsted sites increases with increasing iron content, whereas increased manganese content leads to an increase in the number of strong Lewis acid sites. The promoters do not change the total number of strong acid sites significantly.

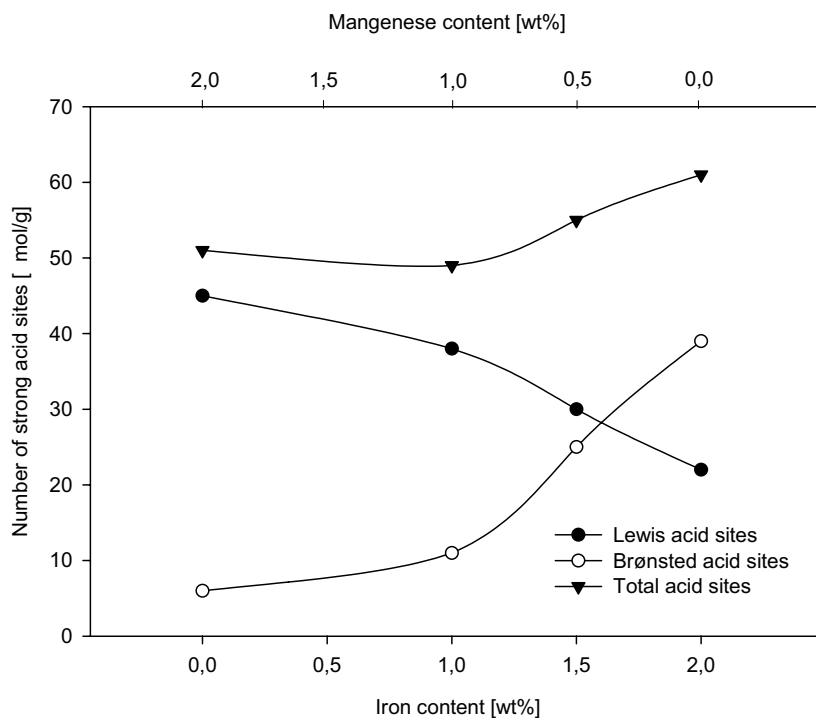


Figure 5.1 The number of strong acid sites as a function of the metal content.

As previously mentioned, Davis *et al.* [82] did not find a correlation between isomerization activity of FMSZ samples and their acidity measured by TPD of benzene. If the acidity is characterized by TPD of a base, e.g. ammonia or benzene, only the total number would be measured. According to our results, obtained in nitrogen and 250°C, the isomerization is catalyzed by the strong Brønsted sites only, while the total number of strong acid sites remains nearly unchanged, hence it would be impossible to explain the differences in activity from TPD alone.

It is difficult from our results to point out the relation between the acidity and other physical or chemical properties of the samples. One important characteristic, except from the IR data, that makes it possible to distinguish between the samples is the decomposition temperature of sulfate in the thermogravimetric analysis. The three catalysts with the strongest acid sites and highest activity lose sulfate at two distinct regions during heating, while the two other only lose sulfate in the high temperature region. Li and Gonzales [104] concluded that two different types of sulfates are present on the surface; one that decomposes at low temperature which is the active one. The other type which decomposes at higher temperature is inactive. This is in line with our observations, though it does not explain why some samples are more acidic than others.

Summary

From the discussion above we find that it is impossible to predict the *n*-butane isomerization activity of a catalyst just from the total number of acid sites and the distribution of their acid strength. It is apparent that it is important to know the strength of the acid sites, but at the same time also to distinguish between Lewis and Brønsted acid sites.

When nitrogen is replaced by hydrogen as the diluting gas, our results indicate that other properties than the acidity of the catalyst influences its catalytic activity. From what is reported in the literature this property is probably connected to the redox properties of the oxides of iron and manganese. We cannot exclude the possibility that there is also a contribution from the redox properties of the FMSZ catalysts in nitrogen atmosphere either, but under these conditions the acid characteristics seem to be the determining property for the conversion of *n*-butane.

5.2 Isomerization of *n*-hexane at elevated pressure

5.2.1 Preliminary catalytic tests

The preliminary catalytic tests showed that the poor stability of the FMSZ catalyst made it very difficult, and in some cases impossible, to estimate the kinetic parameters for the catalyst. Seeing that the FMSZ catalyst was rapidly deactivated in the case of *n*-butane isomerization, it is not unexpected that this catalyst is not stable during *n*-hexane isomerization either. Moreover, its high selectivity to cracking products makes it unsuitable as an isomerization catalyst as well. The PtSZ catalyst is more active, selective and stable than the FMSZ sample. It was therefore decided to continue the investigation on SZ promoted by platinum and make comparison to other noble metals like rhodium, ruthenium and iridium.

5.2.2 The noble metal promoted catalysts

Characterization of the samples

The characterization data show that the crystallinity and the textural properties of the catalysts in this series are identical. The variation in sulfur content is also almost within the limits of the uncertainty of the analysis method. This is not unexpected since all the catalysts originate from the same batch of SZ. The sulfur content of the samples is at the same level as in the studies we compare with [44, 45, 55, 56, 59]. IR spectroscopy of adsorbed pyridine and the TPR analysis are the only characterization techniques employed that show any difference between the samples.

The results from the TPR analysis show two interesting features. Firstly, a shift in the reduction temperature for the main reduction peak is observed when adding a metal to the catalyst. The fact that platinum and other metals enhance the reduction of sulfate has been reported before [53, 118, 121,

122]. In addition, it is reported that metals like platinum and ruthenium catalyze the reduction of SO_2 , formed over pure SZ, to H_2S [53, 121]. The formation of H_2S on our catalysts, even for the unpromoted sample was confirmed by the distinct smell of H_2S from the reactor after the TPR analysis.

The other feature of interest is the reduction peak in the low temperature range, 160-200°C, for RuSZ, RhSZ and IrSZ. This peak is assigned to the reduction of the metal oxide [118, 121]. These metals are thus in the oxidized state after calcination, which is line with Hino and Arata's results from XPS analysis of similar samples [9]. No such low temperature reduction peak is observed for the PtSZ sample which implicates that it is already in the reduced metallic state after calcination. Platinum reduction under air treatment may take place by either thermal decomposition of the platinum oxide or reduction of the platinum oxide by sulfur containing species [122]. The results of Dicko *et al.* [122] suggest that calcination at 600°C is necessary to reduce the platinum oxide. The calcination temperature in our case is 450°C, but still no peak for the reduction of platinum oxide is observed.

Another explanation for the absence of a reduction peak of platinum oxide can be that platinum is present as sulfide or sulfate or an oxide that is harder to reduce. Ebitani *et al.* [95] found that platinum in PtSZ remains in a high oxidation state even after reduction in hydrogen at 400°C. They claim that that in this case platinum is extremely difficult to reduce and therefore is mostly in the cationic state after reduction. This is unreasonable according our results which show that there is a considerable increase in the activity of the PtSZ sample when it is reduced at 300°C compared to the non-reduced sample.

The other property where variance between the samples is observed is the acidity. The acidity characterization does not fully describe the true state of the catalyst at reaction conditions. The samples were pretreated at 450°C before the IR spectroscopy of adsorbed pyridine, which is higher than the pretreatment before the catalytic test (i.e. 300°C). The TPR studies indicate that the sulfate is reduced in hydrogen at temperatures above 300°C, which means that some sulfate is lost from the samples and thus changes the acidity. This is unfortunate, but the analysis was performed after this pretreatment because at 300°C the spectra are not well-defined. The unpromoted sample was pretreated in air at 450°C because of a misunderstanding. This will probably not influence the acidity characterization that much since the TPR analysis shows that the reduction of pure SZ does not start before 450°C.

Correlation between acidity and n-hexane isomerization activity

The activity measurements over the FMSZ catalyst suggest that the *n*-butane isomerization activity is related to the strong Brønsted acid sites of the samples. From the acidity characterization of the noble metal promoted samples no such relation can be found neither for the Brønsted nor the Lewis acid sites, nor does the activity depend on the acid strength of the samples, as shown in Figure 5.2. The same lack of correlation between of acidity is found for all acid strengths and as well for the samples pretreated in helium.

The most active sample, PtSZ reduced in hydrogen, has substantially fewer and weaker acid sites than both SZ and PtSZ pretreated in helium, though the two last samples exhibit much lower catalytic activity. The number of both Lewis and Brønsted acid sites on PtSZ is higher than on IrSZ and RuSZ, and PtSZ contains stronger sites as well. The activity of those catalyst samples are only a third of that of the PtSZ sample, thus this appears to fit with the idea of that the reaction is controlled by the acidity of catalyst. The RhSZ sample also fits into this picture to some extent, though it contains more weak acid sites than PtSZ. The RhSZ sample has substantially more and stronger acid sites than IrSZ and RuSZ, but the activity of RhSZ is comparable to the two other.

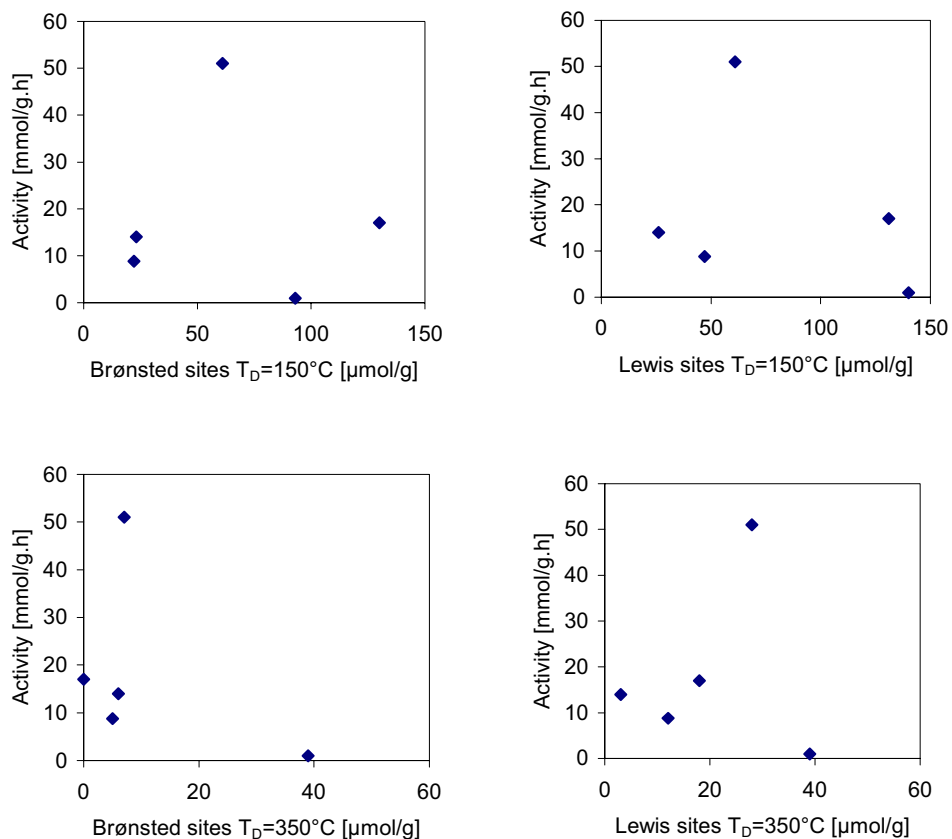


Figure 5.2 Activity of the reduced samples as a function of acid sites. T_D is the desorption temperature of adsorbed pyridine. Reaction conditions: 200°C, 10 bara, $\text{H}_2/n\text{-hexane} = 9$.

The acidity characterization of the PtSZ sample showed that it had less acid sites after reduction than after pretreatment in helium. As already mentioned the reduction temperature before the IR spectroscopy of adsorbed pyridine was higher (450°C) than before reaction (300°C) which means that

it does not necessarily reflect the true state of the catalyst under reaction conditions. It does however illustrate the different effect on acidity caused by the two pretreatments. These results suggest that there are other properties than acidity alone that is determining the catalytic activity. One obvious explanation, with the proposed bifunctional mechanism in mind, can be the promoters and the state of the promoters.

Correlation between promoter and activity

Experimental evidence for the oxidation state of the promoters can be found by TPR analysis. Reduction in hydrogen can have two effects on the properties of metal promoted sulfated zirconia; hydrogen can reduce the metal oxide, like observed in the TPR analysis of RuSZ, RhSZ and IrSZ, and it can reduce sulfate groups.

The activity measurements of PtSZ, IrSZ and RhSZ clearly show that when samples are pretreated in helium the activity is lower than for the equivalent sample reduced in hydrogen. This can be explained by the TPR analysis which shows that the promoters on IrSZ and RhSZ are in the oxidized state before pretreatment. When the metal is reduced it can provide the metal function in a bifunctional catalyst. It can be that it provides a dehydrogenating function and provides olefinic intermediates. Another possible function is that has a function in hydrogen spillover, and is therefore providing protons that increase the acid strength [44] or that it supplies hydrides which increase the rate of desorption [56].

An indication of the oxidation state of the promoting metals can also be found when comparing the activity of the catalysts with different pretreatments. The activity of the helium pretreated samples increases initially, while for the reduced catalysts a slight deactivation is observed. Assuming that the role of the promoter is to provide a site for dehydrogenating the alkanes, like in the classical bifunctional mechanism, the promoter must be in the reduced, metallic state [111]. This fits well with the fact that we observe an initial increase in the conversion, which can be caused by a build up of olefinic intermediates on the catalyst surface like observed for *n*-butane isomerization at low temperatures [20, 72]. An alternative explanation can be that the metal is being reduced initially and becoming more able to produce the olefinic intermediates as the oxides of the promoting metals are reported to be reduced at temperatures below 200°C [118, 121].

However, our results are complicated with respect to the platinum promoted sample and the effect of the pretreating gas. The TPR analysis indicates that platinum on PtSZ is in the Pt⁰ state after calcination, hence a reduction of the catalyst should be unnecessary like it was claimed by Comelli *et al.* [96], the catalytic activity is however, as mentioned above, much higher after reduction treatment. This either means that our conclusion from the TPR analysis is wrong and that platinum is not the reduced form or that it can exist in another form, e.g. as platinum sulfide, that can be harder to reduce, like claimed by Ebitani *et al.* [44].

Kinetic study

The reaction rate can be expressed by a power rate law,

$$r = k \cdot P_{\text{H}_2}^{\alpha} \cdot P_{\text{nC}_6}^{\beta} \quad (5.1)$$

where α and β represent the reaction orders of hydrogen and *n*-hexane, respectively. k is the rate constant which can be expressed by the Arrhenius equation:

$$k = A \cdot e^{-E_A / RT} \quad (5.2)$$

where E_A is the apparent activation energy of the reaction.

The kinetic parameters, α , β and E_A , can in combination with the isomer distribution give an indication of which mechanism that is prevailing over the different catalyst. Information on the role of the different promoters and hydrogen can also be obtained from these data.

The activation energy reported previously for *n*-hexane isomerization via a classical bifunctional mechanism is ranging from 84 – 126 kJ/mol [2, 123-125], this is higher than the values observed in liquid superacidic solutions which is in the range 65-75 kJ/mol [126]. The reaction order of hydrogen in this mechanism is found to be between -1 and 0 because of the inhibiting effect of hydrogen on the formation of olefins. The hydrocarbon reaction order is usually close to 1 [127], but for the bifunctional Pt/zeolite catalysts it is reported to be slightly positive [59, 128].

In the case of the sulfated zirconia catalyst, the dependency of the hydrogen partial pressure on the isomerization rate is reported to be both positive and negative and has as well been reported to go through a maximum. Ebitani *et al.* [44] found that a positive order for hydrogen in *n*-butane isomerization was owing to hydrogen spillover. The *n*-hexane isomerization activity was increasing with increasing hydrogen pressure, and a small positive effect was found for *n*-hexane [55]. A positive effect of both hydrogen and hydrocarbon partial pressures was also found by Iglesia *et al.* [56] on the *n*-heptane isomerization activity of a PtSZ catalyst. Negative orders of hydrogen has been found by Signoretto *et al.* [53] and Sayari *et al.* [81]. A maximum in the conversion as function of hydrogen pressure was found for *n*-butane isomerization [8]. The same was observed in the case of *n*-hexane isomerization by Paal *et al.* [60] and Duchet *et al.* [61, 111]. The hydrogen and *n*-hexane pressures are much lower in the former of those reports than in our study, while in the latter the conditions are comparable to our experiments.

Although the activity of the tested samples differs much, their response to the reaction temperature and the partial pressures of *n*-hexane and hydrogen are fairly similar. All the catalysts, with the exception of the unpromoted SZ sample, show a negative order with respect to hydrogen. The reaction order for *n*-hexane is positive and close to 1 except in the case of the commercial zeolite catalyst, where it is nearly zero. The reaction order is expected to be lower for zeolites than for sulfated zirconia due to the differences in pore structure for these two classes of catalysts.

The reaction order of hydrogen being negative for all metal promoted SZ samples, while for *n*-hexane the order is positive. This is a clear indication to that the isomerization reaction proceeds via the classical bifunctional mechanism, where the role of the metal is to form olefinic intermediates. The activation energy is within the low end of the range reported for bifunctional catalysts, but is still above the typical values for superacids. The activation energy of the commercial catalyst is at the same level as reported for Pt/H-mordenite, Pt/mazzite and Pt/ZSM-22 [128, 129].

The kinetic parameters of IrSZ and PtSZ are almost identical, and the product distributions are similar for the two catalysts. In addition, the product distribution and the kinetic parameters seem to be independent of the pretreatment. From these results it seems like the mechanism is independent of the promoting metal and the oxidation state of the metal, the activity does however change considerably if promoter or pretreatment is changed. This implicates that the number of active sites is the limiting factor. Reduction of the catalyst always gives the most active catalyst, indicating that it is the number of metallic sites that limits the reaction rate.

The high activity of the reduced catalyst compared to the helium pretreated catalyst could be well explained on the basis of the bifunctional mechanism. When the catalyst is being reduced one can assume that the promoting metal will be reduced and thus give a more effective dehydrogenation catalyst. In the case of the helium pretreated catalysts it is likely that there are less metallic sites present on the surface, especially in the case of IrSZ and RhSZ which according to the TPR analysis are in the oxidized state. These catalysts do however seem to follow the same mechanism as the reduced catalyst. One possible explanation can be that the metals are partially reduced. The TPR analysis does not give any information of the degree of oxidation of metals. If the metals are partially reduced they can have some capacity for dehydrogenation of the alkanes, this capacity is increased upon further reduction treatment. The behavior of the unreduced catalysts supports this hypothesis. During the catalytic tests the activity of these samples increased with time on stream, which is the opposite of what is observed for the prereduced samples. The obvious explanation is that the metal on the catalyst is being reduced during the tests. The reaction conditions are reductive due to a large excess of hydrogen. The increase in activity is especially noticeable when the temperature is being increased during the investigation, which implies that the promoter is being reduced. Figure 4.27 shows that during the test of the IrSZ sample the activity is nearly doubled. The trend is the same for the samples of PtSZ and RhSZ when they are pretreated in helium, although the effect is most pronounced for the IrSZ sample. Even though the activity increases during the run it never reaches the level of the reduced samples. The reason probably is that temperature during the catalytic run is lower than 300°C, and it is therefore difficult to achieve a complete reduction of the metal. It is also possible that the presence of hydrocarbons inhibits the reduction.

The PtSZ sample appears to have properties that are different from what has been reported in the literature. The negative reaction order corresponds to a classical bifunctional mechanism, while in the

isomerization reaction the reaction order over other platinum promoted sulfated zirconia catalysts has been reported to be positive or going through a maximum [8, 44, 45, 55, 56, 60].

As mentioned earlier, the catalytic properties of sulfated zirconia are very sensitive to differences in the preparation route. The groups who have found a positive reaction order have impregnated the catalyst with both sulfate and platinum before calcination at 600°C or higher. This one-step impregnation followed by calcination at high temperature probably leads to a stronger interaction between the acidic function (sulfate) and the metal function. And the positive effect of hydrogen has indeed been explained by models with metal-acid ensembles as the active site. These ensembles, where the acid and the metal exist in close proximity, have been given different names like “the collapsed bifunctional site” [59], “the compressed bifunctional site” [60] or a “metal-proton adduct” [11]. None of these models fits our data.

Duchet and coworkers [45] on the other hand impregnated the zirconium hydroxide with sulfate before calcination at 600°C. The crystalline sulfated zirconia was then impregnated with platinum and finally calcined at 480°C. This synthesis route is similar to the one used here, and in addition the catalysts has properties like sulfur content (~2wt%) and a platinum content at a comparable level. These properties makes their work a good basis of comparison.

Duchet *et al.* [45] observe a maximum in *n*-hexane isomerization as function of the hydrogen pressure. The position of this maximum does however shift when the *n*-hexane pressure is increased. When the *n*-hexane pressure is 1 bar, which is the same as our standard conditions, the activity is continuously decreasing, though this is not emphasized by the authors. This confirms our results, but it also points to that the reaction orders can change as the reaction conditions change. We find that the reaction order of the total pressure is close to zero, which implicates that the reaction orders do not change even if the *n*-hexane pressure changes.

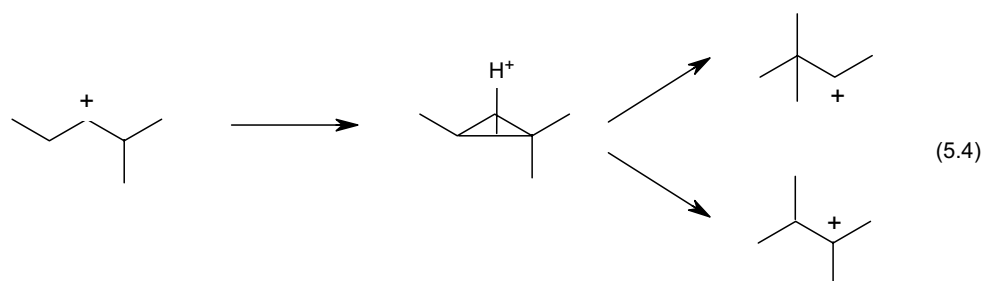
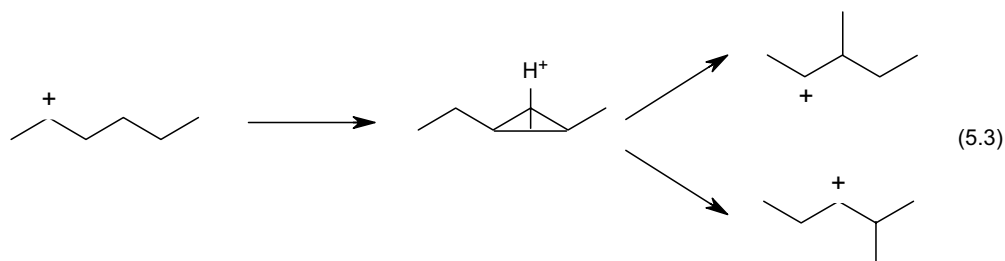
In summary, the kinetic study of the noble metal promoted sulfated zirconia catalysts show that the reaction order of hydrogen is negative while the reaction order of *n*-hexane is close to one for most of the samples. The activation energy is found to be similar to the bifunctional commercial Pt/zeolite catalyst, and the activation energies of both catalysts are within the typical range of bifunctional catalysts. All the results of the kinetic study point to that the classical bifunctional mechanism is prevailing over the noble metal promoted sulfated zirconia.

Product distribution

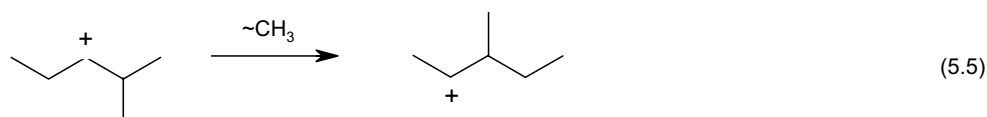
Table 4.9 shows that the isomer distributions of PtSZ, IrSZ, RuSZ, RhSZ and the commercial catalyst are similar. From the distribution of isomers it appears that 2MP, 3MP and 2,3DMB are formed directly from *n*-hexane (e.g. Figure 4.21 and 4.24) and that 2,2DMB is formed consecutively by isomerization of 2,3DMB. The fraction of 2,3DMB is close to the equilibrium level. The ratio between 2MP and 3MP

is approaching to their equilibrium ratio but are present at higher levels than predicted from thermodynamical calculations. 2,2DMB on the other hand is far from the equilibrium composition.

Based on the kinetic parameters the isomerization reaction seems to follow a bifunctional mechanism over the promoted catalysts. According to this mechanism 2,3DMB should be formed consecutively to that of the methylpentanes, with a simultaneous formation of 2,2DMB [128].



The formation of 2,2DMB is the slowest isomerization reaction owing to that it involves the formation of secondary carbenium ion while 2,3DMB involves the more energetically favorable tertiary carbenium ion. This is in accordance with what is observed for all the examined catalysts. It is expected from reaction (5.3) that 2MP and 3MP should be formed at similar rates and therefore be found in equimolar quantities in the product stream [128]. This is indeed observed at very low conversions, but as conversion increases the ratio between 2MP and 3MP approaches the thermodynamic equilibrium because of a rapid isomerization through a methyl shift [128] as shown in equation (5.5).



The unpromoted catalyst on the other hand shows higher selectivities to the dimethylbutanes than the promoted SZ catalysts and the commercial sample, indicating that the reaction proceeds via a different mechanism than the bifunctional one.

Comparison of the different promoters

According to the kinetic parameters and the product distribution, the isomerization of *n*-hexane over noble metal promoted sulfated zirconia proceeds via the classical bifunctional mechanism. The activity of the metals in alkane dehydrogenation is probably an important parameter in determining its isomerization activity. Platinum is well known as a good dehydrogenation catalyst, for instance as the bifunctional Pt/chlorided alumina catalyst used in catalytic reforming.

A comparative study of the dehydrogenation activity of the noble metal examined in this work is, to our knowledge, not reported in the literature. The activities of these metals in hydrogenation of cycloalkenes, which is the reverse reaction, has been examined, though under quite different conditions than in our work [130, 131]. They report that platinum and rhodium have similar activities in cycloalkene hydrogenation, while the activities of iridium and ruthenium are much lower. These results alone can not explain the differences between the metals that we observe in *n*-hexane isomerization.

It is also likely that the promoting metals play other roles than just in the dehydrogenation of the alkanes. One important function is to stabilize the catalytic activity, for example by hydrogenating coke precursors. It may also be that the promoters may affect the acidity of the catalysts, e.g. by facilitating the reduction of sulfates and then reduce the number of Brønsted acid sites. The acidity can also be changed during the reaction by hydrogen spillover, thus the activity of the metals in the dissociative adsorption of hydrogen may also be important.

There may be several properties of the promoting metal that is determining for its activity, and the results do not give any conclusive evidence for the role of the promoter. The kinetic study does however indicate that the bifunctional mechanism is prevailing, thus it would be interesting to investigate the activity of the catalysts in pure hydrogenation/dehydrogenation reactions to clarify the differences in dehydrogenating activity of the promoting metals.

Comparison with the commercial catalyst

The commercial catalyst was less active than the PtSZ sample and therefore the standard reaction temperature during the catalytic tests was set to 235°C for this sample. In Table 4.8 the activity of the both catalysts at 235°C are shown. The activity of the PtSZ sample is 8 times higher than the commercial catalyst under these conditions. The stability of the commercial catalyst is however much better, in fact it was observed a slight increase in activity for this catalyst as shown in Figure 4.36.

Pretreatment

The examination of the effect of the pretreatment procedure, i.e. the temperature and the atmosphere, was not a major objective in this project. Some interesting features were however discovered during the initial experiments.

It is common to activate the catalysts in air in situ before the reaction is started, like it was done before *n*-butane isomerization over the FMSZ catalysts. In case of the series of noble metal promoted catalysts the activation step was skipped since the catalyst already had been precalcined twice. The catalysts were instead pretreated with hydrogen to ensure that the promoting metal would be in the metallic state. In some cases the catalyst was pretreated in helium to examine the effect of the pretreating gas. In the case of the unpromoted SZ sample it should be unnecessary to reduce the catalyst, yet this was done to make sure the history of the samples were as similar as possible.

Figure 4.23 shows that when increasing reduction temperature the catalytic activity is decreasing. This is in line with what is found by van Gestel *et al.* [111], who also reported the same, though it was in a lower temperature range, 150-250°C. They also found that the activity for toluene hydrogenation was more affected by the increase in reduction temperature, and attributed this to sulfur poisoning of platinum sites. The drop in the *n*-hexane isomerization activity was attributed to reduction of sulfate groups leading to a loss of acid sites [111].

We observe a dramatic drop in the activity when the reduction temperature is increased from 300°C to 325°C. This temperature is coincident with the onset of sulfate reduction found from the TPR analysis. It is therefore likely that this drop in activity is due to the loss of surface sulfate. When the reduction temperature is further increased to 337°C the activity diminished to a nearly insignificant level, and nearly all of the sulfate groups are presumably transformed to H₂S after 3 hours reduction at this temperature.

Pretreatment in helium at 300°C gives a catalyst with much poorer activity than after reduction at the same temperature. This can be explained by the change in oxidation state of the promoting metal as described above. When increasing the pretreatment temperature to 337°C the activity is decreased even further, this can reflect that the increase in the temperature alters the hydration state of the catalyst as reported by Hong [62]. The increased temperature can result in less adsorbed water on the surface which leads to a transformation of the Brønsted sites to Lewis sites. The change in hydration state can be a part of the effect we observe with increasing reduction temperature. And the combined effect of reduced Brønsted acidity from the dehydration and loss of surface sulfate groups leads to a more dramatic effect on the acidity.

Deactivation and regeneration

Poisoning of the active sites by coke is one of the most frequently proposed reasons for deactivation of SZ catalysts during alkane isomerization. Alternatively, the activity can be lost by partial reduction of the sulfate groups. Both catalyst deactivation by coke formation and reduction of the sulfur species can be regenerated by reoxidizing the catalyst at temperatures above 400°C [102, 104]. If the catalyst is deactivated by for instance loss of sulfur in the form of H₂S or migration from the surface to the bulk

of the catalyst it will not be possible to regenerate the catalytic activity by reoxidizing. The same is the case if the deactivation is caused by loss of the promoter.

After reoxidizing the catalyst in a 2% oxygen stream at 450°C for 3 hours, followed by reduction by the standard procedure the initial activity was completely recovered for both the PtSZ sample and the unpromoted one. This observation points to two possible causes for deactivation, i.e. coke formation and reduction of sulfate groups. One of the proposed roles of platinum is to prevent coke formation and increase the stability of the SZ catalyst [4, 8, 53, 55]. It is therefore likely that the large difference in stability between PtSZ and unpromoted SZ is due to this stabilizing effect. This conclusion is supported by a XPS analysis of a SZ sample, showing that the deactivation did not result in a change of the oxidation state of sulfur. Instead poisoning of the active sites by coke formation was found to be the main cause of the deactivation [132]. Though coke formation on the catalyst surface is believed to be the main reason for the deactivation of the SZ catalyst, we cannot rule out the possibility of reduction of the sulfur species to be contributing as well.

When platinum is added to the catalyst the deactivation behavior is different, as expected. Figure 5.3 shows the deactivation/regeneration during a catalytic run where the flow of *n*-hexane was interrupted during two periods, but the conditions were otherwise unchanged. The deactivation slope is the same throughout the catalytic test, even in the periods when no *n*-hexane is fed to the reactor. This points to the reduction of sulfate species as the main cause to deactivation since no coke can be formed during these periods, and the reducing hydrogen was always present.

Even though the TPR analysis shows that the onset of sulfur reduction is above 300°C, the sulfur can probably be reduced during catalytic testing. The hydrogen partial pressure is much higher at the reaction conditions, 9 bar compared to 0.07 bar during the TPR analysis, thus the rate of the reduction is quite different.

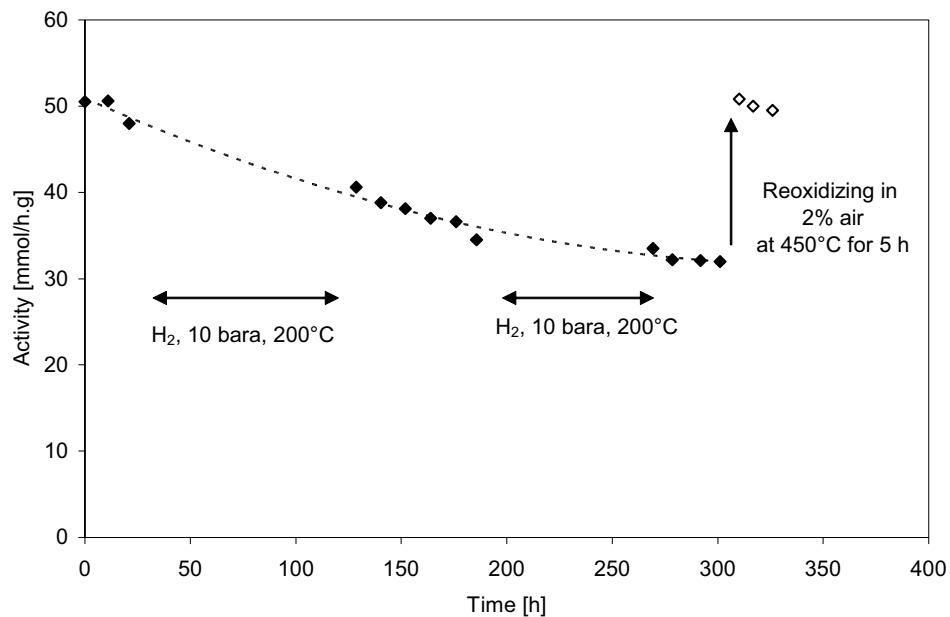


Figure 5.3 Deactivation and regeneration of PtSZ. The activity measurements were taken at standard conditions: 200°C, $P_{\text{TOT}}=10$ bara, $H_2/nC_6=9$. During two periods the *n*-hexane flow was interrupted while the conditions otherwise were unchanged.

The TPR analysis shows that the reduction of sulfur demands a considerably higher temperature on SZ than on PtSZ, thus the contribution of sulfur reduction to the deactivation is believed to be less in the case of SZ. The conclusion is therefore that poisoning of the active sites by coke is the main cause of deactivation for the unpromoted SZ sample, but reduction of sulfate species can not be ruled out. The situation is contrary for the PtSZ sample, reduction of sulfate groups is the main cause of deactivation, but coke formation can be contributing as well.

One obvious way of checking if the catalyst is deactivated by coke formation or sulfur loss is by analyzing the content of these two compounds before and after the reaction. This was difficult because the catalyst was diluted with silicon carbide (SiC) in the catalyst bed to avoid temperature gradients and bypassing of the reactants. The SiC particles were of the same size as the catalyst which made it very difficult to separate them from the catalyst particles, and since it contains carbon it makes the analysis difficult.

5.3 Suggestions for further work

To improve the understanding of the mechanism of the isomerization reaction it is essential to develop a detailed kinetic model for the reaction. This model should involve the individual steps as they are outlined in the classical bifunctional mechanism.

To implement such a model it will be necessary to know the properties of the catalyst better. The properties of main interest, when considering a bifunctional catalyst, are the activity of the metal in the dehydrogenation/hydrogenation reaction and the acidity of the catalyst. For the investigation of the activity of the catalyst in the dehydrogenation/hydrogenation reaction it could be useful to use test reactions. This could for instance be toluene hydrogenation, like van Gestel *et al.* [111] have reported for platinum promoted sulfated zirconia.

In this work it was difficult to obtain well defined IR spectra after pretreating the sample at 300°C. It should be possible to develop a method that can reflect the true state of the catalyst after pretreatment. Alternatively, it should be possible to change the pretreatment procedure before the catalytic test so that it resembles the ideal pretreatment before IR spectroscopy. This could for instance be calcination in situ at 450°C before the standard reduction at 300°C. This alteration in pretreatment gives a procedure that is similar to the regeneration procedure, and should not change the catalyst properties much, like it was observed for the regenerated catalyst.

6 Conclusions

A series of iron and manganese promoted SZ catalysts was prepared, characterized and tested for their catalytic activity in *n*-butane isomerization. The activity at 250°C and atmospheric pressure was related to the physical and chemical properties of the sample. No promoting effect of iron and manganese was found when *n*-butane was diluted in nitrogen. When nitrogen was replaced by hydrogen as the diluting gas the activity of the unpromoted SZ sample was dramatically lowered, while the activity of the promoted catalyst was not significantly changed. The presence of dihydrogen is known to suppress the formation of hydrogen deficient species, like alkenes. These species are crucial in the bimolecular isomerization mechanism. It is therefore likely that the role of iron and manganese is to facilitate the formation of butenes. It is not clear from our work whether the iron and manganese species stabilize the transition state or if they facilitate the formation of alkenes via redox reactions.

If we only consider the promoted samples, the catalytic activity increases with increasing iron/manganese ratio. We also observe that the activity of the samples is clearly correlated with the number of strong Brønsted acid sites. The total number of strong acid sites (i.e. the sum of Brønsted and Lewis sites) does not change significantly when the promoter content is changing, hence no correlation between catalytic activity and the total number of acid sites is found. This underlines the importance of discrimination between Lewis and Brønsted acidity when characterizing the acidity of the samples.

One of the iron and manganese promoted samples was also tested for its activity in *n*-hexane isomerization at elevated pressure. The catalyst was not very active, and it deactivated fast and showed a high selectivity to cracking products as well. Sulfated zirconia promoted by platinum or other noble metals is superior to the FMSZ sample when it comes to activity, stability and selectivity to branched isomers.

Among the noble metal promoted samples the catalyst promoted with platinum was the most active. The samples promoted with rhodium, ruthenium and iridium showed a lower, and similar activity. Common for all the noble metal promoted catalysts is the large increase in activity when catalysts are reduced with hydrogen compared to when they are pretreated in helium. The increase in activity is most likely connected to the reduction of metal oxides of the promoters to ensure that the promoters are in the metallic state. Reduction at too high temperatures does however give lower activity. This is probably due to the reduction of surface sulfate groups leading to a loss of acid sites.

The PtSZ sample is 8 times more active than the commercial isomerization catalyst at 235°C. The stability of the commercial sample is however better, in fact a slight increase in the activity was observed in the long term experiments.

As already mentioned, the noble metal promoted catalysts were more stable than SZ promoted with iron and manganese and unpromoted SZ. The activity of both the platinum promoted and the unpromoted catalyst was completely regenerated after reoxidation in air at 450°C. It appears that presence of the noble metal promoters inhibits the formation of coke, like previously reported in the literature. The deactivation of the PtSZ sample is most likely due to reduction of sulfate groups.

The kinetic study of all the noble metal promoted SZ samples showed reaction orders of hydrogen, *n*-hexane and total pressure that are typical for the classical bifunctional mechanism. A negative reaction order of hydrogen is also observed for the commercial Pt/zeolite catalyst, and the activation energies of two types of catalysts are both within the range that is typical for bifunctional catalysts. All the data point to that noble metal promoted sulfated zirconia is a classical bifunctional catalyst like platinum promoted zeolites and platinum on chlorided alumina.

All the noble metal promoted SZ catalysts and the commercial isomerization catalyst showed close to 100% selectivity to branched hexane isomers, and the isomer distribution is similar for all these catalysts. 2MP, 3MP and 2,3DMB appear to be formed directly from *n*-hexane, while 2,2DMB appears to be formed consecutively. The 2MP/3MP ratio is approaching the equilibrium ratio as the conversion increases, and the 2,3DMB level is close to what is predicted from the thermodynamical calculations. Formation of 2,2DMB involves the formation of a primary carbenium ion, and this isomer is thus far from the equilibrium composition. The isomer distribution being the same for the noble metal promoted catalyst and the Pt/zeolite is another indication that the isomerization proceeds via the bifunctional mechanism over the promoted samples. The unpromoted SZ catalyst shows higher selectivity to cracking products than the promoted samples do. It also shows higher selectivities to dimethylbutanes, which indicates that the reaction proceeds via a different pathway than the bifunctional mechanism over this catalyst.

The observed differences between the different promoters can not be explained from the acidity characterization data. The *n*-hexane isomerization proceeds via the classical bifunctional mechanism, which means that the dehydrogenation activity of the promoting metals must be important. A study of the hydrogenation/dehydrogenation activity of the noble metal promoted catalysts would be useful to clarify this issue.

7 References

- [1] T. Kimura, *Catal. Today* **81**(2003), 57-63.
- [2] M. Belloum, C. Travers and J. P. Bournonville, *Revue de l'institut francais du petrole* **46**(1991), 89-107.
- [3] M. de Boer and C. Johnson, *Catalyst Courier - courier* 33 (1998),
- [4] J. B. Laizet, A. K. Søiland, J. Leglise and J. C. Duchet, *Topics Catal.* **10**(2000), 89-97.
- [5] V. C. F. Holm and G. C. Bailey, *US Patent 3,032,599* (1962), 1-4.
- [6] M. Hino and K. Arata, *J. Am. Chem. Soc.* **101**(1979), 6440.
- [7] G. D. Yadav and J. J. Nair, *Micropor. Mesopor. Mater.* **33**(1999), 1-48.
- [8] F. Garin, D. Andriamasinoro, A. Abdulsamad and J. Sommer, *J Catal* **131**(1991), 199-203.
- [9] M. Hino and K. Arata, *Catal. Lett.* **30**(1995), 25-30.
- [10] S. R. Vaudagna, R. A. Comelli and N. S. Figoli, *React. Kin. Catal. Lett.* **63**(1998), 33-40.
- [11] Ü. B. Demirci and F. Garin, *Catal. Lett.* **76**(2001), 45-51.
- [12] G. A. Mills, H. Heinemann, T. H. Milliken and A. G. Oblad, *Ind. Eng. Chem.* **45**(1953), 134-137.
- [13] C. -Y. Hsu, C. R. Heimbuch, C. T. Armes and B. C. Gates, *J. Chem. Soc. Chem. Commun.* (1992), 1645-1646.
- [14] A. S. Zarkalis, C. Y. Hsu and B. C. Gates, *Catal. Lett.* **29**(1994), 235-239.
- [15] C. -H. Lin and C. -Y. Hsu, *J Chem. Soc. Chem. Commun.* (1992), 1479-1480.
- [16] V. Adeeva, J. W. d. Haan, J. Jänchen, G. D. Lei, V. Schünemann, L. J. M. v. d. Ven, W. M. H. Sachtler and R. A. v. Santen, *J. Catal.* **151**(1995), 364-372.
- [17] D. J. McIntosh, R. A. Kydd and J. M. Hill, *Chem. Eng. Comm.* **191**(2004), 137-149.
- [18] X. Song and A. Sayari, *CatalRev-SciEng.* **38**(1996), 329-412.
- [19] B. S. Klose, R. E. Jentoft, A. Hahn, T. Ressler, J. Kröhnert, S. Wrabetz, X. Yang and F. C. Jentoft, *J. Catal.* **217**(2003), 487-490.
- [20] M. Risch and E. E. Wolf, *Catal. Today* **62**(2000), 255-268.
- [21] O. A. Rokstad, *Personal communications*
- [22] J. A. Ridgway Jr and W. Schoen, *Ind.Eng.Chem.* **51**(1959), 1023-1026.
- [23] Y. Ono, *Catal. Today* **81**(2003), 3-16.
- [24] K. Arata, *Adv. Catal.* **37**(1990), 165-211.
- [25] A. Corma, *Chem. Rev.* **95**(1995), 559-614.
- [26] L. M. Kustov, V. B. Kazansky, F. Figueras and D. Tichit, *J. Catal.* **150**(1994), 143-149.
- [27] C. Morterra, G. Cerrato, F. Pinna and M. Signoretto, *J. Phys. Chem.* **98**(1994), 12373-12381.
- [28] T. Yamaguchi, T. Jin, T. Ishida and K. Tanabe, *Mater. Chem. Phys.* **17**(1987), 3-19.
- [29] T. Lei, J. S. Xu, Y. Tang, W. M. Hua and Z. Gao, *Appl. Catal. A: General* **192**(2000), 181-188.
- [30] M. -T. Tran, N. S. Gnep, G. Szabo and M. Guisnet, *Appl. Catal. A: General* **171**(1998), 207-217.
- [31] K. Ebitani, J. Tsuji, H. Hattori and H. Kita, *J. Catal.* **135**(1992), 609-617.

- [32] B. H. Davis, R. A. Keogh and R. Srinivasan, *Catal. Today* **20**(1994), 219-256.
- [33] K. Arata and M. Hino, *Mater. Chem. Phys.* **26**(1990), 213-237.
- [34] P. Nascimento, C. Akrapoulou, M. Oszagyan, G. Coudurier, C. Travers, J. F. Joly and J. C. Vedrine, *New Frontiers in Catalysis*. (Guszi *et al.*, ed.), **75** Elsevier, Amsterdam, 1993, pp. 1185-1197.
- [35] S. X. Song and R. A. Kydd, *J. Chem. Soc., Faraday Trans.* **94**(1998), 1333-1338.
- [36] K. B. Fogash, G. Yaluris, M. R. González, P. Ouraipryvan, D. A. Ward, E. I. Ko and J. A. Dumesic, *Catal. Lett.* **32**(1995), 241-251.
- [37] M. Hino and K. Arata, *J. Chem. Soc. Chem. Commun.* **18**(1988), 1259-1260.
- [38] G. Larsen and L. M. Petkovic, *Appl. Catal. A: General* **148**(1996), 155-166.
- [39] S. Kuba, P. Lukinskas, R. K. Grasselli, B. C. Gates and H. Knosinger, *J. Catal.* **216**(2003), 353-361.
- [40] S. R. Vaudagna, R. A. Comelli and N. S. Figoli, *Appl. Catal. A: General* **164**(1997), 265-280.
- [41] M. Guisnet, P. Bichon, N. S. Gnep and N. Essayem, *Topics Catal.* **11/12**(2000), 247-254.
- [42] N. Essayem, G. Coudurier, M. Fournier and J. C. Vedrine, *Catal. Lett.* **34**(1995), 223-235.
- [43] K. Na, T. Okuhara and M. Misono, *J. Chem. Soc. Faraday Trans.* **91**(1995), 367-373.
- [44] K. Ebitani, J. Konishi and H. Hattori, *J. Catal.* **130**(1991), 257-267.
- [45] J. C. Duchet, D. Guillaume, A. Monnier, C. Dujardin, J. P. Gilson, J. van Gestel, G. Szabo and P. Nascimento, *J. Catal.* **198**(2001), 328-337.
- [46] B. C. Gates, *Catalytic Chemistry*. John Wiley & Sons, New York, 1992.
- [47] V. Adeeva, H. -Y. Liu, B. -Q. Xu and M. H. Sachtler, *Topics Catal.* **6**(1998), 61-76.
- [48] V. Adeeva, H. -Y. Liu, B. -Q. Xu and W. M. H. Sachtler, *Topics Catal.* **6**(1998), 61-76.
- [49] M. Guisnet, *Acc. Chem. Res.* **23**(1990), 392-398.
- [50] C. Bearez, F. Avendano, F. Chevalier and M. Guisnet, *Bull. Soc. Chim. Fr.* (1985), 346-348.
- [51] C. Bearez, F. Chevalier and M. Guisnet, *Reaction Kinetics and Catalysis Letters* **22**(1983), 405-409.
- [52] V. Adeeva and W. M. H. Sachtler, *Appl. Catal. A: General* **163**(1997), 237-243.
- [53] M. Signoretto, F. Pinna, G. Strukul, P. Chies, G. Cerrato, S. Di Ciero and C. Morterra, *J. Catal.* **167**(1997), 522-532.
- [54] R. Bouiti, *Isomérisation d'alcanes légers sur catalyseurs acides et bifonctionnels Pt-acides.*, Doctoral thesis, Université de Poitiers, France, 2003.
- [55] R. A. Comelli, S. R. Finelli, S. R. Vaudagna and N. S. Figoli, *Catal. Lett.* **45**(1997), 227-231.
- [56] E. Iglesia, S. L. Soled and G. M. Kramer, *J. Catal.* **144**(1993), 238-253.
- [57] J. -M. Manoli, C. Potvin, M. Muhler, U. Wild, G. Resofszki, T. Buchholz and Z. Paal, *J. Catal.* **178**(1998), 338-351.
- [58] M. G. Falco, J. M. Grau and N. S. Figoli, *Appl. Catal. A: General* **264**(2004), 183-192.
- [59] H. Liu, G. D. Lei and W. M. H. Sachtler, *Appl. Catal. A: General* **137**(1996), 167-177.
- [60] J. Manoli, C. Potvin, M. Muhler, U. Wild, G. Resofszki, T. Buchholz and Z. Paál, *J. Catal.* **178**(1998), 338-351.

- [61] J. C. Duchet, D. Guillaume, A. Monnier, J. van Gestel, G. Szabo, P. Nascimento and S. Decker, *Chem. Commun.* **18**(1999), 1819-1820.
- [62] Z. Hong, K. B. Fogash and J. A. Dumesic, *Catal. Today* **51**(1999), 269-288.
- [63] S. X. Song and R. A. Kydd, *Catal. Lett.* **51**(1998), 95-100.
- [64] R. A. Comelli, C. R. Vera and J. M. Parera, *J. Catal.* **151**(1995), 96-101.
- [65] T. Ishida, T. Yamaguchi and K. Tanabe, *Chem. Lett.* (1988), 1869.
- [66] D. A. Ward and E. I. Ko, *J. Catal.* **150**(1994), 18-33.
- [67] D. Tichit, B. Coq, H. Armendariz and F. Figueras, *Catal. Lett.* **38**(1996), 109-113.
- [68] A. Hahn, T. Ressler, R. E. Jentoft and F. C. Jentoft, *Chem. Commun.* (2001), 537-538.
- [69] P. S. Kumbhar, V. M. Yadav and G. D. Yadav, *Chemically Modified Surfaces* **3**(1990), 81-92.
- [70] A. S. C. Brown and J. S. J. Hargreaves, *Green Chemistry* **1**(1999), 17-20.
- [71] F. C. Lange, T. -K. Cheung and B. C. Gates, *Catal. Lett.* **41**(1996), 95-99.
- [72] J. E. Tabora and R. J. Davis, *J. Catal.* **162**(1996), 125-133.
- [73] J. C. Yori and J. M. Parera, *Appl. Catal. A: General* **147**(1996), 145-157.
- [74] S. X. Song, D. J. McIntosh and R. A. Kydd, *Catal. Lett.* **65**(2000), 5-7.
- [75] J. M. M. Millet, M. Signoretto and P. Bonville, *Catal. Lett.* **64**(2000), 135-140.
- [76] E. A. Garcia, E. H. Rueda and A. J. Rouco, *Appl. Catal. A: General* **210**(2001), 363-370.
- [77] M. A. Coelho, W. E. Alvarez, E. C. Sikabwe, R. L. White and D. E. Resasco, *Catal. Today* **28**(1996), 415-429.
- [78] J. A. Moreno and G. Poncelet, *Appl. Catal. A: General* **210**(2001), 151-164.
- [79] S. G. Ryu and B. C. Gates, *Ind.Eng.Chem.Res.* **37**(1998), 1786-1792.
- [80] K. T. Wan, C. B. Khouw and M. E. Davis, *J. Catal.* **158**(1996), 311-326.
- [81] A. Sayari, Y. Yang and X. Song, *J. Catal.* **167**(1997), 346-353.
- [82] A. Jatia, C. Chang, J. D. MacLeod, T. Okubo and M. E. Davis, *Catal. Lett.* **25**(1994), 21-28.
- [83] T. Yamamoto, T. Tanaka, S. Takenaka, S. Yoshida, T. Onari, Y. Takahashi, T. Kosaka, S. Hasegawa and M. Kudo, *J. Phys. Chem. B* **103**(1999), 2385-2393.
- [84] R. K. Scheithauer, E. Bosch, U. A. Schubert, H. Knozinger, T. -K. Cheung, R. E. Jentoft, B. C. Gates and B. Tesche, *J. Catal.* **177**(1998), 137-146.
- [85] T. -K. Cheung and B. C. Gates, *Topics Catal.* **6**(1998), 41-47.
- [86] C. Morterra, G. Cerrato, S. Di Ciero, M. Signoretto, A. Minesso, F. Pinna and G. Strukul, *Catal. Lett.* **49**(1997), 25-34.
- [87] R. Srinivasan, R. A. Keogh and B. H. Davis, *Appl. Catal. A: General* **130**(1995), 135-155.
- [88] T. -K. Cheung, J. L. d'Itri and B. C. Gates, *J. Catal.* **153**(1995), 344-349.
- [89] F. C. Jentoft, A. Hahn, J. Krohnert, G. Lorenz, R. E. Jentoft, T. Ressler, U. Wild, R. Schlogl, C. Hassner and K. Kohler, *J. Catal.* **224**(2004), 124-137.
- [90] C. R. Vera, J. C. Yori and J. M. Parera, *Appl. Catal. A: General* **167**(1998), 75-84.
- [91] W. E. Alvarez, H. Liu and D. E. Resasco, *Appl. Catal. A: General* **162**(1997), 103-119.
- [92] Z. Gao, Y. Xia, W. Hua and C. Miao, *Topics Catal.* **6**(1998), 101-106.
- [93] M. G. Falco, S. A. Canavese, R. A. Comelli and N. S. Figoli, *Appl. Catal. A: General* **201**(2000), 37-43.

- [94] K. Ebitani, H. Konno, T. Tanaka and H. Hattori, *J. Catal.* **135**(1992), 60-67.
- [95] K. Ebitani, H. Konno, T. Tanaka and H. Hattori, *J. Catal.* **143**(1993), 322-323.
- [96] R. A. Comelli, S. A. Canvese, S. R. Vaudagna and N. S. Figoli, *Appl. Catal. A: General* **135**(1996), 287-299.
- [97] M. -D. Appay, J. -M. Manoli, C. Potvin, M. Muhler, U. Wild, O. Pozdnyakova and Z. Paál, *J. Catal.* **222**(2004), 419-428.
- [98] T. Shishido, T. Tanaka and H. Hattori, *J. Catal.* **172**(1997), 24-33.
- [99] G. Larsen, E. Lotero, R. D. Parra, L. M. Petkovic, H. S. Silva and S. Raghavan, *Appl. Catal. A: General* **130**(1995), 213-226.
- [100] J. Weitkamp, P. A. Jacobs and J. A. Martens, *Appl. Catal.* **8**(1983), 123-141.
- [101] T. Buchholz, U. Wild, M. Muhler, G. Resofszki and Z. Paal, *Appl. Catal. A: General* **189**(1999), 225-236.
- [102] K. Föttinger and H. Vinek, *Catal. Lett.* **97**(2004), 131-138.
- [103] S. Y. Kim, J. G. Goodwin and D. Galloway, *Catal. Today* **63**(2000), 21-32.
- [104] B. Li and R. D. Gonzalez, *Appl. Catal. A: General* **165**(1997), 291-300.
- [105] G. Resofszki, M. Muhler, S. Sprenger, U. Wild and Z. Paal, *Appl. Catal. A: General* **240**(2003), 71-81.
- [106] F. T. T. Ng and N. Horvát, *Applied Catalysis A: General* **123**(1995), L197-L203.
- [107] J. C. Yori, J. C. Luy and J. M. Parera, *Appl. Catal.* **46**(1989), 103-112.
- [108] C. Li and P. C. Stair, *Catal. Lett.* **36**(1996), 119-123.
- [109] Z. Paal, U. Wild, M. Muhler, J. -M. Manoli, C. Potvin, T. Buchholz, S. Sprenger and G. Resofszki, *Appl. Catal. A: General* **188**(1999), 257-266.
- [110] K. Arata, *Appl. Catal. A: General* **146**(1996), 3-32.
- [111] J. van Gestel, V. T. Nghiem, D. Guillaume, J. P. Gilson and J. C. Duchet, *J. Catal.* **212**(2002), 173-181.
- [112] S. De Rossi, G. Ferraris, M. Valigi and D. Gazzoli, *Appl. Catal. A: General* **231**(2002), 173-184.
- [113] K. Arata and M. Hino, *Proceedings 9th International Congress on Catalysis Volume 4 Oxide catalysis and catalyst development.* (M. J. Phillips and M. Ternan, eds.), The Chemical Institute of Canada, Ottawa, 1988, pp. 1727-1734.
- [114] S. R. Vaudagna, S. A. Canvese, R. A. Comelli and N. S. Figoli, *Appl. Catal. A: General* **168**(1998), 93-111.
- [115] E. A. Blekkan, A. Holmen and S. Vada, *Acta. Chem. Scand.* **47**(1993), 275-280.
- [116] P. Bichon, Doctoral Thesis, Université de Poitiers, France, 2002.
- [117] H. Scott Fogler, *Elements of Chemical Reaction Engineering.* Prentice Hall, Upper Saddle River, 1992.
- [118] A. Sayari and A. Dicko, *J. Catal.* **145**(1994), 561-564.
- [119] M. -T. Tran, N. S. Gnep, M. Guisnet and P. Nascimento, *Catal. Lett.* **47**(1997), 57-61.
- [120] F. Garin, L. Seyfried, P. Girard, G. Maire, A. Abdulsamad and J. Sommer, *J. Catal.* **150**(1995), 26-32.

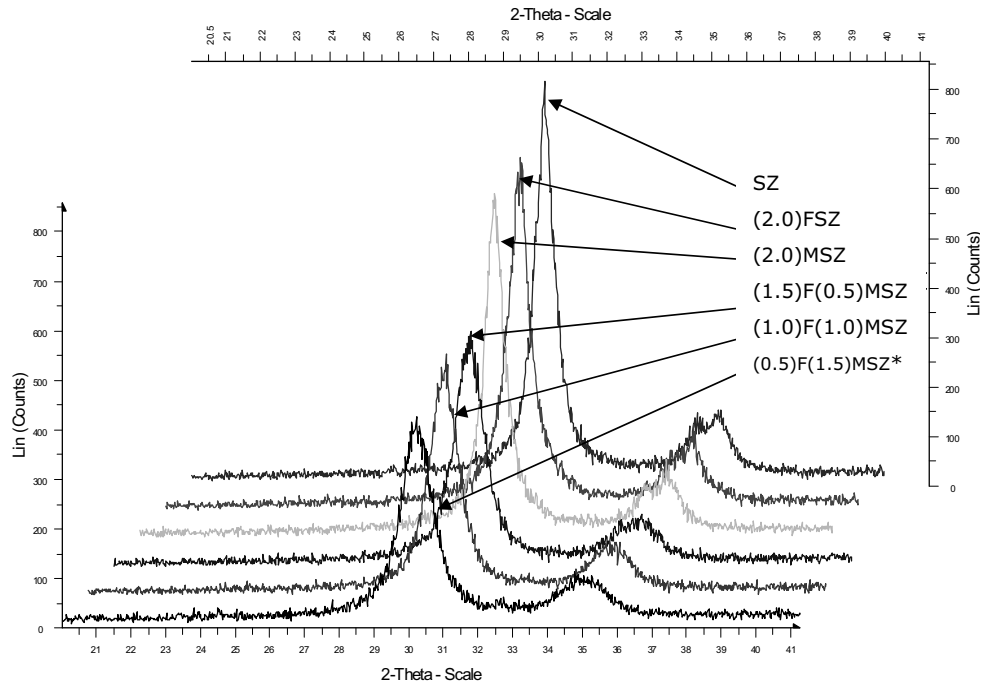
-
- [121] Y. Huang and W. M. H. Sachtler, *Appl. Catal. A: General* **163**(1997), 245-254.
- [122] A. Dicko, X. Song, A. Adnot and A. Sayari, *J. Catal.* **150**(1994), 254-261.
- [123] M. Guisnet, V. Fouche, M. Belloum, J. P. Bournonville and C. Travers, *Appl. Catal.* **71**(1991), 295-306.
- [124] F. Chevalier, M. Guisnet and R. Maurel, *Comptes Rendus des Seances de l'Academie des Sciences, Serie C: Sciences Chimiques* **282**(1976), 3-5.
- [125] J. H. Sinfelt, T. B. Drew, J. W. Hoopes and T. Vermeulen, *Advan. Chem. Eng.* **5**(1964), 37-74.
- [126] D. M. Brouwer and J. M. Oelderik, *Recl. Trav. Chim. Pays Bas* **87**(1968), 721-736.
- [127] U. B. Demirci and F. Garin, *J. Mol. Catal. [A] Chem.* **188**(2002), 233-243.
- [128] J. F. Allain, P. Magnoux, P. Schulz and M. Guisnet, *Appl. Catal. A: General* **152**(1997), 221-235.
- [129] F. J. M. M. de Gauw, J. van Grondelle and R. A. van Santen, *J. Catal.* **206**(2002), 295-304.
- [130] R. L. Augustine, F. Yaghmaie and J. F. Van Peppen, *J. Org. Chem.* **49**(1984), 1865-1870.
- [131] A. S. Hussey, T. A. Shenack and R. H. Baker, *J. Org. Chem.* **33**(1968), 3258.
- [132] R. Marcus, U. Diebold and R. D. Gonzalez, *Catal. Lett.* **86**(2003), 151-156.

List of Appendices

Appendix 1	X-ray diffractograms for the iron and manganese promoted samples	102
Appendix 2	X-ray diffractograms for the noble metal promoted samples	103
Appendix 3	Reproducibility of n-butane isomerization experiments	104
Appendix 4	Selectivities of Fe and Mn promoted SZ	105
Appendix 5	Pore size distribution	109
Appendix 6	Preliminary experiments at high pressure	112

Appendix 1 X-ray diffractograms for the iron and manganese promoted samples

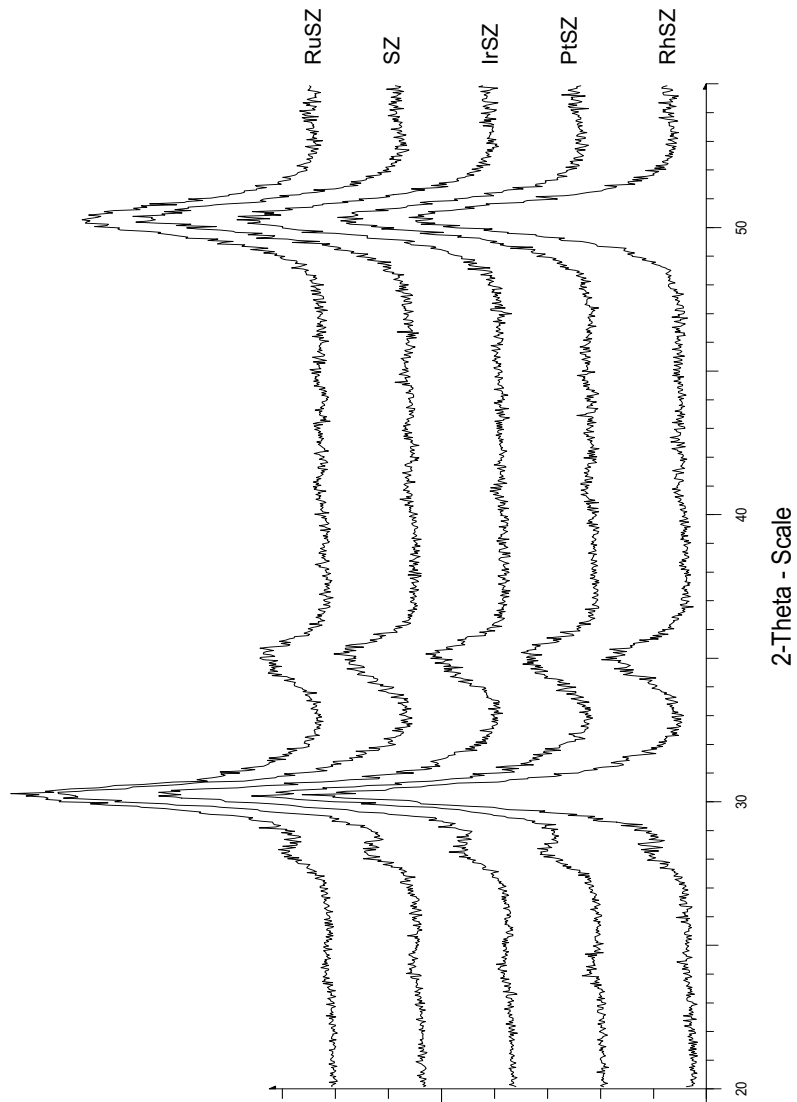
The crystallinity of the samples was characterized by X-ray diffraction (XRD). The XRD spectra were obtained by a Siemens D5005 x-ray diffractometer with Cu K α radiation, scanned at a rate of 2° min⁻¹.



*Further characterization of the sample ((0.5)F(1.5)MSZ) has not been done.

Appendix 2 X-ray diffractograms for the noble metal promoted samples

The crystallinity of the samples was characterized by X-ray diffraction (XRD). The XRD spectra were obtained by a Siemens D5005 x-ray diffractometer with Cu K α radiation, scanned at a rate of 2° min⁻¹.



Appendix 3 Reproducibility of *n*-butane isomerization experiments

To check the reproducibility of the *n*-butane isomerization experiments at atmospheric pressure the (1.5)F(0.5)MSZ sample was tested twice at the same conditions:

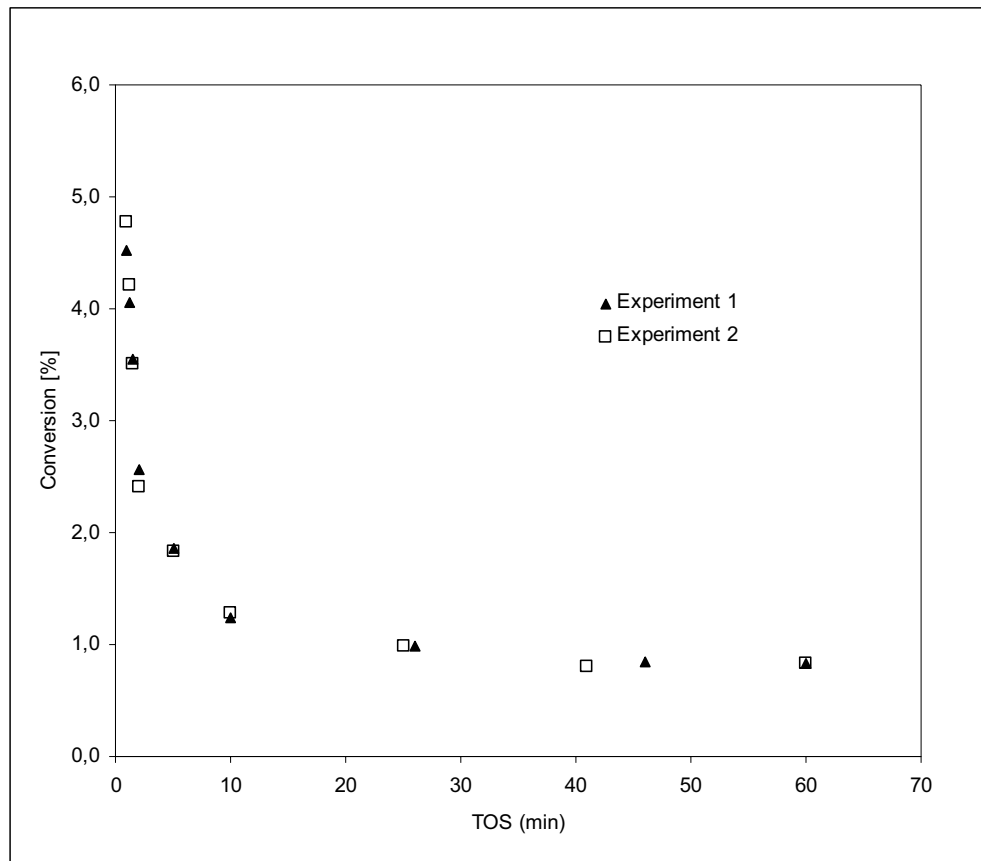


Figure A3.1 Reproducibility of the *n*-butane isomerization experiments. Catalyst: (1.5)F(0.5)MSZ. $T_{\text{reaction}} = 250^{\circ}\text{C}$, $\text{WHSV} = 4.7\text{h}^{-1}$, $\text{N}_2/\text{nC}_4 = 9$. The catalyst was pretreated in air at 450°C .

Appendix 4 Selectivities of Fe and Mn promoted SZ

Product selectivities for n-butane isomerization over Fe and Mn promoted sulfated zirconia are given in figure A2.1 to A2.7. The experiments were all carried out in a nitrogen or a hydrogen atmosphere (diluent/nC4=9) at 250°C and atmospheric pressure and with WHSV= 4.7h⁻¹. All samples calcined *in situ* at 450°C before the reaction is started.

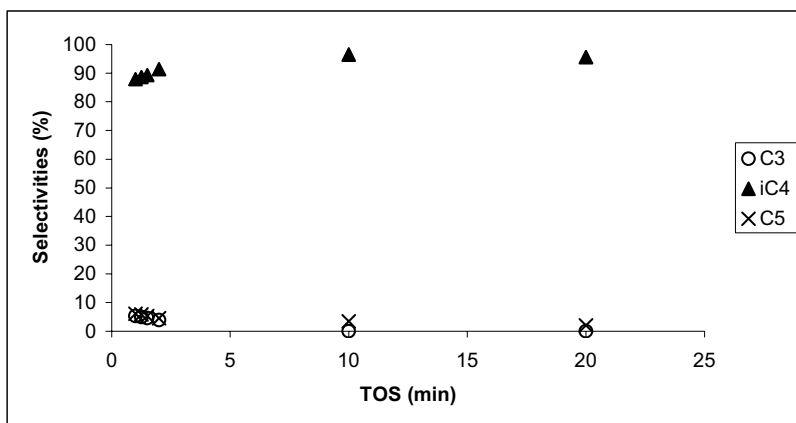


Figure A4.1 Unpromoted sulfated zirconia in nitrogen. (N₂/nC4=9) at 250°C, atmospheric pressure, WHSV= 4.7h⁻¹.

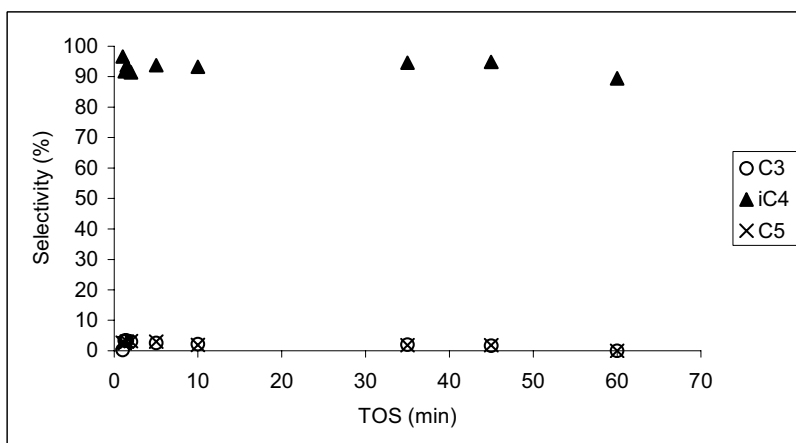


Figure A4.2 (2.0wt%) Mn sulfated zirconia in nitrogen. (N₂/nC4=9) at 250°C, atmospheric pressure, WHSV= 4.7h⁻¹.

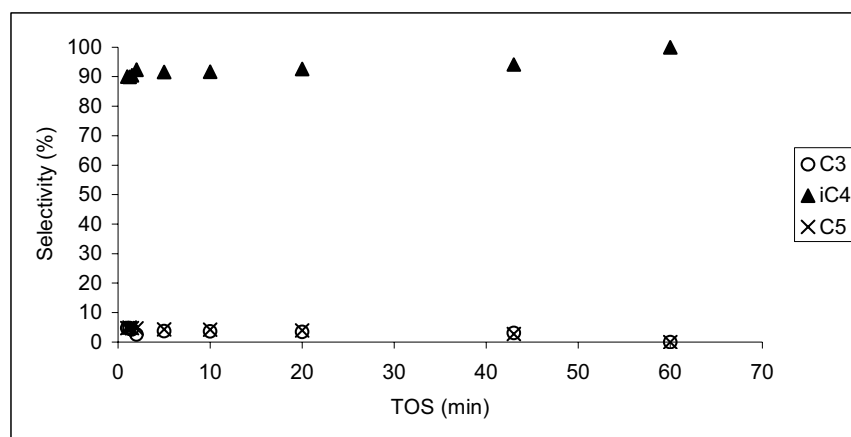


Figure A4.3 (1.0wt%)Fe(1.0wt%)Mn sulfated zirconia in nitrogen. ($N_2/nC_4=9$) at 250°C, atmospheric pressure, $WHSV= 4.7h^{-1}$

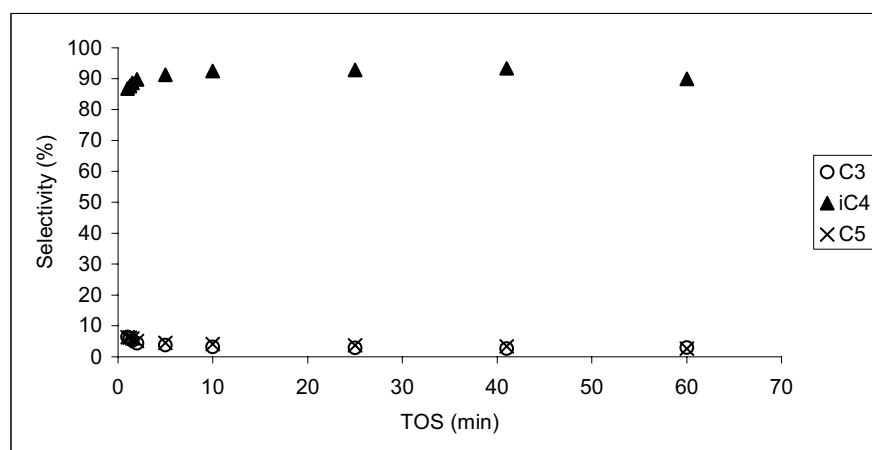


Figure A4.4 (1.5wt%)Fe(0.5wt%)Mn sulfated zirconia in nitrogen. ($N_2/nC_4=9$) at 250°C, atmospheric pressure, $WHSV= 4.7h^{-1}$.

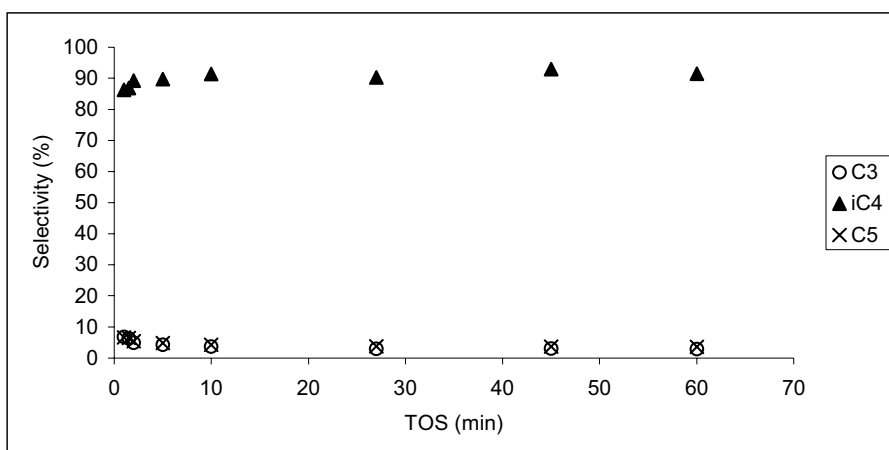


Figure A4.5 (2.0wt%)Fe sulfated zirconia in nitrogen. ($N_2/nC_4=9$) at 250°C, atmospheric pressure, $WHSV= 4.7h^{-1}$.

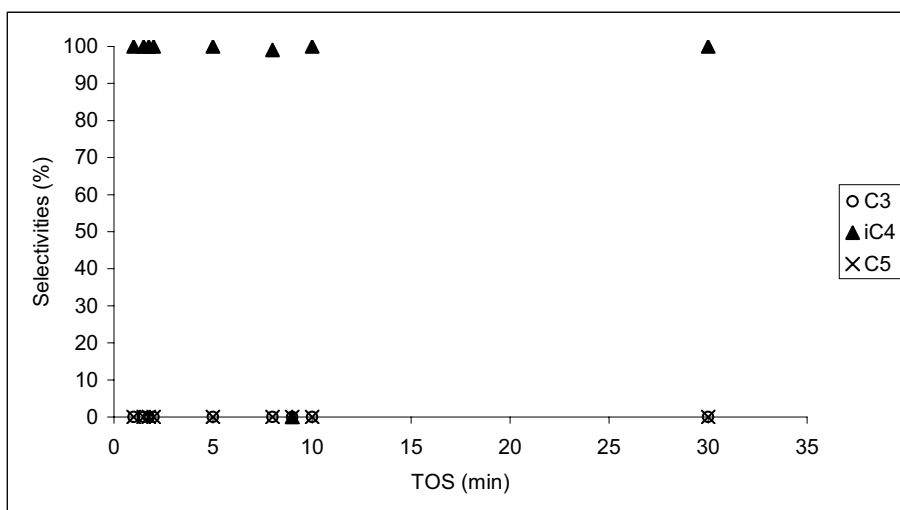


Figure A4.6 Sulfated zirconia in hydrogen. ($H_2/nC_4=9$) at 250°C, atmospheric pressure, $WHSV= 4.7h^{-1}$.

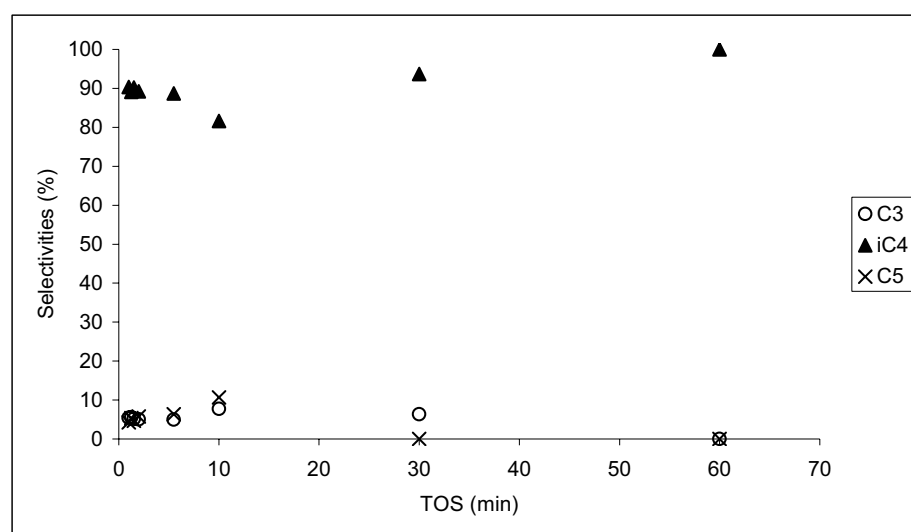


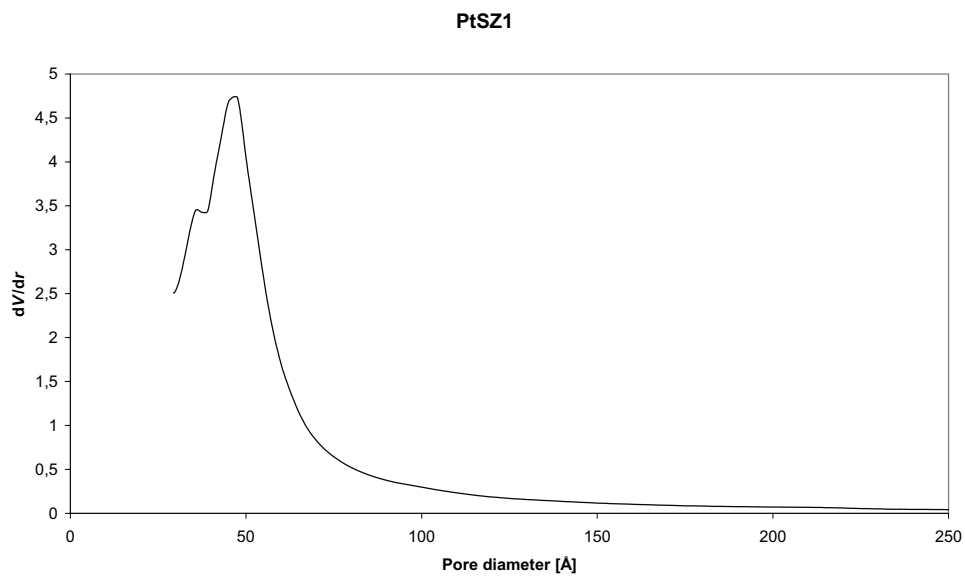
Figure A4.7 (1.5wt%Fe)(0.5wt%Mn) sulfated zirconia in hydrogen. ($H_2/nC_4=9$) at 250°C, atmospheric pressure, $WHSV=4.7h^{-1}$.

Appendix 5 Pore size distribution

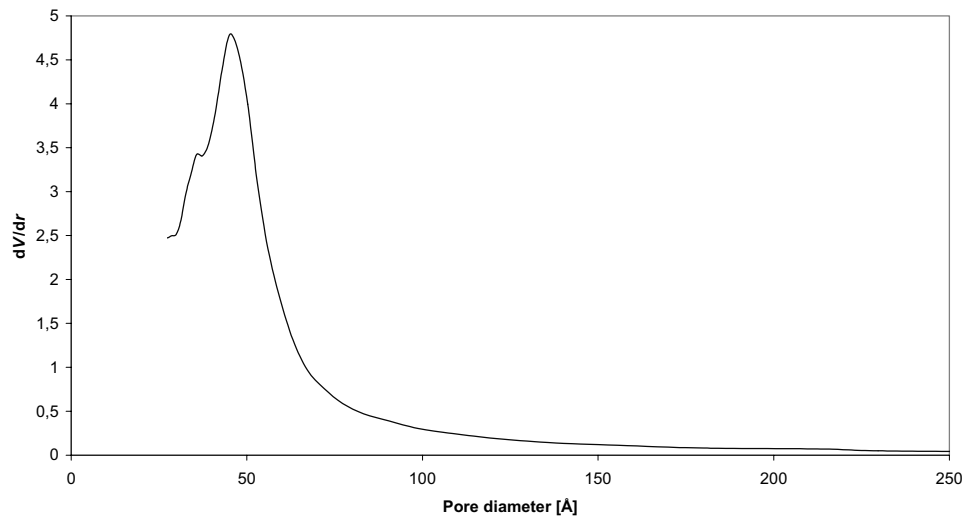
Nitrogen adsorption-desorption isotherms were measured at a Micromeritics TriStar 3000 instrument, and the data were collected at the nitrogen liquid temperature, 77 K. All samples were outgassed at 473 K overnight prior to measurement. The total pore volume and the pore size distribution were calculated from the nitrogen desorption branch applying the Barrett-Joyner-Halenda (BJH) method.

The pore size distribution of all the samples is almost identical as shown in following figures. The BET surface area, mean pore diameter and specific pore volume are also identical.

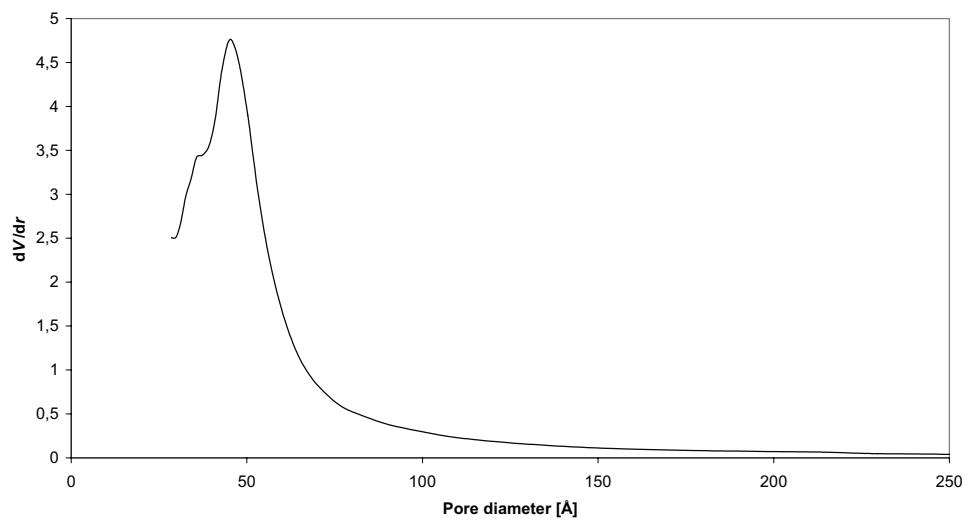
Sample	BET surface area [m ² /g]	Average pore width [nm]	Pore volume [cm ³ /g]
PtSZ	134	46	0.20
IrSZ	133	47	0.20
RuSZ	132	46	0.19
RhSZ	134	47	0.20
SZ	133	47	0.19



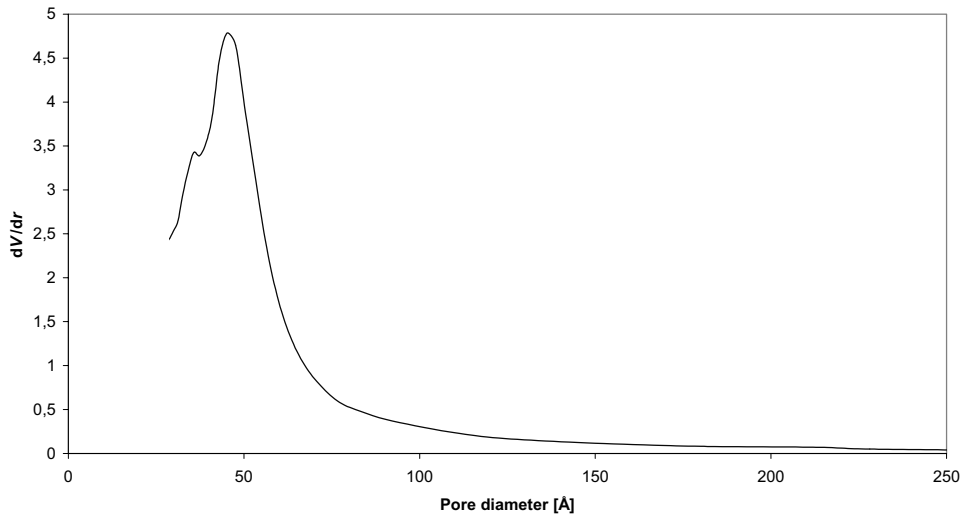
RhSZ



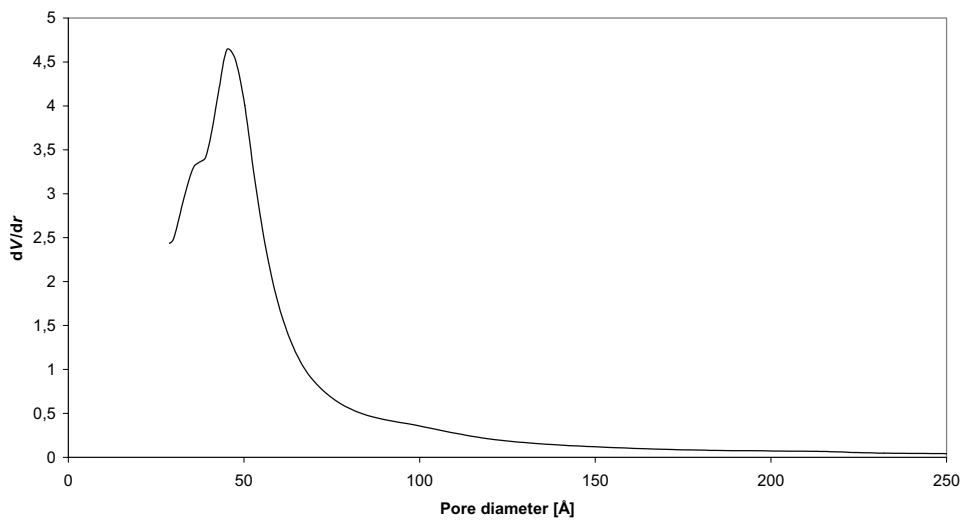
RuSZ



SZ



IrSZ



Appendix 6 Preliminary experiments at high pressure

Platinum promoted sulfated zirconia

The catalytic test was carried out during 6 days, and the results for each day are shown in figure A6.1 to A6.9. Pretreatment procedure and conditions between the experiments can be found in chapter 3.

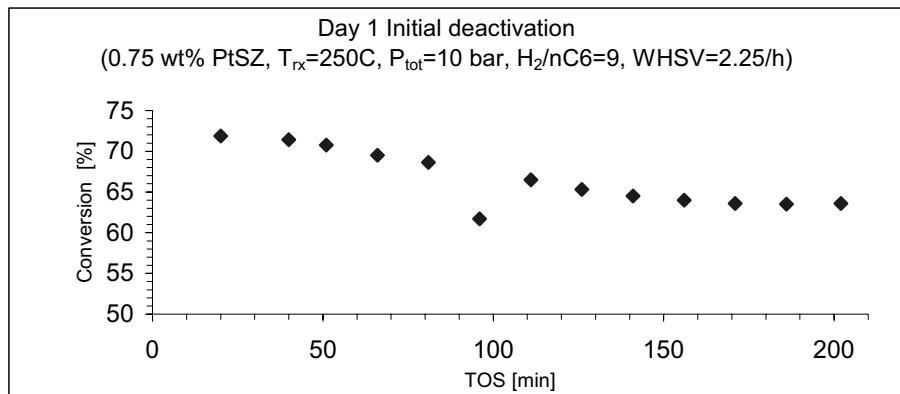


Figure A6.1 Day 1 Initial deactivation

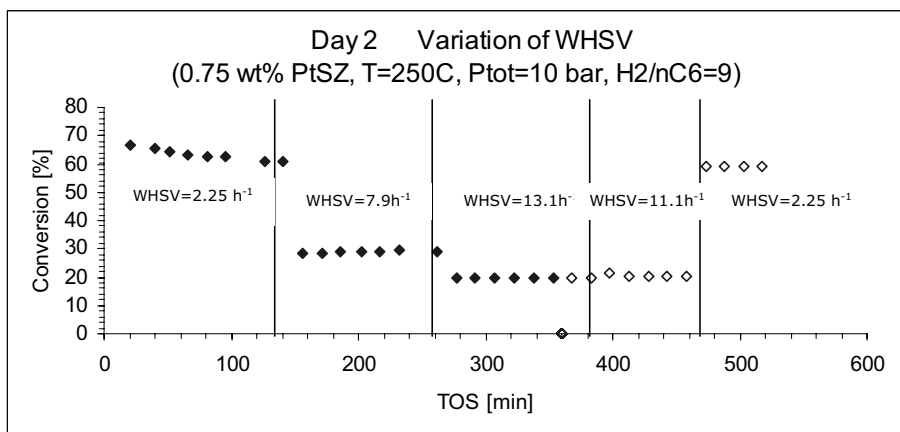


Figure A6.2 Day 2 Effect of WHSV

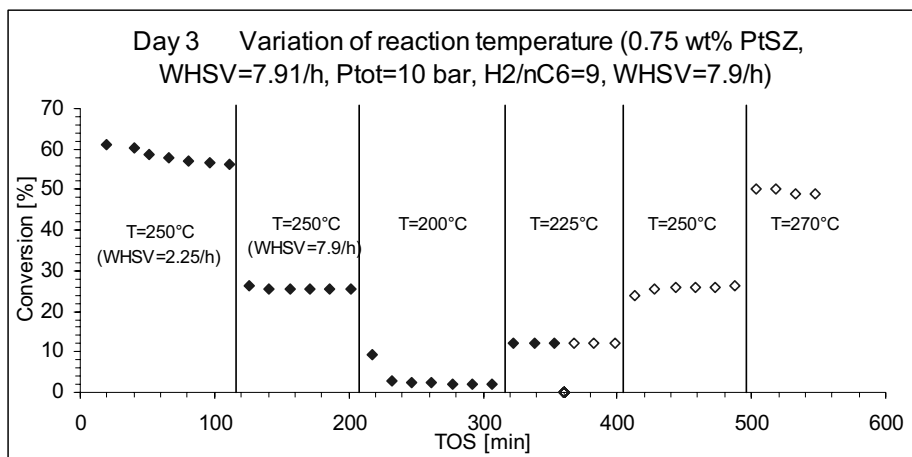
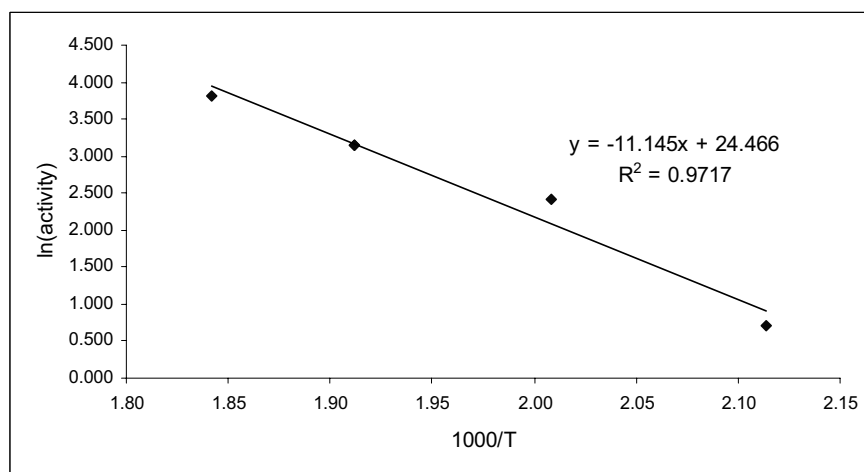


Figure A6.3 Day 3 Effect of temperature

These data are presented as an Arrhenius plot in Figure A6.4. The activation energy was found to be 93 kJ/mol.



$E_a = 93$ kJ/mol

Figure A6.4 Arrhenius plot for *n*-hexane isomerization over PtSZ

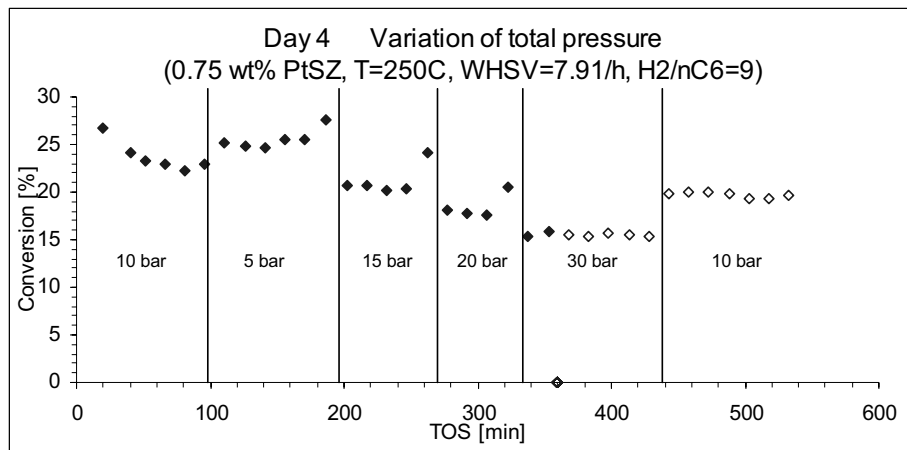
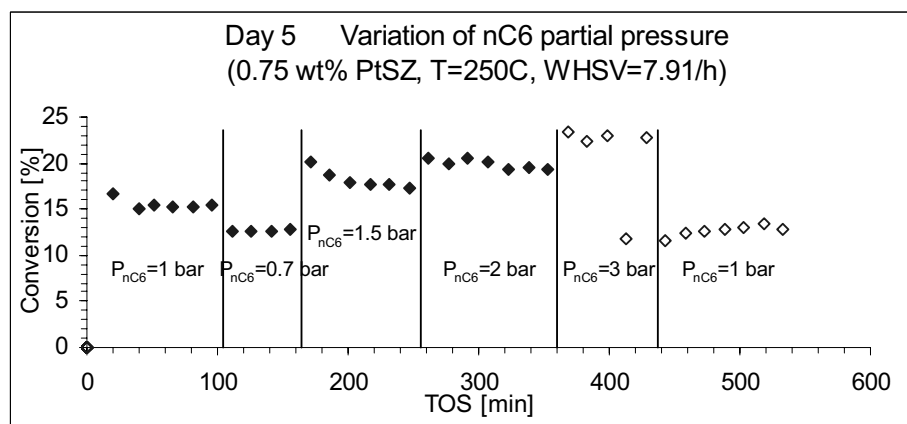


Figure A6.5 Day 4 Effect of total pressure

Figure A6.6 Day 5 Effect of *n*-hexane partial pressure

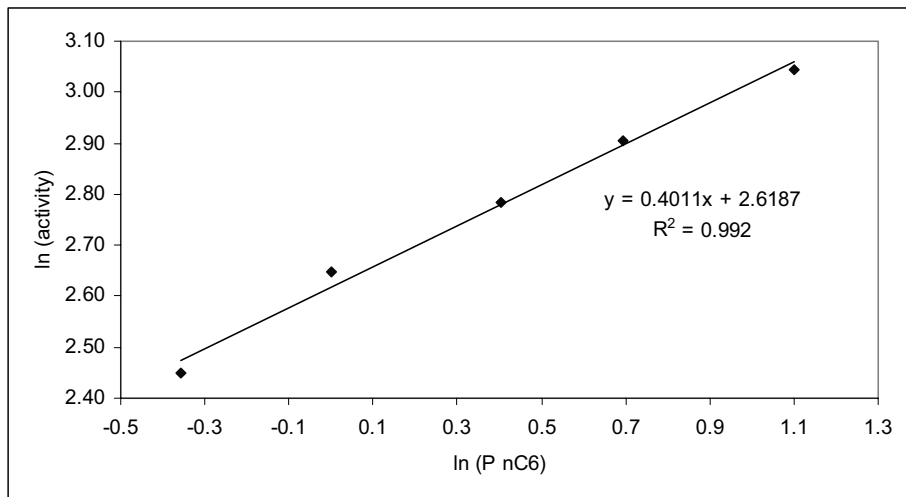


Figure A6.7 Reaction order of *n*-hexane partial pressure.

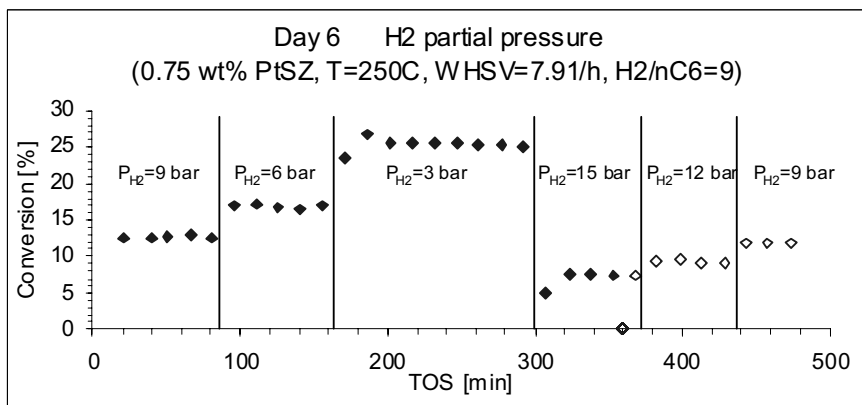


Figure A6.8 Day 6 Effect of hydrogen partial pressure

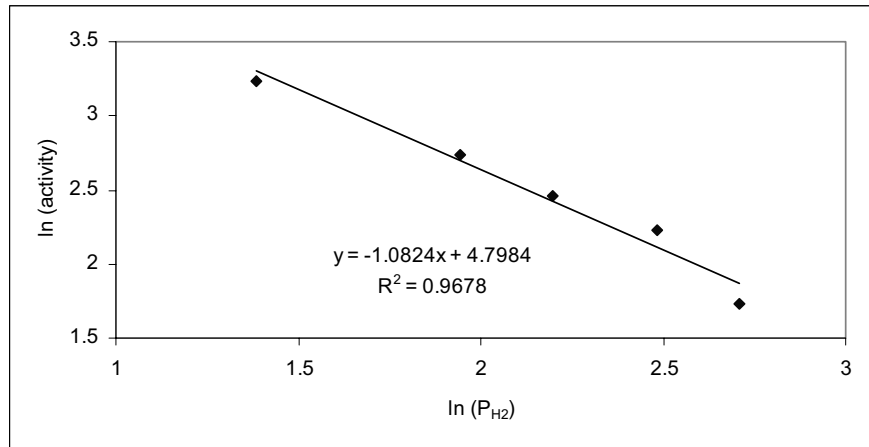


Figure A6.9 Reaction order of hydrogen

Deactivation

The catalyst was continuously deactivated. In Figure A6.10 the deactivation from day to day during the whole experiment with the platinum promoted sample is shown. The conversion at standard conditions at the end of each day was taken as measure for the conversion. After six days the residual activity is approximately 40% of the initial activity.

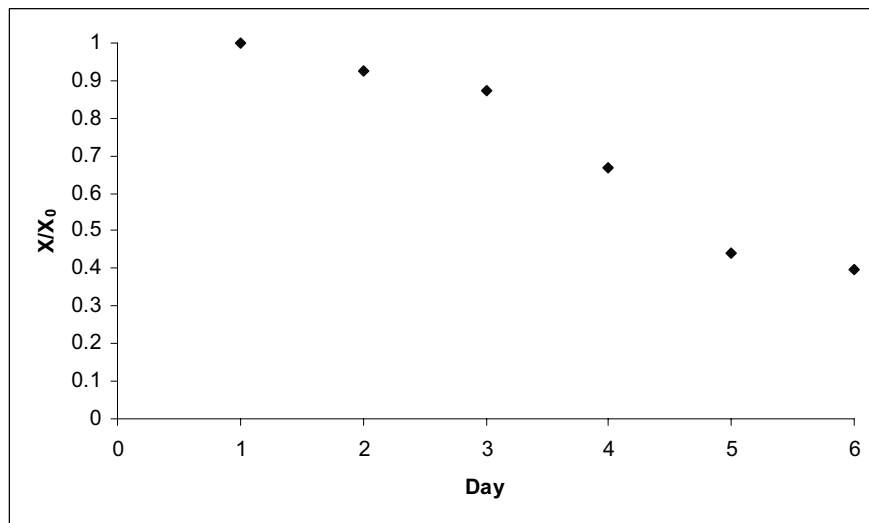


Figure A6.10 Deactivation during experiment for the Pt promoted sulfated zirconia. X_0 – conversion at the end of day 1.

Iron and manganese promoted sulfated zirconia

The catalytic test was carried out during 5 days, and the results for each day are shown in Figure A6.11 to Figure A6.16. Pretreatment procedure and conditions between the experiments can be found in chapter 3.

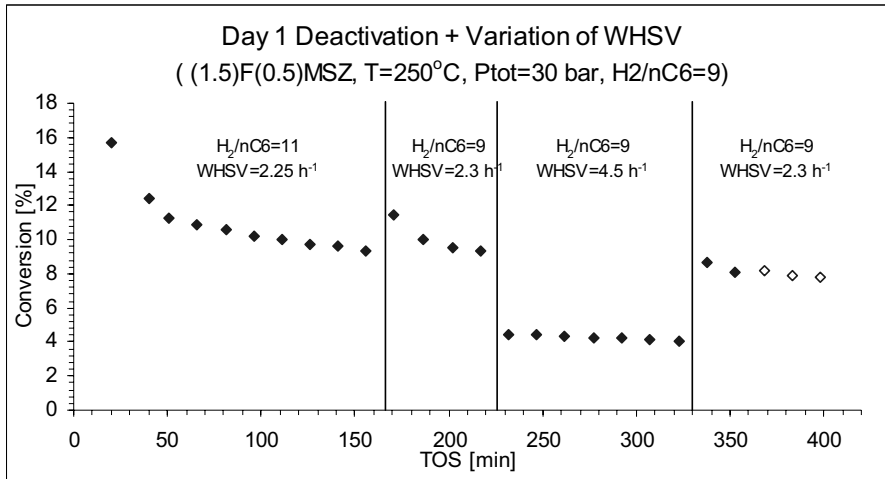


Figure A6.11 Day 1 Initial deactivation and effect of WHSV

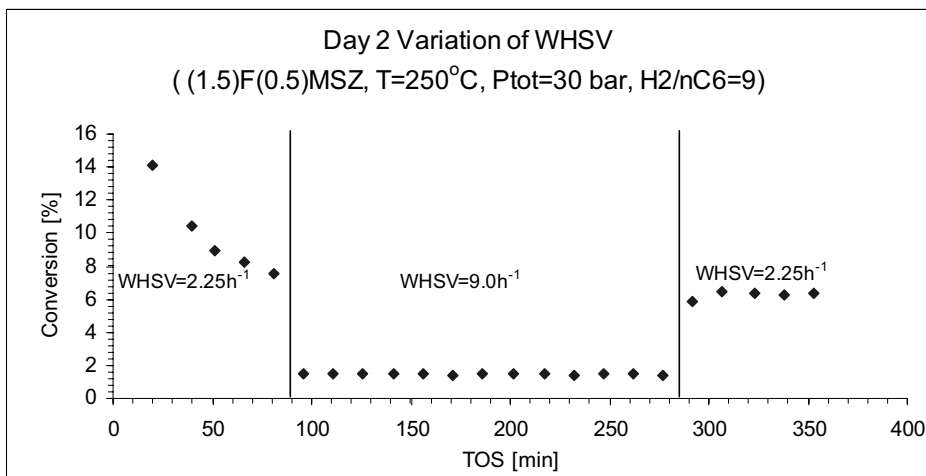


Figure A6.12 Day 2 Effect of WHSV

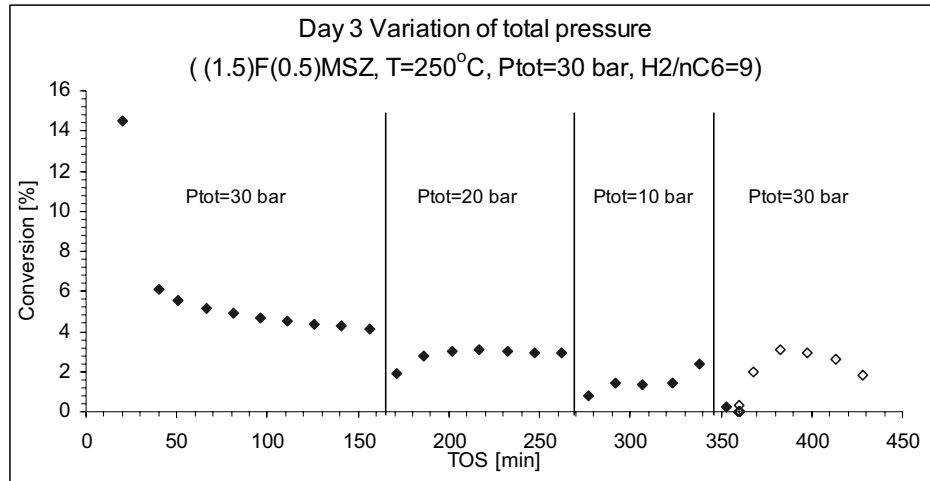


Figure A6.13 Day 3 Effect of total pressure

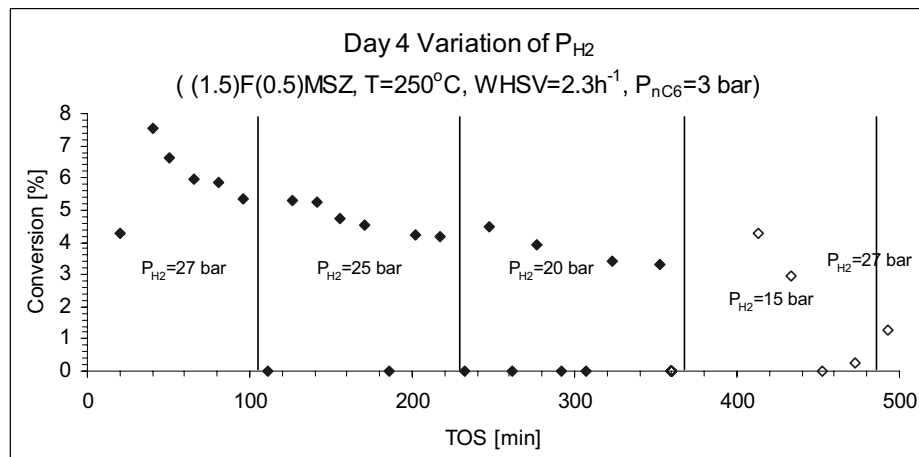


Figure A6.14 Day 4 Effect of hydrogen partial pressure. Points at zero conversion are due to failure in the analysis.

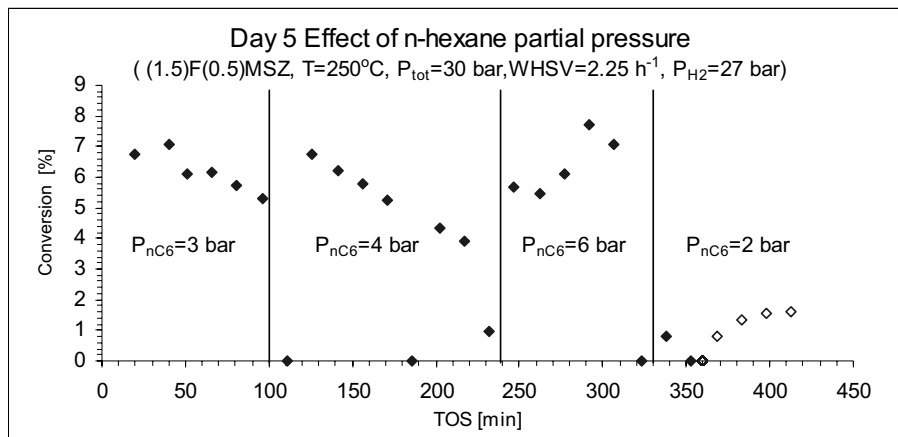


Figure A6.15 Effect of *n*-hexane partial pressure. Points at zero conversion are due to failure in the analysis.

Deactivation

The catalyst was continuously deactivated. In Figure A6.16 the deactivation from day to day during the experiment with the iron and manganese promoted sample is shown. The conversion at standard conditions at the end of each day was taken as measure for the conversion. Only the three first days are shown, after the third day the conversion did not stabilize (Figure A6.14 and Figure A6.15). After three days the residual activity is 33% of the initial activity.

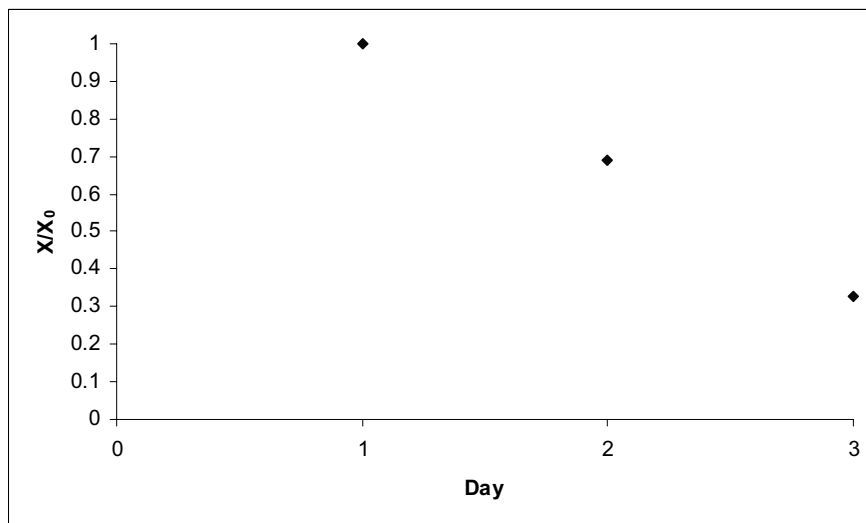


Figure A6.16 Deactivation during experiment for the iron and manganese promoted sulfated zirconia. X₀ – conversion at the end of day 1.